SAMUEL CORDEIRO VITOR MARTINS

HYDRAULIC LIMITATIONS IN DIFFERENT PLANT SPECIES

Thesis submitted to Federal University of Viçosa, as part of the requirements for obtaining the Doctor Scientiae degree in Plant Physiology.

VIÇOSA
MINAS GERAIS – BRASIL
2015

Ficha catalográfica preparada pela Biblioteca Central da Universidade Federal de Viçosa - Câmpus Viçosa

T

M379h
2015

Martins, Samuel Cordeiro Vitor, 1986-
Hydraulic limitations in different plant species / Samuel Cordeiro Vitor Martins. - Viçosa, MG, 2015.
x, 78f. : il. (algumas color.) ; 29 cm.

Orientador : Fábio Murilo da Matta.
Tese (doutorado) - Universidade Federal de Viçosa.
Inclui bibliografia.

1. Fisiologia vegetal. 2. Plantas - Relações hídrica. 3. Controle estomático. I. Universidade Federal de Viçosa. Departamento de Biologia Vegetal. Programa de Pós-graduação em Fisiologia Vegetal. II. Título.

CDD 22. ed. 571.2

SAMUEL CORDEIRO VITOR MARTINS

HYDRAULIC LIMITATIONS IN DIFFERENT PLANT SPECIES

Thesis submitted to Federal University of Viçosa, as part of the requirements for obtaining the Doctor Scientiae degree in Plant Physiology.

APPROVED: February 25th, 2015.

Wagner Luiz Araújo	Raimundo Santos Barros
Leandro Elias Morais	Paulo Eduardo Menezes Silva

Fábio Murilo DaMatta
(Adviser)

To my parents, Vacvenus e Vânia,

You were there in the very first moment I opened my eyes, guided me during my very first steps, and, if I was able to handle a pen and adventure myself into the unknown, all that thanks to you. Unconditional love comes at no price, the deserved thanks, on the other hand, at no possible amount.

To my dear wife, Karina,

I wish I could put in words how much you mean to me, but how could I use something finite to describe the infinite? You are my safe harbor, the one I turn my eyes when I lose hope and need help, the one I will love and want by my side, forever.

If I have seen further, it is by standing on the shoulders of giants.

Sir Isaac Newton

ACKNOWLEDGMENTS

First, I thank God for the gift of life and for creating the beautiful and lovely plants for which I became so passionate about. I will always be grateful for the person who somewhat introduced me to the amazing world of Plant Physiology, Professor Fábio DaMatta. It has been almost teen years of mentorship and, most importantly, friendship; your dedication, tenacity, efficiency and passion for work will be things I will carry for life. Definitely, if one day I turn out to have 10% of your efficiency, I will be on the top! Tim Brodribb, what a nice time I spent in Tasmania under your supervision! Thanks for having me in your house, introducing me to your family and sharing so much with me and Karina! Those moments in Pelverata where I, Karina, you and Jill were planting the lovely conifers and hearing Luca singing, they will always be one of my finest memories. I also had a tremendous time learning scientific process from you and enjoying your passion for life and the world around you. Thanks for letting me dive in the world of hydraulics, conifers, ferns and plant evolution; you provided me so much perspective and I will be eternally grateful for that!

I am also very grateful to my dear labmates and friends in UTAS, Scott and Erin McAdam, Chris Lucani (and his lovely family), Maddy, Ross, Patrick Mitchell, Rachael Berry, Greg Jordan, Mario, Giselle, Paty Machado and the great staff from the School of Biological Sciences. It was great to spend time in your company and to share experiences, you all make my life way easier in Hobart. Specially to Scott, Erin and Chris, you were such nice friends, thanks for that! What a hell of a nice time we had together, hunting Eucs in Tasmania, sharing life stories, learning how to cook and knowing so many interesting and random facts, definitely, you are the best friends anyone can wish for!

To everyone I have met in the University of Sydney, I am so grateful for the opportunity to get to know you all. I am specially grateful to Margaret Barbour, Kevin Simonin and Xin Song, I had the best possible people to introduce me to the isotope world and your expert supervision and solid knowledge made an overall difficult subject much easier to understand, I sincerely hope we will keep our partnership for years to come. I could not forget to thank my two sisters in the CCWF, Bárbara and Carol Muller, without you, my journey in Sydney would have been extremely more difficult and less pleasant!

There are a number of people who I would like to thank for their help and encouragement, without whom I would never have produced this thesis. To all my friends from Viçosa, the department staff and especially the ones from the Coffee and Rice Group, you were my family here and I am happy for how much we have shared in the past ten years. Specially, thanks are due to the Professors Wagner Araújo, Raimundo Barros, Leandro Morais and Paulo Menezes for have participated in my PhD committee. You all are friends and it was a great pleasure to hear your comments and suggestions. I deeply appreciate your efforts in reading my thesis in such short time and doing your best to understand my rambling writing.

Lastly, my family and friends outside the Academia – thank you for your support, encouragement and patience for allowing me to accomplish this dream. Particularly my relatives who were crucial in encouraging my passion for research; and providing such an inspirational example of the value of hard work and striving for improvement.

CONTENTS

RESUMO vii
ABSTRACT ix
GENERAL INTRODUCTION 1
References 3
CHAPTER 1 6
Stomata dynamics are limited by leaf anatomy and hydraulics in ferns and conifers: results from simultaneous measurements of liquid and vapour fluxes in leaves.
1. Introduction 6
2. Materials and Methods 8
3. Results 11
4. Discussion 12
5. Conclusion 16
7. References 16
8. Table and Figures 19
CHAPTER 2 29
Influence of leaf hydraulic parameters defining heavy water enrichment in different species
1. Introduction 29
2. Material and methods 31
3. Results 36
4. Discussion 37
5. Conclusions 40
7. References 41
8. Tables and figures 45
CHAPTER 3 .....
Leaf hydraulic vulnerability in two field-grown coffee cultivars under severe drought conditions
1. Introduction 53
2. Material and methods 55
3. Results 58
4. Discussion 59
5. Conclusions 63
7. References 64
8. Tables and figures 70
GENERAL CONCLUSIONS 78

RESUMO

MARTINS, Samuel Cordeiro Vitor, D.Sc., Universidade Federal de Viçosa, fevereiro de 2015. **Hydraulic limitations in different plant species.** Orientador: Fábio Murilo da Matta.

Características hidráulicas como a condutância hidráulica foliar (K_{leaf}) e capacitância (C_{dyn}) definem os limites operacionais do xilema em nível de folha. Apesar do controle estômático em samambaias e coníferas ser fielmente predito por um modelo hidropassivo, ainda não foi testado se as características hidráulicas podem predizer com sucesso o comportamento estômatico em resposta ao déficit de pressão de vapor (VPD). Além disso, pouco se sabe sobre como características hidráulicas podem influenciar o enriquecimento de água nos locais de evaporação e a velocidade com que ocorre a mistura de água enriquecida e não enriquecida dentro de uma folha. Em um primeiro experimento, foi examinada a resposta estômática a aumentos graduais em VPD em quatro samambaias e duas coníferas estruturalmente diferentes, que abrangem uma grande diversidade em K_{leaf} e C_{dyn}. Os fluxos na fase líquida e gasosa também foram medidos para determinar o potencial hídrico foliar (Ψ_l) em tempo real e sua relação com a condutância estomática (g_s). Foi encontrado que diferentes valores de K_L e C_{dyn} levaram a balanços distintos entre a fase líquida e gasosa impactando significativamente o tempo de resposta para o fechamento estômática, onde o tempo de meia-vida variou de 48-248 segundos. O modelo hidropassivo predisse com sucesso a resposta estômáticas ao VPD em todas as espécies estudadas. Além disso, houve melhora na capacidade de predição do modelo quando assumindo um K_{leaf} dinâmico, sugerindo uma resposta de K_{leaf} ao VPD. De qualquer forma, a magnitude das mudanças em K_{leaf} foi pequena e em acordo com recentes modelos prevendo uma mudança da transpiração perivascular para a periestomática em resposta à aumentos em VPD. Em um segundo experimento, foi estudado o enriquecimento da água foliar em ^{18}O durante o processo tranpiratório em quatro espécies com K_{leaf} e C_{dyn} constrastantes. Evidências adicionais em suporte ao modelo de dois compartimentos para o enriquecimento em ^{18}O em três das quatro espécies foram encontradas. Os dados obtidos também sugerem uma possível interação entre a densidade de venação e tecidos associados às nervuras como determinantes da fração de água não-enriquecida. Além disso, é sugerido que o baixo K_{leaf} apresentando por samambaias, levaria a um aumento da resistência radial para o transporte de água,

restringindo assim a mistura de água entre as frações enriquecidas e não-enriquecidas. Em um terceiro experimento, a vulnerabilidade hidráulica foliar foi avaliada em duas cultivares de café em condições de campo sob forte restrição hídrica de modo a testar a suscetibilidade do café à disfunções hidráulicas. As folhas de café foram caracterizadas como moderadamente tolerantes a disfunções hidráulicas; no entanto, os Ψ_l encontrados sob seca foram suficientes para causar falha hidráulica e abscisão foliar. Após o retorno das chuvas, a recuperação da fotossíntese líquida (A_n) e g_s foi reprimida em diferentes extensões, provavelmente como resultado da perda hidráulica dado que nenhuma evidência para limitações bioquímicas em A_n foi encontrada. Em todo caso, após dois meses de chuvas, a recuperação total de A_n, mas não de g_s, foi observada em folhas expandidas sob seca em comparação com folhas expandidas na estação chuvosa. Sob condições de ampla disponibilidade hídrica, a abertura estômática parece ser regulada de modo a evitar que a perda de condutividade hidráulica alcance níveis maiores do que c. 30% por meio de mecanismos ativos provavelmente relacionados ao ácido abscísico (ABA). No entanto, a alta variabilidade em Ψ_l encontrada sob seca sugere que existe sensibilidade diferencial ao ABA nas folhas, dado que algumas folhas não conseguem alcançar fechamento estômático suficiente para evitar danos no sistema hidráulico. Em conclusão, é demonstrado que a anatomia foliar, através de mudanças em C_{dyn} e/ou no teor de água, tem um efeito significativo sobre a velocidade dos movimentos estomático em coníferas e samambaias. Portanto, o mecanismo passivo de controle estomático pode levar à taxas de fechamento estomático tão rápidas quanto as observadas em angiospermas e também afetar as propriedades do processo de enriquecimento em ^{18}O. Ressalta-se que, no cafeeiro, mais estudos relacionados à sensibilidade ao ABA serão necessários para melhor elucidar a contribuição de mecanismos passivos e ativos no controle estômático. É deveras importante também a determinação da vulnerabilidade hidráulica em caules e raízes, bem como em outras variedades de café para uma adequada avaliação dos efeitos da seca na cultura do café.

ABSTRACT

MARTINS, Samuel Cordeiro Vitor, D.Sc., Universidade Federal de Viçosa, February, 2015. **Hydraulic limitations in different plant species.** Adviser: Fábio Murilo da Matta.

Hydraulic traits such as leaf hydraulic conductance (K_{leaf}) and leaf capacitance (C_{dyn}) define the xylem operational limits at the leaf level. Despite stomata control in ferns and conifers having been proposed to be regulated via a hydropassive model, it remains untested whether hydraulic traits can successfully predict stomata behaviour to changes in vapour pressure deficit (VPD). Additionally, little is known on how hydraulic traits influence leaf water enrichment at the sites of evaporation and the mixing of enriched and unenriched water within a leaf. In a first experiment, we examined the stomata response to stepwise increases in VPD in two ferns and four conifers structurally different covering a large range in K_{leaf} and C_{dyn}. Water vapour and liquid fluxes were also measured in order to determine the online leaf water potential (Ψ_l) and its relationship with stomatal conductance (g_s). We found that different K_L and C_{dyn} led to distinct balances between liquid and vapour phase significantly impacting stomata responsiveness as seen by the differences in stomata closure half-times ranging from 48 to 248 seconds. The hydraulic passive model successfully modelled stomata response to VPD in all species studied. Furthermore, considering a changing rather than a fixed K_{leaf} improved model predictions suggesting VPD-induced changes in K_{leaf}. In any case, the extents of changes were small and in agreement with recent models predicting a shift from perivascular to peristomatal transpiration in response to increases in VPD. In a second experiment, we studied leaf water enrichment in ^{18}O during transpiration in four species with contrasting K_{leaf} and C_{dyn}. Additional evidence in support for the two pool model in three out of four species was found. Our data also suggest a possible interplay between vein density and associated ground tissues as determinants of the fraction of unenriched water. Moreover, we suggest that a low K_{leaf}, leading to an increased radial resistance for water transport in ferns, can have a role constraining the mixing of enriched and unenriched leaf water. In a third experiment, leaf hydraulic vulnerability was assessed in two field-grown coffee cultivars under a severe drought to test coffee susceptibility to hydraulic dysfunctions. Coffee leaves were characterized as moderately tolerant to hydraulic dysfunctions; however, the large negative Ψ_l

experienced under drought were sufficient to cause hydraulic failure and leaf loss. Upon rainfall, A_n and g_s recovery were constrained at different extents probably as a result of hydraulic loss given that no evidence for biochemical limitations to A_n was found. In any case, after two months of rainfall, full recovery of A_n, but not g_s, was observed in leaves expanded under drought in comparison to leaves expanded in the rainy season. Under wet conditions, stomata aperture seems to be regulated to prevent loss of conductivity of reaching levels higher than c. 30% by means of active mechanisms likely ABA-related. However, a high variability in Ψ_l experienced under drought suggests that differential leaf sensitivity to ABA exists as some leaves cannot reach sufficient stomata closure to avoid damaging Ψ_l to occur. In conclusion, we showed that leaf anatomy, through changes in C_{dyn} and/or water content, has a significant effect on the speed of stomata movements in ferns and conifers leading to closure rates as fast as those seen in angiosperms, in addition to affect leaf water enrichment properties. In coffee, further ABA-sensitivity studies are necessary to better elucidate the contribution of passive and active mechanisms controlling coffee stomata. Most importantly, studies to determine hydraulic vulnerability in stems and roots as well in other coffee varieties will be of extreme importance to a proper assessment of the impact climate change will have for the coffee crop.

GENERAL INTRODUCTION

From all environmental resources, water is likely the most important resource determining plant distribution, growth, yield and survival (Engelbrecht et al., 2007; Zhao and Running, 2010). Plants are constantly threatened by the risk of desiccation through exposure to a drying soil or atmosphere and survival hinges on finding a strategy to optimize water loss and carbon gain (Brodribb et al., 2014). Such an optimization is achieved by assigning the control of leaf gas exchange to tiny leaf pores called stomata. Stomata respond rapidly to changes in evaporative demand (e.g. vapour pressure, temperature) or photosynthetic potential (e.g. light intensity, CO_2 partial pressure) by regulating the size of the pore to maintain an optimum balance between evaporation and photosynthesis (Cowan and Farquhar, 1977). These stomatal movements are ubiquitous among plant species, and profoundly affect diurnal and seasonal courses of water and carbon movement between plants and the atmosphere (Hetherington and Woodward, 2003; Farquhar et al., 1993).

As stomata control the transpiration flux, the xylem tissue dictates the hydration state of the leaves relative to the soil. The interdependence of these tissues is such that their development is tightly coordinated (Brodribb et al., 2014) It has been proposed that the point of stomatal closure during drought stress is determined by the vulnerability of the xylem tissue to cavitation under tension (Brodribb & Holbrook, 2003). Thus, the leaf hydraulic conductance (K_{leaf}), defined as the conductance of the pathway between the leaf vein termini and the evaporation sites furthest from the xylem veinlet (Brodribb et al., 2010), sets a physical limit to water demand that cannot be exceeded without risking hydraulic failure and desiccation. The coupling between stomata conductance (g_s) and the need to maintain a proper leaf water balance has often been evidenced by the strong positive scaling between g_s and K_{leaf} (Brodribb et al., 2010). In turn, the significance of K_{leaf} as a potentially limiting component of the vascular system has been further emphasized by the strong hydraulic-photosynthetic coordination observed across a large sample of diverse species (Brodribb et al., 2007).

Despite the importance of K_{leaf} defining the capacity for water supply, its role controlling stomata movements was undermined by the complexity of active mechanisms involving ion-trafficking present in stomata from seed plants (Hetherington and Woodward, 2003). Only recently, with the discovery of an

ancestral hydropassive stomatal behaviour in ferns and lycophytes (Brodribb and McAdam 2011), it became possible to test how hydraulic traits influence stomata behaviour. If stomata respond uniquely to a balance between hydraulic conductance, capacitance and evaporation, modeling stomata dynamics can be extremely simplified.

Leaf capacitance is an important parameter in leaves that defines the dynamics of how leaves respond to fluctuations in transpiration rates or upstream water potential (Blackman and Brodribb, 2011). A contentious matter concerning capacitance is hydraulic compartmentalization, i.e., that only a portion of the leaf tissue actively exchanges water with the transpiration stream. Probing capacitance under evaporative conditions is technically challenging, but, in theory, instantaneous measurements of liquid and water vapour fluxes can shed light on the matter. According to a hydropassive model, any disturbance in steady-state liquid and vapour phases will be dependent on the ratio between K_{leaf} and capacitance to determine the time response to return to a new steady-state phase. Thus, measurements of liquid and vapour phases in addition to K_{leaf} measurements per se have the potential to probe in vivo capacitance.

Another interesting tool that, in theory, integrates K_{leaf} and capacitance is the use of water stable isotopes. During leaf transpiration, leaves become enriched in ^{18}O due to slower diffusion of $H_2{}^{18}O$ through stomata than $H_2{}^{16}O$ and this isotopic signature can be used to estimate the path length (L), defined as the distance that water vapour has to move from the leaf vein until the evaporative surface. The L estimation revealed of special interest for the understanding of water pathways inside the leaf and how those can be influenced by different routes (apoplastic versus symplastic), leaf anatomy and leaf hydraulics (Ferrio et al., 2012). As ^{18}O enrichment happen at the evaporative sites within a leaf, and unenriched water leaves the leaf veins, the degree of mixing between enriched and unenriched water should be dependent on both K_{leaf} and capacitance.

At a plant level, recent work studying interactions between xylem vulnerability and the dynamics of stomatal closure during drought demonstrates that these two traits in combination can predict how trees succumb to drought stress, either by desiccation or starvation (McDowell et al., 2008). In a recent meta-analysis, Choat et al. (2012) reported that several plant species, mainly tropical seed plants, are expected to be highly vulnerable to hydraulic dysfunctions that should be exacerbated

due to the current and ongoing scenarios of increased frequency and severity of drought episodes (Allen et al., 2010). In this context, coffee, one of the most important commodities in the international agricultural trade, it is also one of most threatened species by global climate change where emission scenarios predict up to 50% in reduction of suitable areas for cultivation (Bunn et al., 2014) or even extinction of native populations in Ethiopia (Davis et al., 2012). A recent report by Nardini et al. (2014) stated that coffee leaves are extremely vulnerable to cavitation; however, empirical observations of field-grown coffee show the species to be able to successfully tolerate certain levels of drought. These conflicting results urge for a proper evaluation of hydraulic vulnerability in field-grown coffee plants not only to assess the ecological importance of cavitation but also to resolve the risk of death by hydraulic failure.

In this study, we carried out two experiments in order to elucidate what is the importance of hydraulic traits controlling stomata movements and leaf water enrichment. A third experiment was done to assess hydraulic vulnerability in coffee and to what extent coffee leaves are susceptible to hydraulic failure. Additionally, we developed a technique to probe leaf capacitance in vivo and measure online changes in leaf water potential. This technique allowed us to test whether changes in leaf turgor are responsible for closing stomata in ferns and conifers upon changes in vapour pressure deficit.

References

Allen CD, Macalady AK, Chenchouni H, et al. 2010. A global overview of drought and heat-induced tree mortality reveals emerging climate change risks for forests. Forest Ecology and Management **259**, 660–684.

Blackman CJ, Brodribb TJ. 2011. Two measures of leaf capacitance: insights into the water transport pathway and hydraulic conductance in leaves. Functional Plant Biology **38**, 118.

Brodribb TJ, Feild TS, Jordan GJ. 2007. Leaf maximum photosynthetic rate and venation are linked by hydraulics. Plant Physiology **144**, 1890–1898.

Brodribb TJ, Feild TS, Sack L. 2010. Viewing leaf structure and evolution from a hydraulic perspective. Functional Plant Biology **37**, 488-498.

Brodribb TJ, Holbrook MN. 2003. Stomatal closure during leaf dehydration, correlation with other leaf physiological traits. Plant Physiology **132**, 2166–2217.

Brodribb TJ, McAdam SAM. 2011. Passive origins of stomatal control in vascular plants. Science **331**, 582–585.

Brodribb TJ, McAdam SAM, Jordan GJ, Martins SCV. 2014. Conifer species adapt to low-rainfall climates by following one of two divergent pathways. Proceedings of the National Academy of Sciences of the United States of America **111**, 14489-14493.

Bunn C, Läderach P, Ovalle Rivera O, Kirschke D. 2014. A bitter cup: climate change profile of global production of Arabica and Robusta coffee. Climatic Change. doi 10.1007/s10584-014-1306-x

Choat B, Jansen S, Brodribb TJ, et al. 2012. Global convergence in the vulnerability of forests to drought. Nature **491**, 752–756.

Cowan LR, Farquhar GD. 1977. Stomatal function in relation to leaf metabolism and environment. In Integration of Activity in the Higher Plant. Ed. D.H. Jenning. Cambridge University Press, 471-505.

Davis AP, Gole TW, Baena S, Moat J. 2012. The impact of climate change on indigenous arabica coffee (Coffea arabica): predicting future trends and identifying priorities. PLoS ONE **7**, e47981.

Engelbrecht BMJ, Comita LS, Condit R, Kursar TA, Tyree MT, Turner BL, Hubbell SP. 2007. Drought sensitivity shapes species distribution patterns in tropical forests. Nature **447,** 80–82.

Farquhar GD, Lloyd J, Taylor JA, Flanagan LB, Syvertsen JP, Hubick KT, Wong SC,
Ehleringer JR. 1993. Vegetation effects on the isotope composition of oxygen in atmospheric CO_2. Nature **365**, 368.

Ferrio JP, Pou A, Florez-Sarasa I, Gessler A, Kodama N, Flexas J, Ribas-Carbó M. 2012. The Péclet effect on leaf water enrichment correlates with leaf hydraulic conductance and mesophyll conductance for CO_2. Plant, Cell & Environment **35**, 611–625.

Hetherington AM, Woodward FI. 2003. The role of stomata in sensing and driving environmental change. Nature **424**, 901–908.

McDowell N, Pockman WT, Allen CD, Breshears DD, Cobb N, Kolb T, Plaut J, Sperry J, West A, Williams DG, et al. 2008. Mechanisms of plant survival and mortality during drought: why do some plants survive while others succumb to drought? New Phytologist **178**, 719–739.

Nardini A, Ounapuu-Pikas E, Savi T. 2014. When smaller is better: leaf hydraulic conductance and drought vulnerability correlate to leaf size and venation density across four Coffea arabica genotypes. Functional Plant Biology **41**, 972-983.

Zhao M, Running SW. 2010. Drought-induced reduction in global terrestrial net primary production from 2000 through 2009. Science **329**, 940-943.

CHAPTER 1

Stomata dynamics are limited by leaf anatomy and hydraulics in ferns and conifers: results from simultaneous measurements of liquid and vapour fluxes in leaves.

Samuel CV Martins, Tim J Brodribb, Scott AM McAdam, Ross M Deans, Fábio M. DaMatta

Introduction

Efficiency in resource use appears as central theme in the evolution and function of the vegetative plant body (McAdam and Brodribb, 2012a). Probably the most dynamic example of this behaviour is the management of water use by stomatal valves on the leaf surface. Stomata respond rapidly to changes in evaporative demand (e.g. vapour pressure, temperature) or photosynthetic potential (e.g. light intensity, CO_2 partial pressure) by regulating the size of the pore to maintain an optimum balance between evaporation and photosynthesis (Cowan and Farquhar, 1977). These stomatal movements are ubiquitous among plant species, and profoundly affect diurnal and seasonal courses of water and carbon movement between plants and the atmosphere (Hetherington and Woodward, 2003; Farquhar et al., 1993). The importance of incorporating stomatal behaviour into global circulation models has been recently recognized (Barman, Jain and Liang., 2014; Cramer et al., 2001), but there remains considerable debate about the mechanisms driving stomatal movements, undermining the predictive capacity of models into the future.

In hydrated plants, stomatal responses to changes in evaporative demand (the vapour pressure difference between leaves and the atmosphere: VPD) result in continuous regulation of daytime gas exchange over the timescale of seconds to minutes (Sellin and Lubenets, 2010). Hydraulic models of water balance in the leaf are able to reasonably predict the sensitivity of stomatal conductance to changes in VPD (Oren et al., 1999), but there has been little research into the dynamic behaviour of stomata between steady states. This is a potentially important knowledge gap because the kinetics of stomatal response to changes in VPD, which can be very rapid, must strongly influence the efficiency of water use by plants. Just as slow stomatal responses to changing light intensity lead to suboptimal diurnal ratios of leaf transpiration (E) over net photosynthesis (A) (Lawson and Blatt, 2014), a species responding slowly to changes in VPD must be less efficient in maintaining an optimal diurnal ratio of E/A than a species with fast moving stomata.

A major limitation to predicting how leaves should respond to VPD is uncertainty about the mechanism driving changes in guard cell turgor (Damour et al., 2010). At one end of the hypothetical spectrum, hydropassive control predicts stomatal aperture to be determined directly by leaf hydration (Brodribb and McAdam, 2011; Buckley 2005), while at the other extreme, guard cells are believed to respond to VPD by autonomously synthesized ABA (Bauer et al., 2013). A number of studies indicate an evolutionary transition between an ancestral hydropassive stomatal behaviour in ferns and lycophytes and a derived ABA-dependent control of guard cells in seed plants (McAdam and Brodribb, 2015, 2014, 2012a, 2012b; Brodribb and McAdam 2011). The kinetics of a stomatal response to VPD predicted if guard cells were uniquely controlled by ABA would depend on a number of unknown factors such as the rate of ABA synthesis, catabolism and signalling (Kim et al., 2010). On the other hand, if stomata responded passively to leaf hydration then response time would depend uniquely on the balance between hydraulic conductance, capacitance and evaporation. A tight association between plant hydraulic characteristics and stomatal behaviour in response to water stress has been seen in ferns, consistent with passive stomatal behaviour, but the response of conifers suggests both ABA and hydropassive influences are important (McAdam and Brodribb, 2014 and 2013).

The first step toward understanding the kinetics of stomatal responses to VPD transitions must be to understand how leaf water potential (ψ_l) changes during perturbations in leaf transpiration. This type of "real-time" measure of ψ_l is typically impossible due to the fact that leaf water potential must be measured destructively in a pressure chamber or under very stable conditions using leaf psychrometer. Here we employ a new technique to calculate ψ_l dynamically based upon the measured balance between liquid and vapour fluxes into and out of the leaf (the dual flow technique). This technique allowed us to examine whether stomatal kinetics in fern and conifer species conformed to the expectations of passive control during step changes in VPD. Additionally, it was also possible to estimate leaf hydraulic conductance (K_L) throughout time in a non-destructive manner, which is of extreme importance considering the role K_L has for carbon gain (Brodribb et al., 2007 and 2005) and the recent reports on its dynamic nature (Prado and Maurel, 2013). Furthermore we employed the dual flow technique to examine the importance of hydraulic parameters in determining the speed of stomatal responses to VPD. If passive control is the dominant mechanism, the speed of the response will be dictated by the balance

between dynamic capacitance (C_{dyn}) and hydraulic conductance whereas the magnitude will be dependent on the relationship between guard cell turgor pressure and leaf water potential.

Material and Methods

Plant material and experimental conditions

Potted individuals of the fern species Adiantum capillus-veneris L., Cheilanthes myriophylla Desv., Hypolepis tenuifolia (G.Forst.) Bernh., Pyrrosia lingua (Thunb.) Farw. and the conifers Metasequoia glyptostroboides and Callitris rhomboidea were used in this study. Plants were grown under controlled glasshouse conditions of 25°C/16°C day/night temperatures and 16 h photoperiod, with natural light supplemented by sodium vapour lamps to ensure a minimum 300 μmol quanta m^{-2} s^{-1} at the pot surface. All plants received weekly applications of liquid fertilizer (Aquasol, Hortico Ltd).

C_{dyn} determined by bulk flow

Leaf capacitance was measured directly for each species by calculating the bulk volume of water absorbed by a partially desiccated leaf or shoot while connected to a flowmeter (Blackman and Brodribb, 2012; Brodribb-prometheus wiki). Here, leaf capacitance was calculated as the volume of water taken up by the leaf during a transition from ψ_o to ψ_f :

$C_{dyn} = \sum F / (\psi_o - \psi_f)$

where $\sum F$ is the sum of the flow of water into the leaf during rehydration adjusted for leaf area (mmol m^{-2}) and temperature following Brodribb and Holbrook (2006); ψ_o is the initial leaf water potential (MPa); ψ_f is the final leaf water potential (MPa). Importantly, initial maximum flow (F) in these rehydration plots was determined by fitting an exponential curve through the first 20 s of the rehydration flow data and extrapolating back to the initial point of leaf excision, taking into account the two-three seconds required to connect the sample to the flowmeter. Over this initial 20 s period a single parameter exponential curve always provided a good fit to data ($r^2 > 0.95$).

Liquid and vapour flux measurements

Leaf gas exchange in three-four even-aged leaves was measured using an infrared gas analyser (LI-6400, LI-COR Biosciences) equipped with a conifer chamber (6400-05, LI-COR Biosciences) and liquid flow was measured with a custom-built flowmeter

(for construction details, see: http://prometheuswiki.publish.csiro. au/tiki index.php?page=Constructing+and+operating+a+ hydraulics+flow+meter). First, leaves were excised under degassed? resin-filtered, deionized water, connected to a flowmeter and then fully enclosed in the chamber. Irradiance was provided by a fiber-optic light source, providing a minimum light intensity of 300 μmol quanta m^{-2} s^{-1} at the leaf surface, which was near the light intensity required for saturating g_s. Conditions in the leaf cuvette were controlled at a constant leaf temperature of 22 °C and with VPD regulated by a portable dew point generator (LI-610, LI-COR Biosciences). Upon enclosure in the cuvette, initial VPD was set at 1.0±0.1 kPa and instantaneous gas exchange and liquid flow were logged every 10s. After g_s reached stability, VPD was increased to 2.2±0.3 kPa and maintained until liquid and vapour fluxes matched each other and/or g_s were stable, afterwards VPD was lowered back to initial conditions until g_s had again reached stability. Final Ψ_w was measured using a Scholander pressure chamber and microscope to precisely measure xylem balance pressure. VPD was increased instantly by totally scrubbing the incoming air through a desiccant column (such treatment was faster than changing VPD using the dew point generator). In the same way, VPD was decreased by totally bypassing the desiccant column returning the VPD control to the dew point generator. Due to differences in equilibration time between reference and sample IRGAS, the first two minutes immediately after the VPD transition were discarded and this gap was filled using linear interpolation. Such procedure was feasible since ferns and conifers do not have hydropassive, wrong-way responses (Brodribb and McAdam, 2013a; Franks and Farquhar, 2007).

Leaf water potential and hydraulic conductance reconstructions

Leaf water potential reconstruction was based on a back-calculation method where final Ψ_w was measured and the immediate previous Ψ_w ($\Psi_{w,i}$) calculated by adding to the final Ψ_w the integrated water deficit (or surplus) between vapour and liquid phase converted into MPa by using C_{dyn} as follows:

$$\Psi_{w,\,i} = \Psi_w + (E_{Licor,\,i} - I_{,\,i}) / C_{dyn}$$

$$\Psi_{w,\,i-1} = \Psi_{w,\,i} + (E_{Licor,\,i-1} - I_{,\,i-1}) / C_{dyn}$$

where I is the instantaneous flow rate into the leaf (mmol s^{-1} m^{-2}) as measured by the flowmeter and normalized by projected leaf area and E_{Licor} is the the instantaneous

flow rate out of the leaf (mmol s^{-1} m^{-2}), unit for C_{dyn} is mmol m^{-2} MPa^{-1}. Similarly as Ψ_w, final K_L values (mmol m^{-2} s^{-1} MPa^{-1}) were measured and reconstructed as:

$K_L = -I / \Psi_w$

$K_{L, i} = -I_{,i} / \Psi_{w, i}$

$K_{L, i-1} = -I_{,i-1} / \Psi_{w, i-1}$

An important step for the reconstructions was the assumption that the water supply rate from the xylem equals the steady-state leaf transpiration rate (as predicted by mass balance); thus, the LiCor-6400 and the flowmeter fluxes were matched just before the first step change in VPD. By doing this, we avoided small mismatches between the flowmeter and the LiCor that could produce an artefactual change in Ψ_w and/or K_L. Another control for the technique was to ensure that the back-calculated Ψ_w at the start of the transition (equivalent to the initial Ψ_w) was similar to the final measured Ψ_w when total recovery of g_s was observed. Based on this criterion, we evaluated the technique precision as being 0.009 ± 0.03 MPa which is equivalent to a maximum error of 10% for a final Ψ_w = 0.3 MPa.

Half-times for stomata closure and structural traits

Half-times for stomata closure were estimated by fitting the time-course of g_s closure (step change from low to high VPD) to the following exponential decay model:

$g_s(t) = g_{s\_high\ VPD} + (g_{s\_low\ VPD} - g_{s\_high\ VPD}) * e^{-K*t}$

where $g_{s\_high\ VPD}$ is the final measured g_s at high VPD and $g_{s\_low\ VPD}$ is the steady state g_s at low VPD, t is the time in seconds. The half-times, expressed in seconds, were calculated as ln(2)/K. The rate constant, K, was fitted by non-linear fitting using the software Graph Pad Prism.

Leaf mass per unit area (LMA) was calculated for each of the current species by dividing the dry weight by projected leaf area. The water content per unit leaf area (mol m^{-2}) was calculated for each species by calculating the difference between wet weight and dry weight, converting it to mol (18 g mol^{-1}) and dividing it by projected leaf area.

.

Dynamic passive hydraulic model for stomatal conductance

To test whether stomata responded to changes in Ψ_w and VPD in a way that was consistent with passive hydraulic control of leaf hydration in the light, we used the dynamic, stepwise model described by Brodribb and McAdam (2011). Primarily, the model predicts g_s in a stepwise fashion based solely on the relationship between g_s

and Ψ_w which was determined for each individual assuming a linear relationship between the two variables and constant K_L. Each relationship comprised three pairs of g_s and Ψ_w values obtained at the end of the transition, at the end of high VPD phase and immediately before the increase in VPD. Final Ψ_w was measured and the other values were estimated as $\Psi_w = E_{Licor}/K_L$.

In the model, Ψ_w was calculated by adding to the initial leaf water potential from the previous iteration of the model ($\Psi_{w,\,i}$) the calculated change in Ψ_w over one second. The change Ψ_w was determined as the theoretical maximum change in Ψ_w (without the effects of stomatal closure or leaf capacitance) that would result from the instantaneous evaporative demand (E) and hydraulic supply (K_L) of the leaf, less the change in Ψ_w as a result of leaf capacitance (C_{dyn}) and the instantaneous evaporative demand and hydraulic supply for a time (t) of one second:

$$-\Psi_w = \frac{E}{K_L} - \left(\left(\frac{E}{K_L} - \Psi_{w,i}\right) \times e^{\frac{tK_L}{C_{dyn}}}\right)$$

It was used as inputs to the model: an initial single E_{Licor} and g_s values and the VPD time-course in addition to the hydraulic parameters and the linear relationship between g_s and Ψ_w. We modelled two scenarios, one with constant K_L and other with the observed K_L estimated with the dual-flow technique. In both scenarios, we also modelled how the g_s time-course would be changed considering ±50% in C_{dyn}.

Results

The conifers and ferns here studied covered a large range in K_L and C_{dyn} ranging from 0.7 to 7.5 mmol m^{-2} s^{-1} MPa^{-1} and 150 to 2100 mmol m^{-2} MPa^{-1}, respectively (Table 1). Across species, C_{dyn} was correlated with water content and LMA ($r=0.8$, $P<0.05$), but neither trait was correlated with K_L ($r=0.5$, $P>0.05$). The half-times for the decrease in g_s upon change in VPD were highly correlated with C_{dyn} ($r=0.96$, $P<0.05$) and less strongly correlated with K_L ($r=0.75$, $P<0.05$) indicating C_{dyn} has a major role determining the speed of the g_s response to VPD than K_L (Fig. 1). Indeed, the variability in K_L and C_{dyn} rendered half-times for stomata closures as fast as 48 seconds (Hypolepis) and as slow as 239 seconds (Callitris).

The range in K_L and C_{dyn} was responsible for distinct patterns in the liquid and vapour fluxes into and out of the leaf as can be seen in Fig. 2. High capacitance species such as Callitris, Metasequoia and Pyrrosia saw increasing water deficits (higher vapour than liquid flow) for up to 14 minutes whereas in low capacitance species (Cheilantes,

Adiantum and Hypolepis) water deficit increased for periods as short as 4 minutes. All species showed a decrease in g_s upon increase in VPD, but diverged in their magnitude: Callitris had the largest decrease (c. 47%) and Cheilanthes the lowest (c. 21%) while the other species averaged a 36% decrease (Fig. 3). No significant hysteresis was observed upon return to the initial VPD with at least 91% recovery of initial gs for all species.

The leaf water potential reconstructions as affected by VPD showed increases and decreases accordingly to exponential decay and rise functions (Fig. 4) and differed within and between species in agreement with the variability in their hydraulic properties. Species with a similar magnitude in the g_s response to VPD but presenting different K_L exhibited contrasting Ψ_w reconstructions; Metasequoia, with a K_L twice as high in comparison with Adiantum, had minor changes (<0.1 MPa) in Ψ_w during the VPD transitions whereas Adiantum was calculated to experience a drop of 0.3MPa in Ψ_w during the transition from 1.1-2.2kPa VPD. Our K_L reconstructions were characterized by constant K_L until the increase in VPD where, afterwards, maximum changes (increases and decreases) in K_L were +14% and -23% (Fig. 5). Upon return to initial VPD conditions, the most recurrent pattern for the conifers was K_L values returning to values slightly lower (c. 10%) in comparison to initials whereas total recovery was mostly observed for the ferns..

We performed a modelling exercise to test to what extent our observed data agreed with the predictions of a passive hydraulic model. First, we showed the impact of changes in C_{dyn} while keeping constant K_L (Fig. 6). Good agreement was found between modelled and observed data with Callitris and Hypolepis averaging a R^2 of 0.81, Pyrrosia, 0.99 and the other species 0.91. Apart from Pyrrosia, the remaining species exhibited a bi-modal relationship where the g_s decrease was underestimated and the increase was overestimated by the hydraulic model. This pattern was remarkably seen in Callitris and Hypolepis because even changes of ±50% in C_{dyn} could not fit the observed data (Fig. 6). Second, we tested whether a changing K_L could improve the hydraulic model predictions. Using the reconstructed K_L by the dual-flow technique as an input to the model, the R^2 were significantly improved for all species (Fig. 7), with exception of Pyrrosia, which had already been optimally explained by the single K_L model (Fig. 6). The new R^2 was 0.88 for Callitris, 0.96 for Adiantum and Hypolepis, and 0.98 for Metasequoia and Cheilanthes.

Discussion

We developed a technique to perform "real-time" measurements of leaf water potential by monitoring the balance between liquid and vapour fluxes into and out of leaves. Such technique also allowed us to probe predicted hydraulic properties of leaves in addition to test whether changes in K_L in response to VPD occurred or not in a diverse sample of structurally different ferns and conifers.

Our dual-flow measurements (Fig. 2) showed visually how different K_L and C_{dyn} led to distinct balances between liquid and vapour phase significantly impacting stomata responsiveness as seen by the differences in stomata closure half-times (Table 1). Most importantly, these half-times were highly correlated with C_{dyn} (Fig. 1) evidencing a major role for this trait across species with enormous variation in stomatal anatomical traits such as stomata density, size or length (Zhang et al, 2014; Franks and Beerling, 2009). This observation contrasts with recent reports suggesting stomatal size as a major determinant of closure speed (Raven 2014) emphasizing the role of stomata size dictating its speediness (Drake et al., 2013). Although this difference strongly supports evidence that stomatal closure in angiosperms is driven by size-dependent metabolism (e.g anion trafficking), but not in ferns and conifers (McAdam and Brodribb, 2015). Altogether, our data shows that the deceptively simple passive hydraulic control present in ferns can be as efficient and fast in closing stomata in comparison to the complex active mechanism operating in angiosperms (Brodribb and McAdam, 2013b). It is important to note that such "efficiency" takes place in response to variables affecting leaf hydration such as changes in VPD. On the other hand, it is recognized the superior efficiency of angiosperm stomata in response to environmental factors related to photosynthetic signalling (e.g. light and CO_2) as ferns are not able to attain high water use efficiency (WUE) under changing light and CO_2 conditions (Brodribb and McAdam, 2013b and 2012).

A pre-requisite for a passive hydraulic control is the direct effect of changes in leaf water content on guard cell turgor and, in turn, stomata aperture. We showed, for the first time, the extent of water deficits developed in situ during stomata closure. The deficits (c. 0.2-0.3 MPa, Fig. 4) were in the range known to cause substantial changes in g_s in three out of four ferns here studied (McAdam and Brodribb, 2013). Recently, the gymnosperm Metasequoia was also shown to behave close passively under favourable water conditions and actively when leaf water potential approached the turgor loss point (McAdam and Brodribb, 2014). Despite the minor changes in Ψ_w (<

0.1 MPa) observed for this species, McAdam and Brodribb (2015) found a 0.2 MPa difference between low and high VPD for a 62% decrease in g_s. Thus, it seems Metasequoia has a steeper relationship between Ψ_w and g_s and further studies are necessary to understand how minor changes in bulk Ψ_w can cause significant decreases in g_s. Nevertheless, Zwieniecki et al. (2007) studied the hydraulic design of Metasequoia among other species and proposed that the species is likely to have a relatively weak hydraulic connection between the vein and the rest of the leaf resulting in a lower water potential of the epidermis than that of the xylem. In any case, our Ψ_w reconstructions were based on C_{dyn} which is believed to more accurately represent the water fraction in tissues that readily exchange water with the transpiration stream (Blackman and Brodribb, 2011) and a strong correlation was observed between the half-times for stomata closure and C_{dyn} (Fig. 1).

Despite the increasing amount of studies reporting that K_L can vary rapidly in response to factors such as leaf hydration, light, temperature or nutrient supply (Prado and Maurel, 2013; Lopez et al., 2013; Baazis et al., 2012; but see Rockewell et al., 2011), we did not find major changes in K_L in response to VPD (c.±20%, Fig. 5) whereas increases in K_L in response to light can be as high as 100% (Scoffoni et al., 2008). Given the high susceptibility of some ferns such as Adiantum to drought damage (McAdam and Brodribb, 2013), increase in K_L would be extremely advantageous in improving the leaf water status under conditions of higher transpiration thus protecting the vascular tissue of reaching water potentials that could lead to hydraulic failure. In contrast, we observed decreases in K_L in Adiantum and Hypolepis under high VPD but there was K_L recovery upon return to low VPD. Given the g_s recovery to initial levels, we discarded cavitation as the cause of reduced K_L since it is highly unlikely that refilling would have occurred in such short time frame (Zwieniecki et al. 2013). Besides cavitation, tracheid deformation (Zhang et al., 2014), leaf shrinkage and changes in living cells outside the xylem such as aquaporin deactivation (Scoffoni et al., 2014) would also be able to cause reversible changes in K_L, but acting mostly on the outside-xylem component (K_{ox}) of K_L. In fact, Adiantum and Hypolepis had the lowest LMA, water content (Table 1) and visually very fragile fronds; producing a combination of traits that would make them very susceptible to leaf shrinkage. It remains to be seen using anatomic studies of fronds exposed to low

and high VPD whether or not structural changes can have a role explaining these K_L changes.

Recent papers by Rockwell et al. (2014) and Buckley (2014) added a new dimension to understand changes in K_L and it is related to where water evaporates within the leaf and how environmental factors and/or leaf anatomy can change the conductance of the gas phase, symplastic and apoplastic pathways. Briefly, most part of evaporation can occur as soon liquid water leaves the bundle sheath (perisvacular) or within the vicinity of the stomatal pore (peristomatal); a higher resistance in the apoplastic pathway (e.g. caused by thin cell walls) would lead to higher perivascular transpiration whereas a low resistance in the apoplast (e.g. as function of thick cell walls) will contribute to a more prominent peristomatal transpiration (Scoffoni 2014). The gas phase conductance will be more or less important depending on the temperature gradients within the leaf and a higher internal vapour transport will render a higher apparent K_L (Rockwell et al., 2014).

The observed increases in K_L upon increase in VPD (Fig. 5) as well as their magnitude (c. 14%) fit well within the context proposed by Rockwell et al. (2014) and Buckley (2014) as follows: according to Rockwell (2014), an increase in transpiration following leaf exposure from humid to dry air (high VPD) would pull the distribution of evaporation towards stomata, in turn, developing temperature gradients within the leaf due to decreased temperature in the epidermal surface as function of an enhanced evaporative heat loss. Such gradients could raise the contribution of the vapour phase conductance, increasing, in last instance, K_L. Indeed, such an explanation is compatible with the positive covariation observed between liquid flow and K_L: as liquid flow decreases because of stomata closure, so does the temperature gradient diminishing the contribution of the gas phase and reducing K_L as clearly observed in Callitris and Cheilanthes (Fig. 5), the two species with the highest transpiratory fluxes.

Despite the observed changes in K_L, we tested to what extent the assumption of a constant K_L, as originally used in the passive hydraulic model (McAdam and Brodribb 2014; Brodribb and McAdam, 2011), would compromise the model predictions. Even when assuming a constant K_L, more than 78% of the variation in g_s was explained by the model which is reasonably good considering its simplicity (Fig. 6). When taking in account the observed changes in K_L, the model explained 88% of the variation in Callitris and nearly all the variation (>96%) was explained for the

other species (Fig. 7). Although it is not practical using a changing K_L from a modelling perspective, the message here is to show how a passive hydraulic model successfully explains stomata behaviour and its usefulness in modelling parameters such as WUE between changes in VPD in ferns and conifers. The drawback is the need to obtain steady state g_s for both low and high VPD in order to parameterize the Ψ_w and g_s relationship, but the fact that the linear approximation gave good results facilitates such task.

Conclusion

We present a novel technique to measure online changes in Ψ_w and K_L allowing us to demonstrate the importance of hydraulic parameters in determining g_s dynamics in response to VPD. Our data shows that leaf anatomy, through changes in dynamic capacitance and/or water content, has a significant effect on the speed of stomata movements in ferns and conifers leading to closure rates as fast as those seen in angiosperms. One important application for the technique will be the opportunity to investigate in more depth whether changes in K_L are a result of the interplay among different pathways for water transport within the leaf as function of leaf anatomy. At last, given the importance of K_L and C_{dyn} in the context of WUE optimization for ferns and conifers, it will be interesting to access the variability of such traits in species thriving in different environments where rapid changes in WUE would be advantageous.

References

Baaziz KB, Lopez D, Rabot A, Combes D, Gousset A, Bouzid S, Cochard H, Sakr S, Venisse JS. 2012. Light-mediated K(leaf) induction and contribution of both the PIP1s and PIP2s aquaporins in five tree species: walnut (Juglans regia) case study. Tree Physiology **32**, 423–434.

Barman R, Jain AK, Liang M. 2014. Climate-driven uncertainties in modeling terrestrial gross primary production: a site level to global-scale analysis. Global Change Biology **20**, 1394–1411.

Bauer H, Ache P, Lautner S, et al. 2013. The stomatal response to reduced relative humidity requires guard cell-autonomous ABA synthesis. Current Biology **23**, 53–57.

Blackman CJ, Brodribb TJ. 2011. Two measures of leaf capacitance: insights into the water transport pathway and hydraulic conductance in leaves. Functional Plant Biology **38**, 118.

Brodribb TJ, Holbrook NM, Zwieniecki MA, Palma B. 2005. Leaf hydraulic capacity in ferns, conifers and angiosperms: impacts on photosynthetic maxima. The New Phytologist **165**, 839–846.

Brodribb TJ, Holbrook NM. 2006. Declining hydraulic efficiency as transpiring leaves desiccate: two types of response. Plant, Cell & Environment **29**, 2205–2215.

Brodribb TJ, Feild TS, Jordan GJ. 2007. Leaf maximum photosynthetic rate and venation are linked by hydraulics. Plant Physiology **144**, 1890–1898.

Brodribb TJ, McAdam SAM. 2011. Passive origins of stomatal control in vascular plants. Science **331**, 582–585.

Brodribb TJ, McAdam SAM. 2013. Abscisic acid mediates a divergence in the drought response of two conifers. Plant Physiology **162**, 1370–1377.

Brodribb TJ, McAdam SAM. 2013. Unique responsiveness of angiosperm stomata to elevated CO2 explained by calcium signalling. PloS One **8**, e82057.

Buckley TN. 2005. The control of stomata by water balance. The New Phytologist **168**, 275–292.

Buckley TN. 2014. The contributions of apoplastic, symplastic and gas phase pathways for water transport outside the bundle sheath in leaves. Plant, Cell & Environment. (in press)

Cramer W, Bondeau A, Woodward FI, et al. 2001. Global response of terrestrial ecosystem structure and function to CO_2 and climate change: results from six dynamic global vegetation models. Global Change Biology **7**, 357–373.

Cowan LR, Farquhar GD. 1977. Stomatal function in relation to leaf metabolism and environment. In Integration of Activity in the Higher Plant. Ed. D.H. Jenning. Cambridge University Press, 471-505.

Damour G, Simonneau T, Cochard H, Urban L. 2010. An overview of models of stomatal conductance at the leaf level. Plant, Cell & Environment **33**, 1419–1438.

Drake PL, Froend RH, Franks PJ. 2013. Smaller, faster stomata: scaling of stomatal size, rate of response, and stomatal conductance. Journal of Experimental Botany **64**, 495–505.

Farquhar GD, Lloyd J, Taylor JA, Flanagan LB, Syvertsen JP, Hubick KT, Wong SC,

Ehleringer JR. 1993. Vegetation effects on the isotope composition of oxygen in atmospheric CO_2. Nature **365**, 368.

Franks PJ, Farquhar GD. 2007. The mechanical diversity of stomata and its significance in gas-exchange control. Plant Physiology **143**, 78–87.

Franks PJ, Beerling DJ. 2009. Maximum leaf conductance driven by CO_2 effects on stomatal size and density over geologic time. Proceedings of the National Academy of Sciences of the United States of America **106**, 10343–10347.

Hetherington AM, Woodward FI. 2003. The role of stomata in sensing and driving environmental change. Nature **424**, 901–908.

Kim TH, Bohmer M, Hu H, Nishimura N, Schroeder JI. 2010. Guard cell signal transduction network: advances in understanding abscisic acid, CO_2, and Ca_{2+} signaling. Annual Review of Plant Biology **61**, 561–591.

Lawson T, Blatt MR. 2014. Stomatal size, speed, and responsiveness impact on photosynthesis and water use efficiency. Plant Physiology **164**, 1556–1570.

Lopez D, Venisse JS, Fumanal B, Chaumont F, Guillot E, Daniels MJ, Cochard H, Julien JL, Gousset-Dupont A. 2013. Aquaporins and leaf hydraulics: poplar sheds new light. Plant & Cell Physiology **54**, 1963–1975.

McAdam SAM, Brodribb TJ. 2012a. Stomatal innovation and the rise of seed plants. Ecology Letters **15**, 1–8.

McAdam SAM, Brodribb TJ. 2012b. Fern and lycophyte guard cells do not respond to endogenous abscisic acid. The Plant Cell **24**, 1510–1521.

McAdam SAM, Brodribb TJ. 2013. Ancestral stomatal control results in a canalization of fern and lycophyte adaptation to drought. The New Phytologist **2**, 429–441.

McAdam SAM, Brodribb TJ. 2014. Separating active and passive influences on stomatal control of transpiration. Plant Physiology **164**, 1578–1586.

McAdam SAM, Brodribb TJ. 2015. The evolution of mechanisms driving the stomatal response to vapour pressure deficit. Plant physiology. (in press)

Oren R, Sperry JS, Katul GG, Pataki DE, Ewers FW, Phillips N, Schäfer KVR. 1999. Survey and synthesis of intra- and interspecific variation in stomatal sensitivity to vapour pressure deficit. Plant, Cell & Environment **22,** 1515–1526.

Prado K, Maurel C. 2013. Regulation of leaf hydraulics: from molecular to whole plant levels. Frontiers in Plant Science **4**, 255.

Raven JA. 2014. Speedy small stomata? Journal of Experimental Botany **65**, 1415–1424.

Rockwell FE, Holbrook NM, Zwieniecki MA. 2011. Hydraulic conductivity of red oak (Quercus rubra L.) leaf tissue does not respond to light. Plant, Cell & Environment **34**, 565–579.

Rockwell FE, Holbrook NM, Stroock AD. 2014. The competition between liquid and vapor transport in transpiring leaves. Plant Physiology **164**, 1741–1758.

Scoffoni C, Pou A, Aasamaa K, Sack L. 2008. The rapid light response of leaf hydraulic conductance: new evidence from two experimental methods. Plant, Cell & Environment **31**, 1803–1812.

Scoffoni C, Vuong C, Diep S, Cochard H, Sack L. 2014. Leaf shrinkage with dehydration: coordination with hydraulic vulnerability and drought tolerance. Plant Physiology **164**, 1772–1788.

Scoffoni C. 2014. Modelling the outside-xylem hydraulic conductance: towards a new understanding of leaf water relations. Plant, Cell & Environment. (in press)

Sellin A, Lubenets K. 2010. Variation of transpiration within a canopy of silver birch: effect of canopy position and daily versus nightly water loss. Ecohydrology **3**, 467 – 477.

Zhang S-B, Sun M, Cao K-F, Hu H, Zhang J-L. 2014. Leaf photosynthetic rate of tropical ferns is evolutionarily linked to water transport capacity. PloS One **9**, e84682.

Zhang Y, Rockwell FE, Wheeler JK, Holbrook NM. 2014. Reversible deformation of transfusion tracheids in Taxus baccata is associated with a reversible decrease in leaf hydraulic conductance. Plant Physiology **165**, 1557–1565.

Zwieniecki MA, Brodribb TJ, Holbrook NM. 2007. Hydraulic design of leaves: insights from rehydration kinetics. Plant, Cell & Environment **30**, 910–921.

Zwieniecki MA, Melcher PJ, Ahrens ET. 2013. Analysis of spatial and temporal dynamics of xylem refilling in Acer rubrum L. using magnetic resonance imaging. Frontiers in Plant Science **4**, 265.

Table 1 – Hydraulic and anatomic traits for the six sampled species. Leaf hydraulic conductance, K_L (mmol m^{-2} s^{-1} MPa^{-1}); Dynamic capacitance, C_{dyn} (mmol m^{-2} MPa^{-1}); Half-times for stomata closure, $t_{1/2\_gs}$ (seconds); Water content, W (mol m^{-2}) and leaf mass per unit leaf area, LMA (g m^{-2}). Values are averages ± standard deviation.

	K_L	C_{dyn}	$t_{1/2\_gs}$	W	LMA

Callitris	7.5±0.29	2100±62	239±24	31.8±6.2	202±44
Metasequoia	4.1±0.45	1022±252	125±27	13.1±1.6	47±11
Pyrossia	0.7±0.31	531±26	136±15	26.2±2.5	142±13
Cheilanthes	2.5±0.39	347±121	73±7	8.0±1.2	49±8
Adiantum	2.1±0.25	203±92	55±12	5.6±0.5	25±2
Hypolepis	2.7±0.14	150±50	48±3	6.0±0.9	38±8

Figure legends

Figure 1. Plots showing the significant relationships between the half-times for stomata closure upon increase in VPD from 1.0±0.1 to 2.2±0.3 kPa and the dynamic capacitance (C_{dyn}, mmol m^{-2} MPa^{-1}) or water content (W, mol m^{-2}). Species with a higher C_{dyn} or W tended to have longer half-times. Plotted values are averages ± standard deviation.

Figure 2. Dynamic changes in the fluxes of liquid and vapour phase water into and out of leaves. A representative individual of each species is shown. Increases or decreases in fluxes denote when vapour pressure deficit (VPD) was increased or decreased in a step change from 1.0±0.1 to 2.2±0.3 kPa and vice-versa. The period when the vapour flux (red line) was higher than the liquid flux (blue line) corresponded to water deficit (leaf drying) and the opposite, liquid higher than vapour, water surplus meaning the leaf was rehydrating. Species with higher capacitance tended to have an extended period of deficit/surplus. Note the difference in the fluxes scales to take in account the different magnitudes among species.

Figure 3. Leaf water potential reconstructions based on water deficit calculations from liquid and vapour fluxes and capacitance. Three individual reconstructions are shown for each species. The drop and rise in Ψ_w correspond to the water deficits or surpluses developed by increase or decrease in VPD. The species were connected to a flowmeter supplying pure water, thus source water potential was c. 0 MPa. Note that Pyrrosia has a different scale in comparison to the other species due to a lower leaf hydraulic conductance.

Figure 4. Trajectories of stomatal conductance (g_s) as leaves were exposed to a reversible sequence of VPD transitions from 1.0±0.1 to 2.2±0.3 kPa and returning to initial VPD. Three individual trajectories are shown for each species. Note the scale for Callitris was different from the other species due to a higher g_s.

Figure 5. Leaf hydraulic conductance reconstructions (K_L) based on the dual-flow technique. Three individual reconstructions are shown for each species. The increases

in K_L were coupled to the increase in VPD for Callitris,Metasequoia and Cheilanthes and decreases in K_L marked the transitions for Adiantum and Hypolepis, the change in K_L behaviour was due to the return to low VPD. Note the difference in scales for Callitris and Pyrrosia and the K_L insensitivity to VPD in Pyrrosia.

Figure 6. Examples of fitting the passive closure model to the observed stomatal dynamics. A single individual of each species is shown to facilitate comparison between observed and modelled data; the colour code for the individual follows the previous figures but the amount of observations was reduced for sake of clarity. In each case, dynamic behaviour of g_s mirrored the behaviour of a passive hydraulic model (dark grey lines) using a constant K_L as input. A ±50% variation around the mean measured dynamic capacitance (C_{dyn}) is depicted as light grey lines. Note the differences in both scales in order to improve comparison between observed and modelled data.

Figure 7. Dynamic stomata behaviour when operating as passive-hydraulic valves in response to perturbations in VPD. Same details as figure 6 but the dynamic behaviour of g_s was modelled with the passive hydraulic model using the estimated dual-flow K_L shown in figure 5 as input. Note the increase in R^2 in comparison with the previous figure with the modelling assuming constant K_L.

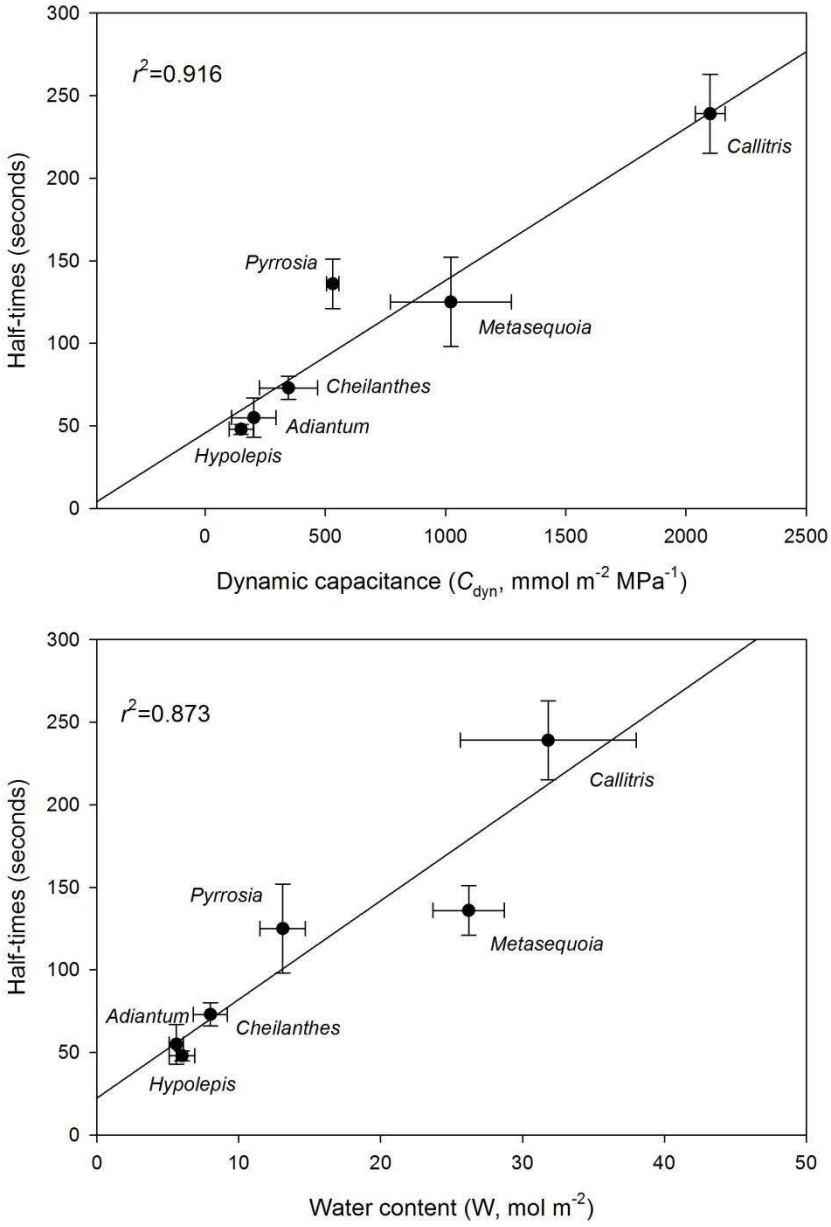
r^2=0.916
Callitris
Pyrrosia
Metasequoia
Cheilanthes
Adiantum
Hypolepis
Half-times (seconds)
Dynamic capacitance (C_{dyn}, mmol m^{-2} MPa^{-1})
r^2=0.873
Callitris
Pyrrosia
Metasequoia
Adiantum
Cheilanthes
Hypolepis
Half-times (seconds)
Water content (W, mol m^{-2})

Figure 1.

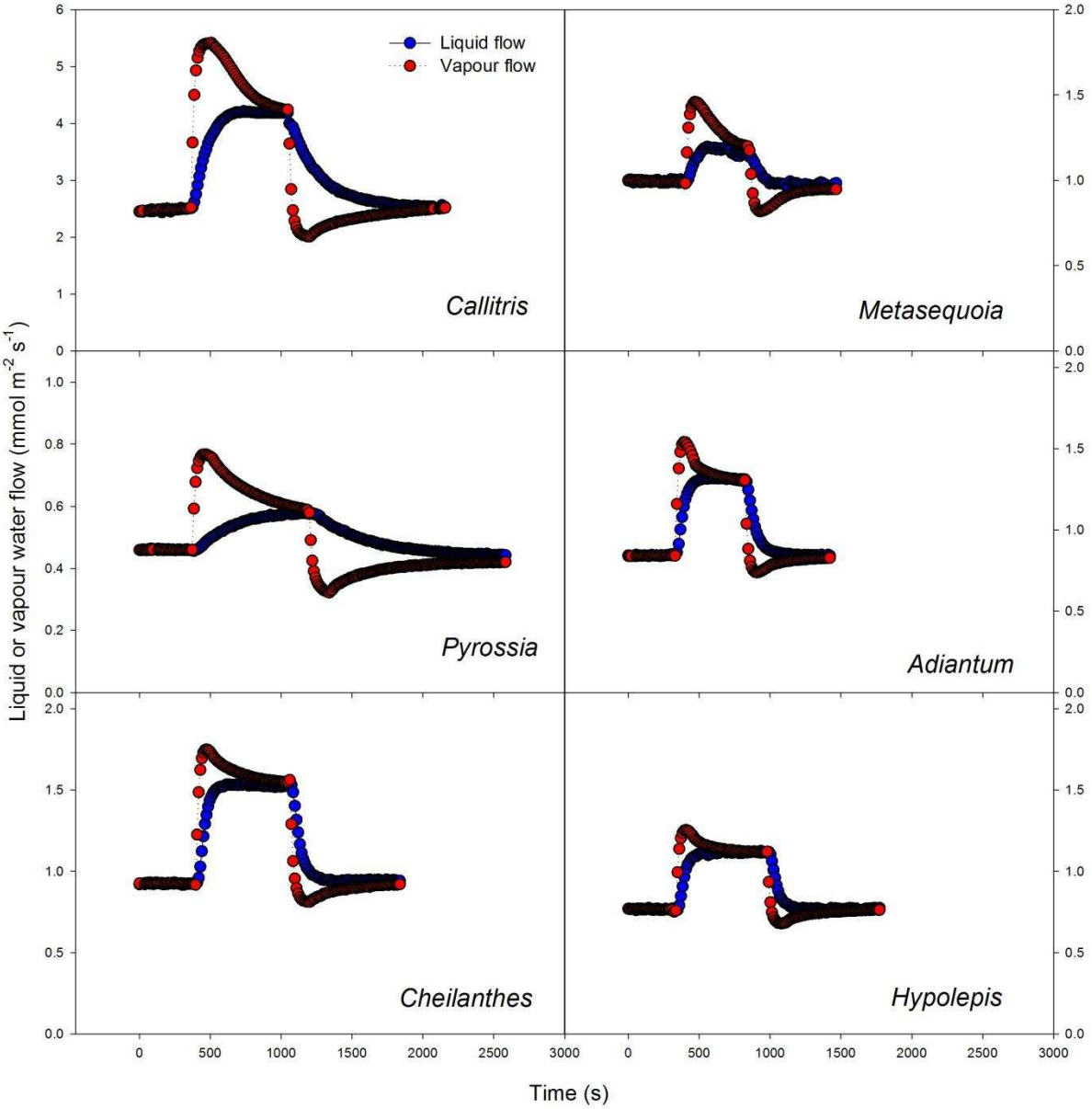
Liquid flow
Vapour flow
Callitris
Metasequoia
Pyrossia
Adiantum
Cheilanthes
Hypolepis
Liquid or vapour water flow (mmol m-2 s-1)
Time (s)

Figure 2.

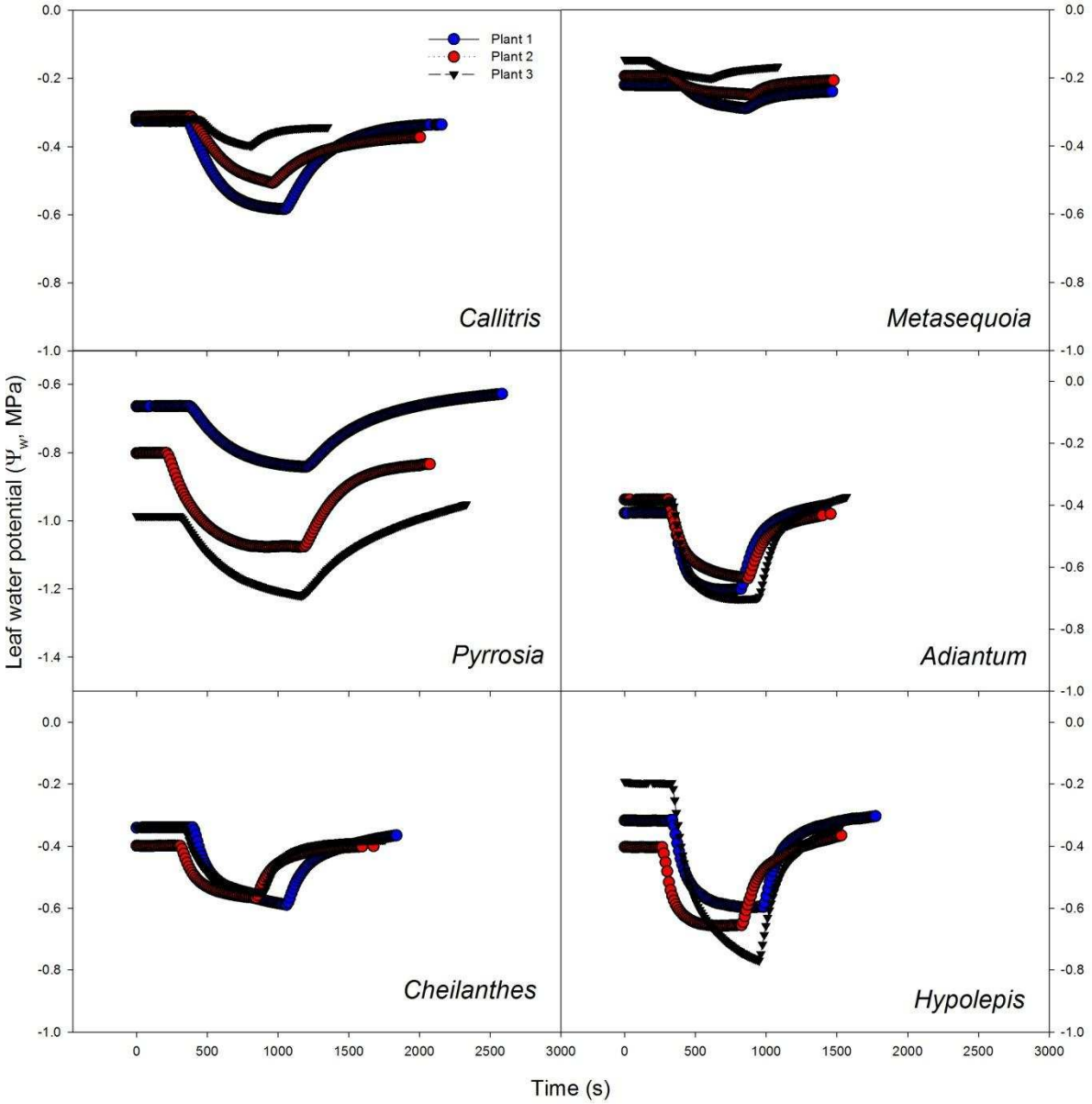
Plant 1
Plant 2
Plant 3
Callitris
Metasequoia
Pyrrosia
Adiantum
Cheilanthes
Hypolepis
Leaf water potential (Ψw, MPa)
Time (s)

Figure 3.

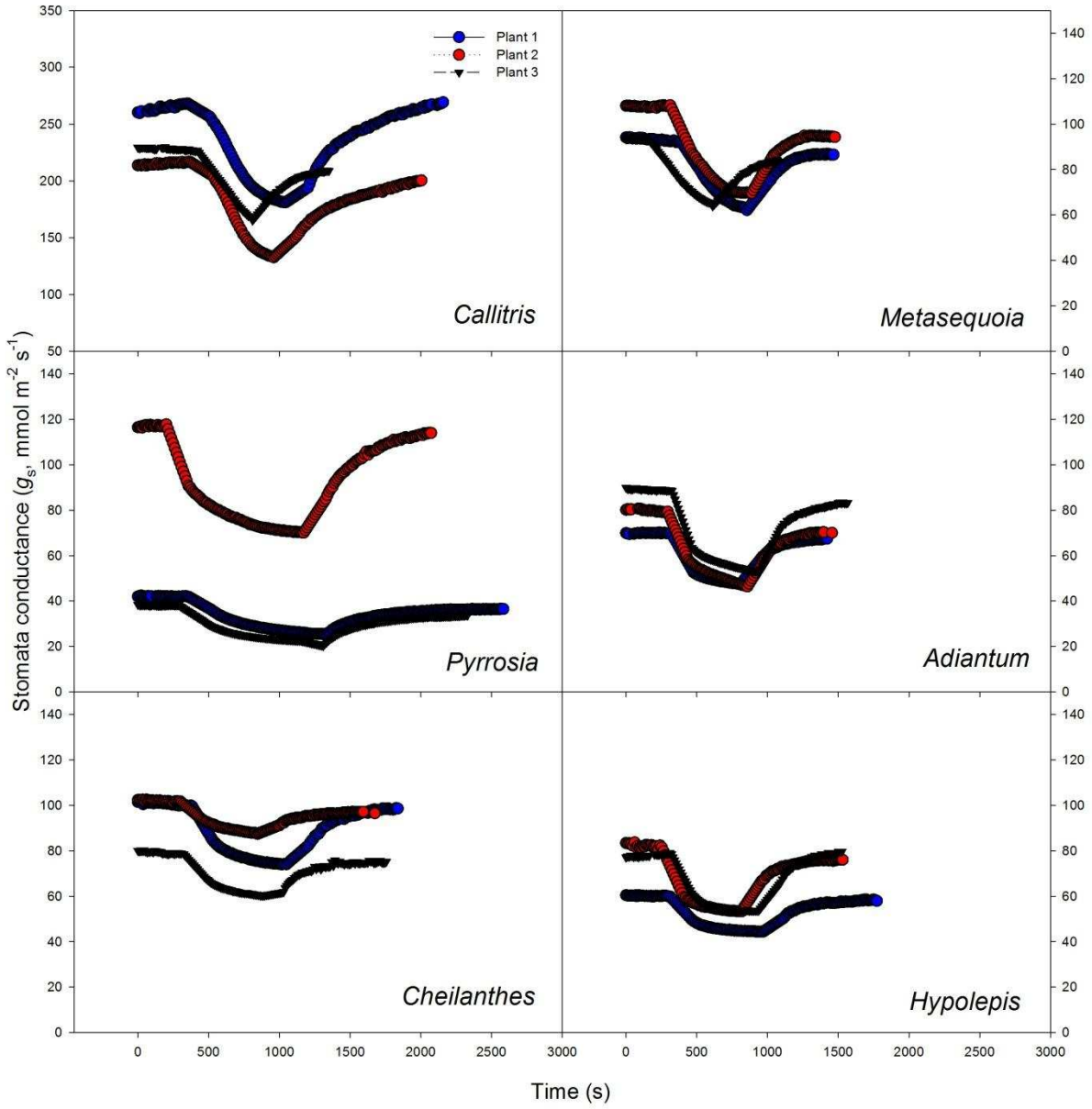
Plant 1
Plant 2
Plant 3
Callitris
Metasequoia
Pyrrosia
Adiantum
Cheilanthes
Hypolepis
Stomata conductance (g_s, mmol m^{-2} s^{-1})
Time (s)

Figure 4.

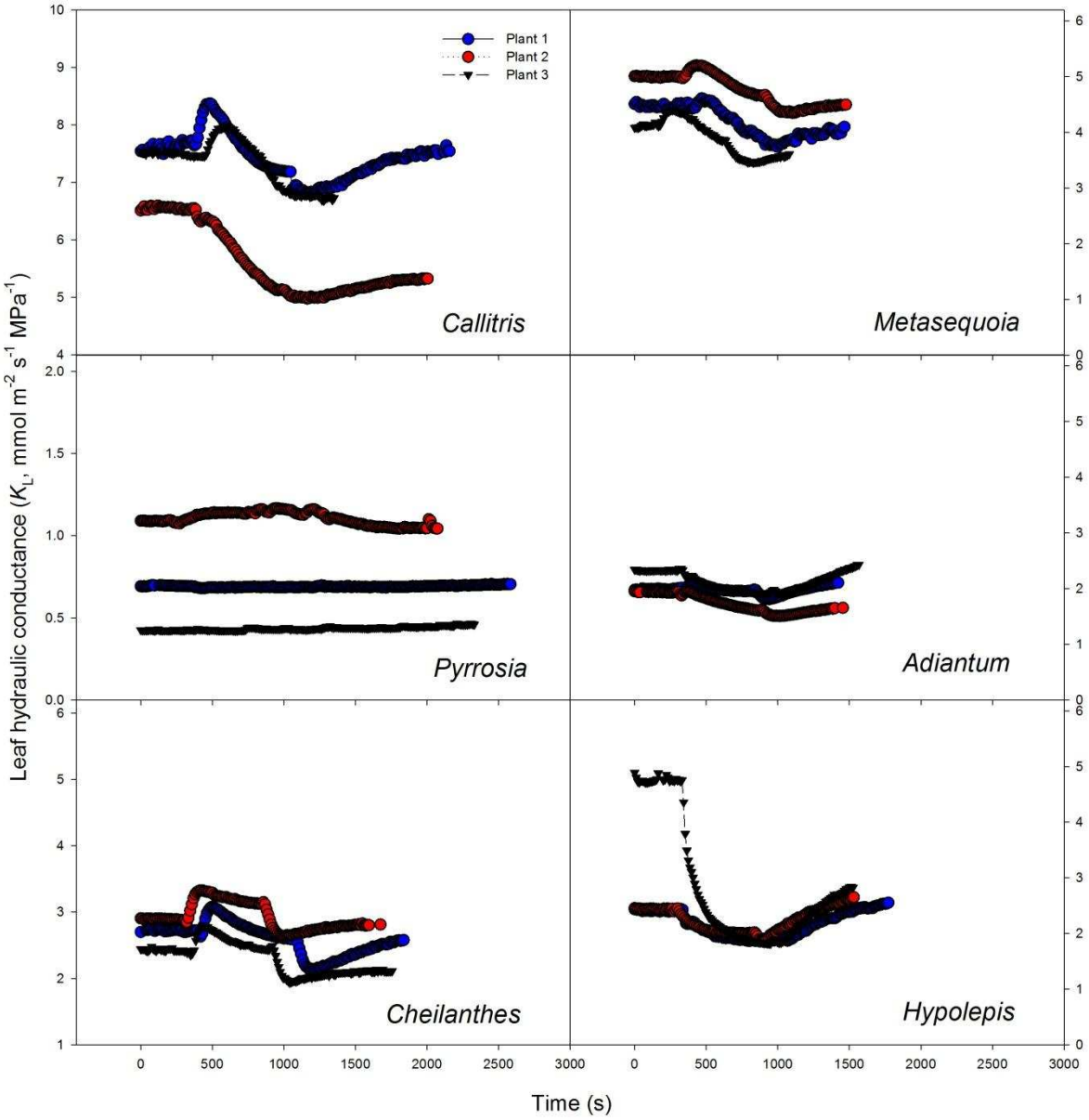
Plant 1
Plant 2
Plant 3
Callitris
Metasequoia
Pyrrosia
Adiantum
Cheilanthes
Hypolepis
Leaf hydraulic conductance (K_L, mmol m^{-2} s^{-1} MPa^{-1})
Time (s)

Figure 5.

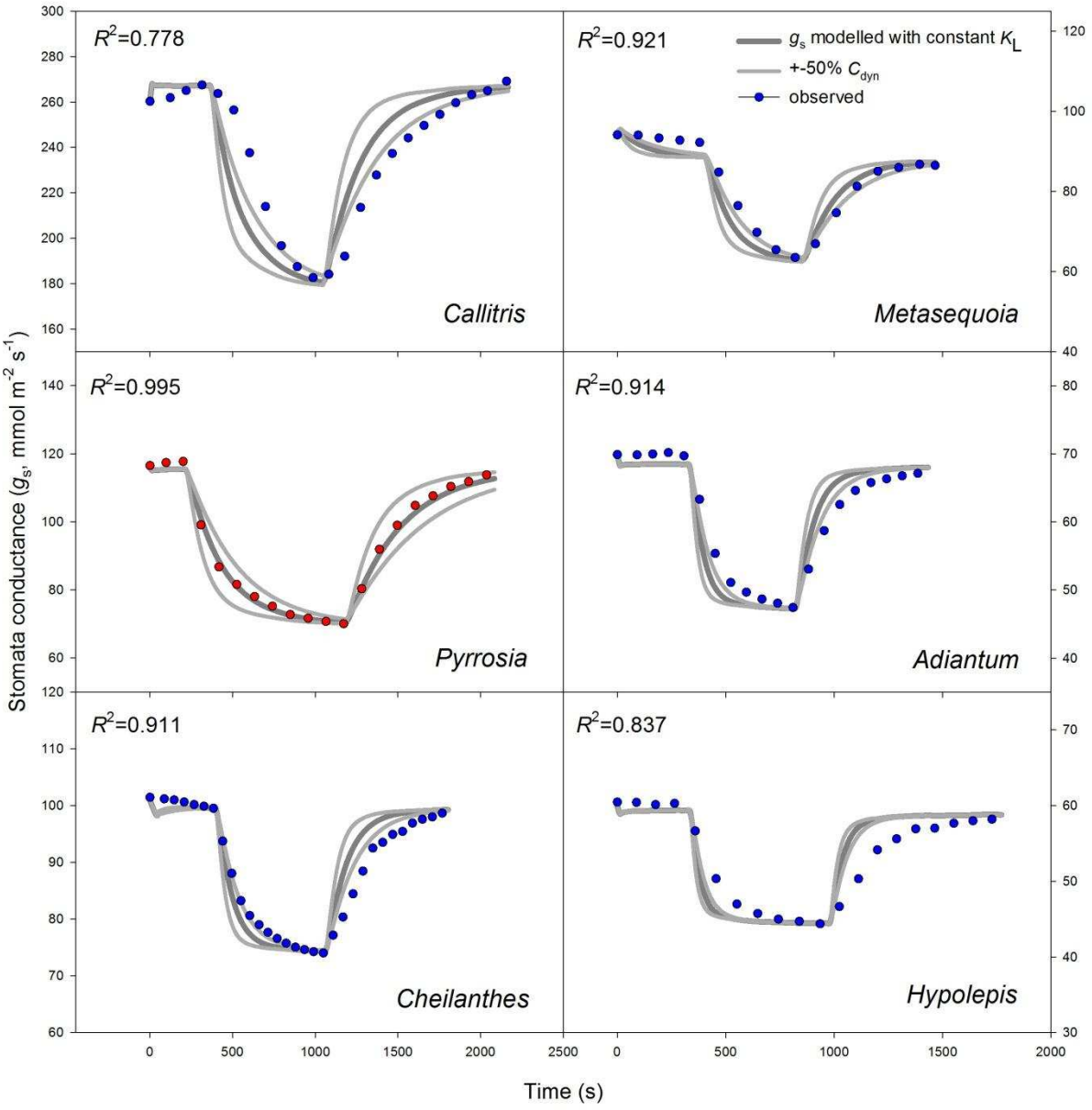
R^2=0.778
R^2=0.921
g_s modelled with constant K_L
+-50% C_{dyn}
observed
Callitris
Metasequoia
R^2=0.995
R^2=0.914
Pyrrosia
Adiantum
R^2=0.911
R^2=0.837
Cheilanthes
Hypolepis
Stomata conductance (g_s, mmol m^{-2} s^{-1})
Time (s)

Figure 6.

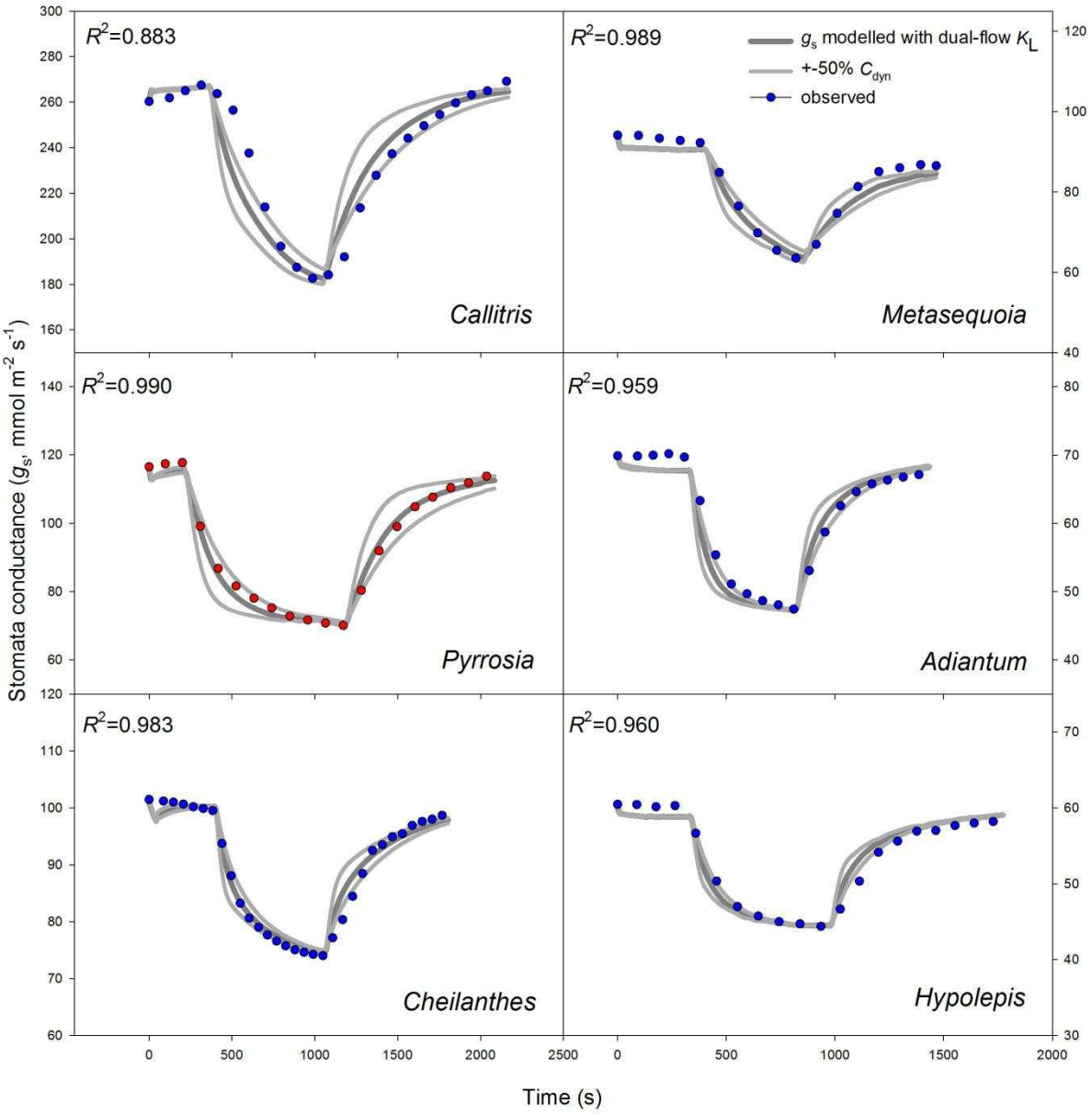
R^2=0.883
Callitris
R^2=0.989
g_s modelled with dual-flow K_L
+-50% C_{dyn}
observed
Metasequoia
R^2=0.990
Pyrrosia
R^2=0.959
Adiantum
R^2=0.983
Cheilanthes
R^2=0.960
Hypolepis
Stomata conductance (g_s, mmol m^{-2} s^{-1})
Time (s)

Figure 7.

CHAPTER 2

Influence of leaf hydraulic parameters defining heavy water enrichment in different species

Samuel CV Martins, Xin Song, Kevin A Simonin, Margaret M Barbour, Tim J Brodribb, Fábio M DaMatta

Introduction

Water stable isotopes ($H_2{}^{18}O$, $H_2{}^{17}O$ and ^2H_2O) are one of the most useful and dynamic tools to study plant water relations. Since there is no isotopic fractionation (meaning no isotopic enrichment or depletion) during water uptake and transport, it is feasible to distinguish plant water acquisition from different sources provided they have different isotopic signatures. At the leaf level, as fractionation occurs during transpiration enriching lamina leaf water, such enrichment will contribute to the organic matter isotopic composition reflecting, at the short term, the leaf evaporative conditions. Essential to all these applications is an understanding of how environmental conditions are translated into these isotopic signals (Werner et al., 2012; Barbour 2007).

During leaf transpiration, leaves become enriched in ^{18}O due to slower diffusion of $H_2{}^{18}O$ through stomata than $H_2{}^{16}O$. This isotopic signature has proven useful for the study of several aspects including its combination with ^{13}C to distinguish stomatal and non-stomatal effects on water user efficiency (Farquhar et al., 2007). It also allows measurements of integrated stomatal conductance (Barbour et al., 2000) and the estimation of the path length (L), which can be defined as the distance water vapour has to move from the leaf vein until the evaporative surface. On the other hand, leaf hydraulic conductance (K_{leaf}) is defined as the conductance of the pathway between the leaf vein termini and the evaporation sites furthest from the xylem veinlet (Brodribb et al., 2010). From the above definitions, L and K_{leaf} should integrate two continuums within a leaf: the point where liquid water changes to the vapour phase at the evaporation sites. Thus, the L and K_{leaf} estimations revealed to be of special interest for the understanding of water pathways inside the leaf and how those can be influenced by different routes (apoplastic versus symplastic, Song et al., 2013), leaf anatomy and leaf hydraulics (Ferrio et al., 2012).

The Craig and Gordon (1965) model of evaporation for well-mixed surfaces and further modified to be applied to leaf transpiration (Dongmann et al. 1974; Farris and Strain 1978; Farquhar et al. 1989; Flanagan et al. 1991; Farquhar and Lloyd 1993;

Harwood et al. 1998; Farquhar and Cernusak 2005) provides the mechanistic link to understand water enrichment in leaves. The model estimates enrichment at the evaporative sites within a leaf ($\Delta^{18}O_{es}$) and usually $\Delta^{18}O_{es}$ is higher than the actual measured bulk leaf water enrichment ($\Delta^{18}O_L$) implying an incomplete mixing of bulk lamina water with enriched water at the evaporative sites. Thus, two theories were proposed to reconcile such discrepancy. The first theory, the two-pool model, explains that a lower $\Delta^{18}O_L$ is due to the mixing of one enriched plus one unenriched pool. The unenriched pool is associated to water in the leaf veins because water fractionation does not occur in the xylem. The other pool reflects water near the evaporative surfaces where fractionation takes place thus enriching liquid water at these sites. The second theory concerns the Péclet effect inclusion into the Craig-Gordon model (Farquhar and Lloyd, 1993) where the final $\Delta^{18}O_L$ is a result from two competing processes: back diffusion of enriched water coming from the sites of evaporation as opposed by advection of unenriched water leaving the leaf veins. The main difference between the models is that advection is proportional to leaf transpiration (E); thus, the higher the E, the lower the mixing. As some studies observed that the fraction of unenriched water was usually associated to a higher E (Walker et al. 1989; Flanagan et al. 1991, 1994), the two-pool model was largely ignored since it is insensitive to variations in E.

Despite the wide acceptance of the Péclet effect by the isotope community due to its sound theoretical basis and empirical observations, unequivocal evidence for the phenomenon was not provided in the past years. Only recently the advent of laser-based spectrometry has allowed some technical challenges to be overcome and assumptions to be tested (see details in Song et al., 2015). Therefore, Song et al. (2015) conducted a careful and thorough study using cotton leaves with the aim of testing the core of the Péclet theory: the proportional difference in $\Delta^{18}O_L$ to $\Delta^{18}O_{es}$ (f_{sw}) as associated to E. The authors did not find support for the Péclet effect concluding that the two-pool model is a more straightforward and simpler mechanism to explain leaf water enrichment.

Renewed interest in the field of water stable isotopes, mainly considering the existence of some reports supporting the Péclet effect (Cernusak et al., 2003; Barbour et al. 2004; Gessler et al., 2007) has appeared recently (Song et al., 2015). As mentioned above, there are several studies discussing the importance of the L parameter as a constant required to correct parameterize the Craig-Gordon model on

its steady and non-steady state formulation (Farquar and Cernusak, 2005; Kahmen et al., 2008). Hence, if the Péclet effect turns out to be not valid, a reappraisal of the Craig-Gordon model will be necessary in order to better understand why leaves become enriched and improve predictions of the model.

In addition to the absence of a positive covariance between f_{sw} and E, support for the two-pool model would also come from differences in the fraction of unenriched water as function of leaf anatomy traits affecting the size of the unenriched pool such as vein density and structure. If water pools in a leaf are static, the degree of mixing between enriched and unenriched water is expected to be dependent on both K_{leaf} and dynamic leaf capacitance (C_{dyn}) as well. As K_{leaf} includes the conductances in series of the vein xylem and the mesophyll pathways outside the xylem (Scoffoni et al., 2014), it is expected that an increased radial resistance would restrict the diffusion of heavy $H_2{}^{18}O$ within the leaf. C_{dyn} concerns the amount of leaf tissues that readily exchange water with the transpiration stream (Blackman and Brodribb, 2011). Thus, leaves with a large C_{dyn} should take longer to reach a new isotopic steady-state upon perturbations in leaf transpiration. Despite these apparently important roles for K_{leaf} and C_{dyn} in understanding leaf water enrichment, no study to date have evaluated the influence of both hydraulic parameters at the same time.

Here, we carried out a study using four species strongly differing in their anatomical properties and encompassing different plant functional groups in order to enlighten our knowledge on the mechanisms controlling leaf water enrichment. More specifically, we tested whether the two-pool model or the inclusion of Péclet effect into the Craig-Gordon model better explain our observed results and to what extent hydraulic traits influence leaf water enrichment.

Material and Methods

Plant Material and Experimental Design

Potted individuals of cotton (Gossypium hirsutum L.) and Adiantum (Adiantum capillus-veneris L.) were grown in a humidity- and temperature-controlled growth cabinet, with day/night temperature set at 28/18 °C and relative humidity at 75%. Photosynthetically active radiation (PAR) at the leaf level was approx. 600 μmol m^{-2} s^{-1}. Aprox. 1-m tall Eucalypt (Eucalyptus polyanthemus Sch.) and pine (Pinus pinaster) were grown in a glasshouse at the Centre for Carbon, Water and Food

(Camden, NSW, Australia), with natural light. Plants were well watered daily with tap water.

Gas Exchange, K_{leaf} and Water Vapor Isotope Measurements

Measurements were performed using a Licor-6400xt photosynthesis system (LiCor Inc., NE, USA) equipped with a custom-made leaf cuvette of area 38 cm^2, coupled to a Los Gatos Research (TIWA-45EP, Los Gatos Inc., Mount View, CA, USA) water vapor isotope analyzer. At the beginning of each measurement, a first or second true leaf (cotton), completely expanded leaf (Eucalypt), frond (Adiantum) or a standard length of needles (Pine) were fully placed into the cuvette and sealed around the petiole with Terostat. Average leaf temperature was measured at two points on the leaf using two thermocouples wired in parallel and gas exchange monitored at one minute intervals. The air stream entering the cuvette was completely dried, so that water vapor of the air exiting the cuvette was entirely derived from leaf transpiration. The exiting air stream was sent via tubing to the laser spectrometer, programmed to measure $\delta^{18}O_v$ at 5-second intervals. The leaf remained with its petiole or stipe under pure water throughout the experiment and was kept the leaf in cuvette for sufficiently long time till $\delta^{18}O_{trans}$ was stable and close to $\delta^{18}O_{sw}$ (judged in practice by $\delta^{18}O_{trans}$ approaching -4‰, the known source water $\delta^{18}O$). Upon completion of the measurement, the leaf was detached and leaf water potential was measured with a Scholander-type pressure chamber (model 1000, PMS Instruments, Albany, NY, USA) and K_{leaf} was then calculated using the following equation:

$$K_{leaf} = -E / \Psi_l$$

where E is the transpirational flux and Ψ_l is the leaf water potential at steady state conditions. After leaf water potential measurements, the leaf was photographed for later determination of the one-sided leaf area using ImageJ (ImageJ 1.45s, http://imagej.nih.gov/ij). The petiole/stipe and leaf/needle samples were separately sealed into two glass vials immediately after photographing. All samples were stored at -20°C until water extraction via vacuum distillation.

In total, 12, 12, 5 and 20 gas-exchange measurements were performed in cotton, eucalypt, pinus and Adiantum, respectively. The different number of measurements was due to the need to obtain a variation in leaf transpiration in order

to test for the Péclet effect. The extended number in Adiantum is due to a second set of measurements performed in order to calculate time constants of water enrichment.

C_{dyn} determined by bulk flow

Leaf capacitance was measured directly for each species by calculating the bulk volume of water absorbed by a partially desiccated leaf or shoot while connected to a flowmeter (Blackman and Brodribb, 2012; Brodribb-prometheus wiki). Here, leaf capacitance was calculated as the volume of water taken up by the leaf during a transition from ψ_o to ψ_f :

$C_{dyn} = \sum F / (\psi_o - \psi_f)$

where $\sum F$ is the sum of the flow of water into the leaf during rehydration adjusted for leaf area (mmol m^{-2}) and temperature following Brodribb and Holbrook (2006); ψ_o is the initial leaf water potential (MPa); ψ_f is the final leaf water potential (MPa). Importantly, initial maximum flow (F) in these rehydration plots was determined by fitting an exponential curve through the first 20 s of the rehydration flow data and extrapolating back to the initial point of leaf excision, taking into account the two-three seconds required to connect the sample to the flowmeter. Over this initial 20 s period a single parameter exponential curve always provided a good fit to data ($r^2 > 0.95$).

Isotope Calibration and Analysis

Calibration of the $\delta^{18}O$ measurements from the laser spectrometry was performed at the end of each day of measurements, as detailed in Simonin et al. (2013). Petiole and leaf water were separately extracted using cryogenic vacuum distillation method of West et al. (2006). Water isotope analysis was performed by first equilibrating water in sealed 27 mL vials with 2% CO_2 and then analyzing $\delta^{18}O$ of the equilibrated CO_2 using a Los Gatos Research (CCIA-36D, Los Gatos Inc., Mount View, CA, USA) carbon isotope analyzer. For the detailed description of the protocol refer to Loucos et al. (2014). All molar isotope ratios were expressed as enrichment above source water (subscript source water or sw) on a per mil basis by $\Delta = [(R_{sample} / R_{source\_water}$ or $R_{transpired\_water})] * 1000‰$, where $R = {}^{18}O/{}^{16}O$.

Leaf water models

Two pool model

According to the two-pool model, with isotope ratio expressed as enrichment above source water (subscript sw), $\Delta^{18}O_{L\_sw}$ can be expressed as:

$$\Delta^{18}O_{L\_sw} = (1- \varphi)\Delta^{18}O_{es\_sw} \quad (1)$$

where $\Delta^{18}O_{L\_sw}$ and $\Delta^{18}O_{es\_sw}$ refer to isotope enrichment of leaf and evaporative site (subscript es) water above source water respectively. Eqn. 1 expresses the extent of deviation of $\Delta^{18}O_{L\_sw}$ from $\Delta^{18}O_{es\_sw}$ as the function of φ, which should in principle vary with leaf anatomy.

Péclet effect

Leaf laminar water isotope enrichment ($\Delta^{18}O_{L\_sw}$) is conventionally modelled from the isotopic enrichment at the evaporative site ($\Delta^{18}O_{es\_sw}$) and the Péclet effect, as the following (Farquhar and Lloyd 1993):

$$\Delta^{18}O_{L\_sw} = \Delta^{18}O_{e\_sw} \frac{1-e^{-\wp}}{\wp} \quad (2)$$

Here, $\wp$ denotes the dimensionless Péclet number, which is the ratio of advection of unenriched vein water via transpiration stream to back diffusion of the enriched water from the evaporative site, or

$$\wp = \frac{LE}{CD} \quad (3)$$

Where E is leaf transpiration rate (mol m^{-2}) and L denotes the scaled effective pathlength (m) for water movement within the leaf lamina, C is the density of water ($55.56\ 10^3$ mol m^{-3}) and D is the diffusivity of $H_2{}^{18}O$ in water (Cuntz et al., 2007).

We denote the term f_{sw} to describe the proportional difference of $\Delta^{18}O_{L\_sw}$ from $\Delta^{18}O_{es\_sw}$, or

$f_{sw} = 1- (\Delta^{18}O_{L\_sw} / \Delta^{18}O_{es\_sw})$ (4)

Note f_{sw} and φ (from the two pool model) have the same mathematical meaning, however, f_{sw} should increase with an increase in $\wp$ if the lamina radial Péclet effect concept is valid. By extension, and under the implicit assumption of the Péclet model that L is a species-specific constant, one can also expect that f_{sw} should increase with increasing E for a given species.

Craig-Gordon model

The Craig-Cordon model in its general form can be adapted to determine $\delta^{18}O_{es}$ under both steady-state and non steady-state conditions, as the following (Harwood et al. 1998; Gillon and Yakir 2000):

$$\delta^{18}O_{es} = \delta^{18}O_{trans} + \varepsilon^{+} + \varepsilon_k + ({}^{w_a}/_{w_i} * (\delta^{18}O_v - \varepsilon_k - \delta^{18}O_{trans})) \quad (5)$$

Where w_a/w_i and subscript v refer to the ambient to intercellular molar fraction of water vapor, and water vapor respectively. ε^{+} is temperature-dependent equilibrium fractionation factor (Bottinga and Craig 1969) and ε_κ is kinetic fractionation factor co-determined by stomatal (r_s) and boundary layer (r_b) resistances as $\varepsilon_\kappa = (28r_s+18.7r_b)/(r_s+r_b)$ (Merlivat, 1978; Barkan and Luz, 2007; Luz et al., 2009).

Because $\delta^{18}O_v$ is the same as $\delta^{18}O_{trans}$ under our experimental setting (detailed above), Eqn. 5 can be be re-written and converted to the conventional source water based $\Delta^{18}O$ notation:

$$\Delta^{18}O_{es\_sw} = \Delta^{18}O_{trans\_sw} + \varepsilon^{+} + \left(1 - {}^{w_a}/_{w_i}\right)\varepsilon_k \quad (6)$$

In summary, the above equation predicts $\Delta^{18}O_{es\_sw}$ as function of the isotopic composition of transpired water ($\Delta^{18o}{}_{trans\_sw}$), leaf temperature ($\varepsilon^{+}$ component), relative humidity (w_a/w_i component) and stomatal and boundary later resistances (ε_κ).

Leaf water isotopic turnover

In a different set of Adiantum, we calculated the time constants for leaf water isotopic turnover following Farquhar and Cernusak (2005), but considering two combinations. Only Adiantum plants were used for this analysis because they rapidly reach constant g_s and w_a/w_i, thus allowing leaf enrichment to be function only of internal mixing of enriched and unenriched water.

The first combination considers the leaf as having a single pool of water totally contributing to isotope enrichment (thus considering $\Delta^{18}O_{es\_sw} = \Delta^{18}O_{L\_sw}$) as follows:

$\tau = (W\alpha^{+}\alpha_k) / gw_i$ (7)

where $\alpha^{+} = 1 + \varepsilon^{+}$, $\alpha_k = 1 + \varepsilon_k$, τ is leaf water residence time (s); W is leaf water content (mol m^{-2}); g is total leaf conductance (stomata plus boundary layer conductance; mol

m^{-2} s^{-1}); and w_i is the mole fraction of water vapour inside the leaf (mol mol^{-1}). W was estimated based on measurements of five leaves per species, and the average value for each species was used in the calculations. Leaf mass per unit area (LMA) was calculated for each of the current species by dividing the dry weight by projected leaf area.

The second combination considers the leaf as having two pools of water: the unenriched pool, which is not prone to fractionation and the second pool which is prone to evaporation (and fractionation) as follows:

$\tau_\varphi = (W\alpha^+ \alpha_k)(1-f_{sw}) / gw_i$ (8)

Where f_{sw} is the fraction of unenriched water calculated according to equation 4.

Residence times were measured using the following equation:

$\Delta^{18}O_{es\_sw}$ (t)= $\Delta^{18}O_{es\_sw\_final}$ + ($\Delta^{18}O_{es\_sw\_initial}$ - $\Delta^{18}O_{es\_sw\_final}$) $*e^{-t/\tau}$

where $\Delta^{18}O_{es\_sw\_final}$ is the final measured $\Delta^{18}O_{es\_sw}$ at the end of the transition and $\Delta^{18}O_{es\_sw\_initial}$ is the first measured $\Delta^{18}O_{es\_sw}$, t is the time in seconds. The time constant, τ, was fitted by non-linear fitting using the Solver feature in software Excel.

Statistical analyses

Data are expressed as the means ± standard error. Student's t-tests were used to compare the parameters between treatments. All statistical analyses were carried out using Microsoft Excel.

Results

The species here studied covered a large range in K_L and C_{dyn} ranging from 0.9 to 8.8 mmol m^{-2} s^{-1} MPa^{-1} and 203 to 1237 mmol m^{-2} MPa^{-1}, respectively (Table 1). Across species, C_{dyn} was correlated with water content (W) ($r=0.76$, $P<0.05$). The lowest K_L, C_{dyn}, leaf mass per unit area (LMA) and W were observed in Adiantum whereas the highest C_{dyn} and W were observed in cotton. Eucalypt and pine presented similar K_L but contrasting C_{dyn}.

We observed a large variation in $\Delta^{18}O_{es\_sw}$ and $\Delta^{18}O_{L\_sw}$ values, ranging from 15.5 to 27.6‰ and 19.8 to 36.1‰, respectively. As it would be expected, all $\Delta^{18}O_{es\_sw}$ values were higher than their $\Delta^{18}O_{L\_sw}$ counterparts and both parameters correlated ($r^2=0.73$, Fig.1). Overall, Adiantum occupied the upper end of the relationship, being more enriched in ^{18}O than the other species in agreement with a lower g_s and w_a/w_i ratio (Fig. 2 and 3). There was a considerable overlap in g_s for the

other species, however, in average, the pine and eucalypt presented the higher (176 mmol m^{-2} s^{-1}), cotton, the intermediate (116 mmol m^{-2} s^{-1}) and Adiantum, the lower (47 mmol m^{-2} s^{-1}) g_s values (Fig. 2). Notably, K_{leaf} presented the same ranking as g_s (Table 1), evidencing the coupling between both parameters.

The $\Delta^{18}O_{L\_sw}$ values were negatively correlated with g_s (r^2=0.52, Fig. 2) and the w_a/w_i ratio (r^2=0.75, Fig. 3). Indeed, despite a large variation in g_s (from 22 to 272 mmol m^{-2} s^{-1}), 86% of the variation in $\Delta^{18}O_{es\_sw}$ was explained by changes in w_a/w_i (Fig. 3).

The relationship between E and f_{sw} was tested and only the pine presented a significant linear relationship (Fig. 4). The average f_{sw}, representing the fraction of unenriched water, were 0.25±0.06 (means±s.d.), 0.17±0.05 and 0.20±0.05 for Adiantum, cotton and eucalypt, respectively. No significant difference (P>0.05) were observed for f_{sw} between cotton and eucalypt, although both species were significantly different (P<0.05) from Adiantum.

Regarding the Péclet effect, we found a large range in the L parameter (8 to 172 mm) with cotton, pine and eucalypt being not significantly different from each other (L c. 29 mm) whereas Adiantum was different from all other species (L c. 94 mm, P<0.001). L and K_{leaf} presented a negative relationship (R^2=0.57, Fig. 5) but largely driven by the Adiantum data.

Oxygen isotope enrichment of transpired water above source water ($\Delta^{18}O_{trans\_sw}$) showed a considerable variation during the time-course of the measurements ranging from -17 to 2‰ (Fig. 6). All species started with a depleted $\Delta^{18}O_{trans\_sw}$ and ended with values around zero, indicating the isotopic composition of transpired water relaxed to that of source water, condition known as the isotopic steady-state (ISS). Eucalypt and pine demanded c. 100 min to reach stable g_s and E, whereas cotton and Adiantum demanded c. 50 and 20 min, respectively. Upon the increase in VPD for c. 30 min, it was noticeable the increases in E most likely due to minor changes in g_s leading to a new state of depleted $\Delta^{18}O_{trans\_sw}$ values going towards enrichment. After returning the VPD to initial conditions, cotton and eucalypt presented slightly enriched stable $\Delta^{18}O_{trans\_sw}$ values at c. 150 min after leaf clamping, whereas $\Delta^{18}O_{trans\_sw}$ in cotton and Adiantum continued to increase until reaching $\Delta^{18}O_{trans\_sw}$ close to 0‰ indicating those samples reached the ISS. Noteworthy, the ISS was reached at c. 55 and 180 min after leaf clamping for Adiantum (lowest C_{dyn})

and cotton (highest C_{dyn}), respectively. Adiantum displayed the highest $\Delta^{18}O_{es\_sw}$ enrichments (from c. 22 to 32‰) while the pine had minor increments (c. 3 ‰) in $\Delta^{18}O_{es\_sw}$. Cotton and eucalypt had intermediate increases in comparison with the other species depending on their initial $\Delta^{18}O_{es\_sw}$ values.

Our second set of Adiantum measurements were performed to measure time constants for leaf water isotopic turnover (τ) is shown in Figure 7. There was a large variation in final g_s and $\Delta^{18}O_{es\_sw}$ which contributed to measured τ ranging from 9 to 60 minutes. In contrast, calculated τ considering the leaf as having a single water pool, ranged from 34 to 92 minutes. We observed positive correlations (r ranging from xx to xx) between measured and calculated τ. For Adiantum, measured τ had a better agreement (values closer to the 1:1 line) with calculated τ_φ considering the two pool model. Considering the single pool τ model, where all water in the leaf contributes to the transpiration strem, calculated τ would overestimate measured τ by c. 250%.

Discussion

We observed a general relationship between $\Delta^{18}O_{es\_sw}$ and $\Delta^{18}O_{L\_sw}$ values (Fig. 1) in species as diverse as a fern and a herbaceous angiosperm with large differences in g_s and leaf anatomy as denoted by the differences in C_{dyn}, K_{leaf} and LMA (Table 1 and Fig. 2). Evaluation of the Craig-Gordon model and the factors controlling $\Delta^{18}O_{es\_sw}$ provides support for our findings. First, as seen in Fig. 3, relative humidity (w_a/w_i) is, by far, the major factor controlling variations in $\Delta^{18}O_{es\_sw}$ since 86% of its variation was explained by the w_a/w_i ratio and additional 13% by variation in $\Delta^{18}O_{trans\_sw}$ (data not shown). Thus, intrinsic variation due to leaf temperature and g_s accounted for just 1%. Thus, for isotopic studies aimed on finding genotypic differences in g_s, it is strongly advisable to minimize variations in w_a/w_i and $\Delta^{18}O_{trans\_sw}$ as discussed in Barbour et al. (2000). The same is valid when studying factors controlling $\Delta^{18}O_{L\_sw}$ as 74% of the variation was explained only by changes in w_a/w_i, thus leaving 26% to be explained by other factors. On the other hand, such general relationship between $\Delta^{18}O_{es\_sw}$ and $\Delta^{18}O_{L\_sw}$ demonstrate that isotopic signature in leaf water is a reliable indicator of evaporative conditions. As a result, it may be useful to assess the degree of coupling between stomata and their surrounding atmosphere in closed canopies (Tausend et al., 2000). Such evaluation is challenging

using traditional gas-exchange as forced ventilation is necessary to homogenize the air within the chamber, minimizing the contribution of boundary layer.

Regarding the Péclet effect, from the four species here studied, only the pine behaved as predicted by the theory, i.e., presented a positive covariance between f_{sw} and E. The other species showed a non significant f_{sw} versus E relationship (Fig. 4), and thus do not support the Péclet theory in line with the findings of Song et al (2015). Interestingly, the only species that agreed with the predictions of the Péclet theory was the pine with its needle-shaped leaves. We believe that single-vein needles behave similar to grasses where progressive enrichment occurs along the leaf blade (Helliker and Ehleringer, 2000) and is dependent on E. These species are better described by the Péclet effect (when considering longitudinal and radial effects, Farquhar and Gan (2002)) or the string-of-lakes model of Gat and Bowser (1991), and therefore both models better describes leaf water enrichment for grasses than the conventional Craig-Gordon model.

Contrary to our hypothesis, no clear relationship was observed between f_{sw} and anatomical and hydraulic traits (W, LMA, C_{dyn} and K_{leaf}). We found similar estimates of f_{sw} for cotton and eucalypt (Fig. 4) even though these species presented clear differences in leaf anatomy due to their herbaceous and sclerophyll nature as seen by the different LMA (Table 1). Cotton had a higher C_{dyn} than eucalypt leaves which would initially lead us to expect a higher f_{sw}. However, eucalypt leaves usually have bundle sheath extensions and a very high packing of the mesophyll with minimal differentiation between spongy and palisade parenchyma (Blackman and Brodribb, 2011). As closely packed cells would provide negligible air spaces for evaporative enrichment (Gan et al., 2002), it is possible that eucalypt mesophyll cells have the potential to store a large amount of relatively unenriched water. Adittionaly, bundle sheath area is proposed to have a role in storing water and acting a a capacitor to cope with sudden evaporative surges under windy conditions and/or increases in VPD (Griffiths et al, 2013). In fact, we found eucalypt to have a high capacity for water supply since g_s was nearly insensitive to changes in VPD (Fig. 6). Our data suggest that, besides vein density, mesophyll packing and the bundle sheath surface area are likely to interact in determining the fraction of unenriched water.

Interestingly, in the context of the two-pool model, the highest f_{sw} values were found for Adiantum (Fig. 4) where the lower vein densities presented by ferns (Brodribb et al., 2007; Zhang et al., 2014) led us to expect a lower f_{sw}. On the other

hand, as Adiantum presented the lowest K_{leaf} (Table 1) it is plausible to argue that increased resistances in the liquid phase would reduce the back diffusion of enriched water from the evaporative surfaces and, as a consequence, also reduce the mixing of enriched and unenriched water. Noteworthy, such explanation is comparable with the L concept of the Péclet effect and, in fact, we estimated L values in the upper range reported in the literature (Wang et al., 1998) as well with a negative relationship between L and K_{leaf} (Fig. 5). Nevertheless, such values were extremely variable (Fig. 5, from 51 to 141 mm) and likely to be a mathematical artefact of f_{sw} not being correlated with E rather than reflecting differences in water pathways within the leaf as suggested by Song et al. (2013) and criticized by Cernusak and Kahmen (2013).

The time-courses of leaf water enrichment showed how $\Delta^{18}O_{trans\_sw}$ (Fig. 6) can be dynamic and instantly responsive to changes in humidity. That highlights its usefulness as a tool to study the leaf water compartment prone to enrichment or depletion of ^{18}O during transpiration. The observed behaviour was consistent with the expected considering leaf hydraulic parameters. The species with a high K_{leaf} (eucalypt and pine) had higher g_s and their isotopic composition of transpiration ($\Delta^{18}O_{trans\_sw}$) reach values close to 0‰ faster than cotton (highest C_{dyn}); that implies a higher degree of mixing between enriched and unenriched water. In fact, $\Delta^{18}O_{Trans\_sw}$ = 0‰ denotes the isotopic steady-state (ISS), condition when the isotopic composition of transpired water is equal to that of source water being supplied trough the xylem. At this point, leaf water becomes sufficiently enriched that the exit of heavy and light molecules through the stomata matches that of the supply of water from the xylem (Farquhar et al., 2007). Most importantly, our results point out to a pivotal role for W and C_{dyn} governing such dynamics because Adiantum, the species with the lowest water content and lowest K_{leaf}, completely changed its evaporative site enrichment and reach the ISS in a matter of one hour or less (Fig. 7). That suggests an interaction between the size of the compartment (W or C_{dyn}) and the rate of water supply (K_{leaf}) governing leaf water enrichment. To a certain extent, one factor can compensate for the other, as the pine had a high K_{leaf} and also a high C_{dyn} but demanded similar time to eucalypt (high K_{leaf} and low C_{dyn}) to reach the ISS. On the other hand, cotton with a lower K_{leaf} and a high C_{dyn}, demanded the longest time to reach the ISS, as both parameters contribute to a slower water turnover.

We calculated different variations of time constants for leaf water isotopic turnover (τ) treating transpiration as coming from: a single pool of water (τ) or two

pools (enriched and unenriched) (τ_φ). It was clear that considering the leaf as a single pool of water was not a valid assumption because calculated τ using the whole water content largely overstimated the observed values. On the other hand, considering the leaf as comprising two-pools led to a better agreement with measured values. However, calculated τ_φ still overestimated measured values by c. 54%. Thus, additional factors other than the fraction of unenriched water (f_{sw}) constrain the mixing of enriched and unenriched water. As discussed above, a lower K_{leaf} increasing the resistance of extra-xylary water pathways may have an important role constraining water mixing within the leaf. In any case, such results clearly demonstrate that conventional models are missing important details regarding how transpiration enrichment develops in leaves throughout time and may be related to unaccounted effects of K_{leaf}, vein enrichment, hydraulic isolation and/or spatial heterogeneity. It has been only recently that Rockwell et al. (2014) and Bucley (2014) drew attention to the fact that the evaporation sites within the leaf can be variable depending on leaf anatomy and/or environmental conditions causing internal temperature gradients such as irradiance and VPD. Inclusion of a changing evaporative site in current water isotope models as function of environmental variables does seems promising in shedding light on the multifaceted relationships involving ^{18}O enrichment.

Conclusion

Our study provided additional evidence in support for the two pool model in three out of four species with contrasting leaf structure and draws attention for a possible interplay between vein density and associated ground tissues as determinants of the fraction of unenriched water. A high degree of mixing between enriched and unenriched water was associate to a high K_{leaf} and a low C_{dyn}. We propose that an increased radial resistance for water transport in Adiantum may have a role constraining the mixing of enriched and unenriched water and highlight the usefulness of species with low water content in the study of water stable isotopes given the reduced time required to reach the ISS. Altogether, our results emphasize the need to better understand time-course of leaf water enrichment in order to improve current models and envisage that the use of species with contrasting structure can provide valuable information on how leaf structure affects water enrichment. At last, it is crucial to evaluate to what extent a low K_{leaf} affects the estimate of the fraction of unenriched water and ferns offer a unique opportunity to address that since most species have a low K_{leaf} but a high diversity in water content and C_{dyn}.

References

Barbour M, Fischer R, Sayre K, Farquhar G. 2000. Oxygen isotope ratio of leaf and grain material correlates with stomatal conductance and grain yield in irrigated wheat. Functional Plant Biology **27**, 625–637.

Barbour MM, Roden JS, Farquhar GD, Ehleringer JR. 2004. Expressing leaf water and cellulose oxygen isotope ratios as enrichment above source water reveals evidence of a Peclet effect. Oecologia **138**, 426-435.

Barbour MM. 2007. Stable oxygen isotope composition of plant tissue: a review. Functional Plant Biology **34**, 83-94.

Barkan E, Luz B. 2007. Diffusivity fractionations of $H_2{}^{16}O/H_2{}^{17}O$ and $H_2{}^{16}O/H_2{}^{18}O$ in air and their implications for isotope hydrology. Rapid Communications in Mass Spectrometry, **21**: 2999-3005.

Blackman CJ, Brodribb TJ. 2011. Two measures of leaf capacitance: insights into the water transport pathway and hydraulic conductance in leaves. Functional Plant Biology **38**, 118.

Blackman CJ, Brodribb TJ, Jordan GJ. 2012. Leaf hydraulic vulnerability influences species' bioclimatic limits in a diverse group of woody angiosperms. Oecologia **168**, 1–10.

Bottinga Y, Craig H. 1969. Oxygen isotope fractionation between CO_2 and water and isotopic composition of marine atmospheric CO_2. Earth and Planetary Science Letters **5**, 285.

Brodribb TJ, Feild TS, Jordan GJ. 2007. Leaf maximum photosynthetic rate and venation are linked by hydraulics. Plant Physiology **144**, 1890–1898.

Brodribb TJ, Feild TS, Sack L. 2010. Viewing leaf structure and evolution from a hydraulic perspective. Functional Plant Biology **37**, 488-498.

Brodribb TJ, Holbrook NM. 2006. Declining hydraulic efficiency as transpiring leaves desiccate: two types of response. Plant, Cell & Environment **29**, 2205–2215.

Buckley TN. 2014. The contributions of apoplastic, symplastic and gas phase pathways for water transport outside the bundle sheath in leaves. Plant, Cell & Environment. doi: 10.1111/pce.12372

Cernusak LA, Wong SC, Farquhar GD. 2003. Oxygen isotope composition of phloem sap in relation to leaf water in Ricinus communis. Functional Plant Biology **30**, 1059-1070

Cernusak LA, Kahmen A. 2013. The multifaceted relationship between leaf water ^{18}O enrichment and transpiration rate. Plant, Cell & Environment **36**, 1239–1241.

Craig H, Gordon LI. 1965. Deuterium and oxygen-18 variations in the ocean and the marine atmosphere. In Proceedings of a Conference on Stale Isotopes in Oceanographic Studies and Palaeotemperautres (ed. E. Tongiorgi), pp. 9–130. Lischi and Figli, Pisa, Italy.

Cuntz M, Ogée J, Farquhar GD, Peylin P, Cernusak LA. 2007. Modelling advection and diffusion of water isotopologues in leaves. Plant Cell & Environment **30**, 892-909

Dongmann G, Nurnberg HW, Förstel H, Wagener K. 1974. On the enrichment of $H_2{}^{18}O$ in the leaves of transpiring plants. Radiation and Environmental Biophysics **11**, 41–52.

Farquhar GD, Hubick KT, Condon AG, Richards RA. 1989. Carbon isotope discrimination and water-use efficiency. In Stable Isotopes in Ecological Research (eds P.W. Rundel, J.R. Ehleinger & K.A. Nagy), pp. 21–46. Springer-Verlag, New York.

Farquhar GD, Lloyd J. 1993. Carbon and oxygen isotope effects in the exchange of carbon dioxide between terrestrial plants and the atmosphere. In 'Stable isotopes and plant carbon–water relations'. (Eds JR Ehleringer, AE Hall, GD Farquhar) pp. 47–70. Academic Press, San Diego.

Farquhar G, Gan K. 2002. On the progressive enrichment of the oxygen isotopic composition of water along a leaf. Plant, Cell & Environment **26**, 801-819.

Farquhar GD, Cernusak LA. 2005. On the isotopic composition of leaf water in the non-steady state. Functional Plant Biology **32**, 293-303.

Farquhar GD, Cernusak LA, Barnes B. 2007. Heavy water fractionation during transpiration. Plant Physiology **143**, 11–18.

Farris F, Strain BR. 1978. The effects of water-stress on leaf $H_2{}^{18}O$ enrichment. Radiation and Environmental Biophysics **15**, 167–202.

Ferrio JP, Pou A, Florez-Sarasa I, Gessler A, Kodama N, Flexas J, Ribas-Carbó M. 2012. The Péclet effect on leaf water enrichment correlates with leaf hydraulic conductance and mesophyll conductance for CO_2. Plant, Cell & Environment **35**, 611–625.

Flanagan LB,Comstock JP, Ehleringer JR. 1991. Comparison of modeled and observed environmental influences on the stable oxygen and hydrogen isotope composition of leaf water in Phaseolus vulgaris L. Plant Physiology **96**, 588–596.

Flanagan LB, Phillips SL, Ehleringer JR, Lloyd J, Farquhar GD. 1994. Effects of changes in leaf water oxygen isotopic composition on discrimination against $C^{18}O^{16}O$ during photosynthesis. Australian Journal of Plant Physiology **21**, 221–234.

Gan KS, Wong SC, Yong JWH, Farquhar GD. 2002. ^{18}O spatial patterns of vein xylem water, leaf water, and dry matter in Gossypium leaves. Plant Physiology **130**, 1008–1021.

Gat JR, Bowser C. 1991. The heavy isotope enrichment of water in coupled evaporative systems. In Stable Isotope Geochemistry: a Tribute to Samuel Epstein (eds H.P. Taylor, J.R. O'Neil & I.R. Kaplan), pp. 159–168. The Geochemical Society, St Louis, MO, USA.

Gessler A, Peuke AD, Keitel C, Farquhar GD. 2007. Oxygen isotope enrichment of organic matter in Ricinus communis during the diel course and as affected by assimilate transport. New Phytologist **174**, 600-613.

Gillon J, Yakir D. 2000. Internal conductance to CO_2 diffusion and $C^{18}OO$ discrimination in C3 leaves. Plant Physiology **123**, 201–213.

Griffiths H, Weller G, Toy LFM, Dennis RJ. 2013. You're so vein: bundle sheath physiology, phylogeny and evolution in C3 and C4 plants. Plant, Cell & Environment **36**, 249–261.

Harwood KG, Gillon JS, Griffiths H, Broadmeadow MSJ. 1998. Diurnal variation of $\Delta^{13}CO_2$, $\Delta C^{18}O^{16}O$ and evaporative site enrichment of $\Delta H_2{}^{18}O$ in Piper aduncum under field conditions in Trinidad. Plant, Cell & Environment **21**, 269–283.

Helliker BR, Ehleringer JR. 2000. Establishing a grassland signature in veins: 18O in the leaf water of C3 and C4 grasses. Proceedings of the National Academy of Sciences **97**, 7894–7898.

Kahmen A, Simonin K, Tu KP, Merchant A, Callister A, Siegwolf R, Dawson TE, Arndt SK. 2008. Effects of environmental parameters, leaf physiological properties and leaf water relations on leaf water delta^{18}O enrichment in different Eucalyptusus species. Plant, Cell & Environment **31**, 738–751.

Loucos KE, Simonin KA, Song X, Barbour MM. 2014. Observed relationships between leaf $H_2{}^{18}O$ Peclet effective length and leaf hydraulic conductance reflect

assumptions in Craig-Gordon model calculations. Tree Physiology **doi**: 10.1093/treephys/tpu110

Luz B, Barkan E, Yam R, Shemesh A. 2009. Fractionation of oxygen and hydrogen isotopes in evaporating water. Geochimica et Cosmochimica Acta **73**: 6697-6703.

Merlivat L. 1978. Molecular diffusivities of $H_2{}^{16}O$, $HD^{16}O$, and $H_2{}^{18}O$ in gases. Journal of Chemical Physics **69**, 2864-2671.

Rockwell FE, Holbrook NM, Stroock AD. 2014. The competition between liquid and vapor transport in transpiring leaves. Plant Physiology **164**, 1741–1758.

Scoffoni C, Vuong C, Diep S, Cochard H, Sack L. 2014. Leaf shrinkage with dehydration: coordination with hydraulic vulnerability and drought tolerance. Plant Physiology **164**, 1772–1788.

Simonin KA, Roddy AB, Link P, Apodaca R, Tu KP, Hu J, Dawson TE, Barbour MM. 2013. Isotopic composition of transpiration and rates of change in leaf water isotopologue storage in response to environmental variables. Plant, Cell & Evironment **36**, 2190–2206.

Song X, Barbour MM, Farquhar GD, Vann DR, Helliker BR. 2013. Transpiration rate relates to within- and across-species variations in effective path length in a leaf water model of oxygen isotope enrichment. Plant, Cell & Environment, 1338–1351.

Song X, Loucos KE, Simonin KA, Farquhar GD, Barbour MM. 2015. Measurements of transpiration isotopologues and leaf water support a two pool leaf water model at the whole leaf level. New Phytologist . doi: 10.1111/nph.13296

Tausend PC, Meinzer FC, Goldstein G. 2000b. Control of transpiration in three coffee cultivars: the role of hydraulic and crown architecture. Trees **14,** 181-190.

Walker CD, Leaney FW, Dighton JC, Allison GB. 1989. The influence of transpiration on the equilibration of leaf water with atmospheric water vapor. Plant, Cell & Environment **12**, 221–234.

Wang XF, Yakir D, Avishai M. 1998. Non-climatic variations in the oxygen isotopic compositions of plants. Global Change Biology **4**, 835–849.

Werner C, Schnyder H, Cuntz M, et al. 2012. Progress and challenges in using stable isotopes to trace plant carbon and water relations across scales. Biogeosciences **9**, 3083–3111.

West AG, Patrickson SJ, Ehleringer JR. 2006. Water extraction times for plant and soil materials used in stable isotope analysis. Rapid Communications in Mass Spectrometry **20**, 1317-1321.

Zhang SB, Sun M, Cao KF, Hu H, Zhang JL. 2014. Leaf photosynthetic rate of tropical ferns is evolutionarily linked to water transport capacity. PloS One **9**, e84682.

Table 1 – Hydraulic and anatomic traits for the four sampled species. Leaf hydraulic conductance, K_L (mmol m^{-2} s^{-1} MPa^{-1}); Dynamic capacitance, C_{dyn} (mmol m^{-2} MPa^{-1}); Water content, W (mol m^{-2}) and leaf mass per unit leaf area, LMA (g m^{-2}). Values are averages ± SE.

	K_{leaf}	C_{dyn}	W	LMA
Adiantum	0.9±0.1	203±92	3±0.1	19±0.6
Cotton	4.8±0.6	1237±151	18.7±0.5	71±6
Eucalypt	7.1±0.6	395±55	15±0.5	215±3
Pine	8.8±1.3	982±123	13.2±1.5	127±7

Figure legends

Figure 1. Plot showing the significant relationship between the ^{18}O enrichment at the evaporative sites ($\Delta^{18}O_{es\_sw}$) and bulk leaf water ^{18}O enrichment ($\Delta^{18}O_{L\_sw}$) across four species. Both enrichments were expressed as enrichment above source water (sw). $\Delta^{18}O_{es\_sw}$ is calculated with the Craig-Gordon model using relative humidity, leaf temperate and stomata conductance as inputs. $\Delta^{18}O_{L\_sw}$ is the actual measured ^{18}O enrichment in the leaf lamina obtained through leaf water extraction and ^{18}O measurement using laser-based spectrometry. As all $\Delta^{18}O_{es\_sw}$ were higher than the $\Delta^{18}O_{L\_sw}$ counterparts, that implies incomplete mixing of water at the evaporation sites with lamina leaf water.

Figure 2. Relationship between stomata conductance (g_s) and bulk leaf water ^{18}O enrichment ($\Delta^{18}O_{L\_sw}$) across four species. Leaves become more enriched in ^{18}O as stomata close, in our conditions the closure was mainly due to a decreased relative humidity. A large range in g_s within species was function of each leaf adjusting itself to evaporative conditions as dry-air was sent to gas-exchange chamber (see details in Material and Methods).

Figure 3. Bulk leaf water ^{18}O enrichment ($\Delta^{18}O_{L\_sw}$, empty symbols) and evaporative site water enrichment ($\Delta^{18}O_{es\_sw}$, filled symbols) plotted against the ratio of ambient to intercellular vapour mole fraction (w_a/w_i). The w_a/w_i ratio is one of the components of the Craig-Gordon model of leaf water enrichment used in the calculus of $\Delta^{18}O_{es\_sw}$. The high r^2 indicates the w_a/w_i ratio is the major factor controlling variation in both

$\Delta^{18}O_{L\_sw}$ and $\Delta^{18}O_{es\_sw}$. Thus, $\Delta^{18}O_{L\_sw}$ largely reflects the relative humidity surrounding the leaf. Symbols legend: triangles = Adiantum, circles = Eucalypt, squares = Cotton and diamonds = Pine.

Figure 4 The correlation between the fraction of unenriched water (f_{sw}) and transpiration rate (E) for all leaves measured. f_{sw} was calculated as $1-\Delta^{18}O_{L\_sw}/\Delta^{18}O_{es\_sw}$. The Péclet theory predicts that f_{sw} should increase with increasing E for a given species. A higher E would lead to a higher rate of advection of unenriched water from the xylem opposing the back diffusion of enriched water from the evaporative sites, thus increasing f_{sw}. As a result, species presenting a non-significant f_{sw} and E relationship do not support the Péclet effect. Only the pine showed a significant relationship between f_{sw} and E identified by the fitted solid line.

Figure 5. The relationship between Péclet effective length (L) and leaf hydraulic conductance (K_{leaf}). L concerns the distance water vapour has to move from the leaf vein until the evaporative surface and is a fitted parameter from the Péclet theory. K_{leaf} is a measure of hydraulic capacity reflecting the resistances to liquid flow from leaf xylem until the evaporative sites.

Figure 6. Time course of stomata conductance (g_s), transpiration rates (E), the measured stable oxygen isotope enrichment of transpiration ($\Delta^{18}O_{trans\_sw}$), and the leaf water enrichment at the evaporative sites ($\Delta^{18}O_{es\_sw}$). The isotopic steady-state (ISS) is the value when $\Delta^{18}O_{trans\_sw}$ is equal to zero, indicating the isotopic composition of transpiration is equal to that of source water. Leaves with a higher K_{leaf} presented higher g_s and leaves with a lower dynamic leaf capacitance demanded longer times to reach the ISS. Note the increase in VPD and return to initial conditions (see increases in E marking the step increase and decrease in VPD). Averages from three-four individuals are shown.

Figure 7. Time course of stomata conductance (g_s), the measured stable oxygen isotope composition of transpiration ($\delta^{18}O_{trans}$), the leaf water enrichment above source water at the evaporative sites ($\Delta^{18}O_{es\_sw}$), ratio of ambient to intercellular vapour mole fraction (w_a/w_i), measured time constants (τ), calculated single-pool time constants (τ_{single}) and the two-pool model time constants (τ_{φ}). Measured time constant was obtained as described in Material and Methods. Calculated τ_{single} and τ_{φ}were calculated from water content, stomata conductance and the fraction of unenriched water (f_{sw}). Briefly, τ_{single} assumes that the whole water content participates in water

enrichment whereas τ_{φ}consider only the water fraction prone to enrichment (1- f_{sw}). f_{sw} is calculated from isotopic measurements as $f_{sw} = 1-\Delta^{18}O_{L\_sw} / \Delta^{18}O_{es\_sw}$.

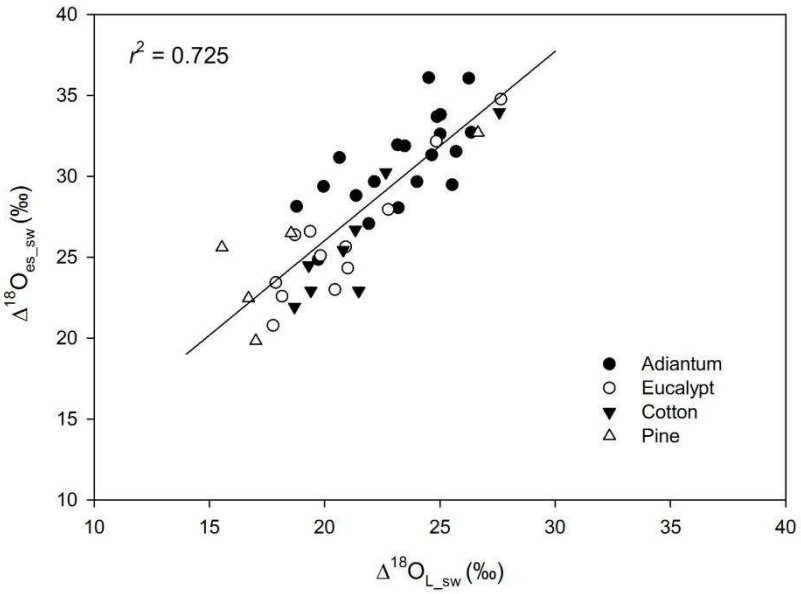

Figure 1.

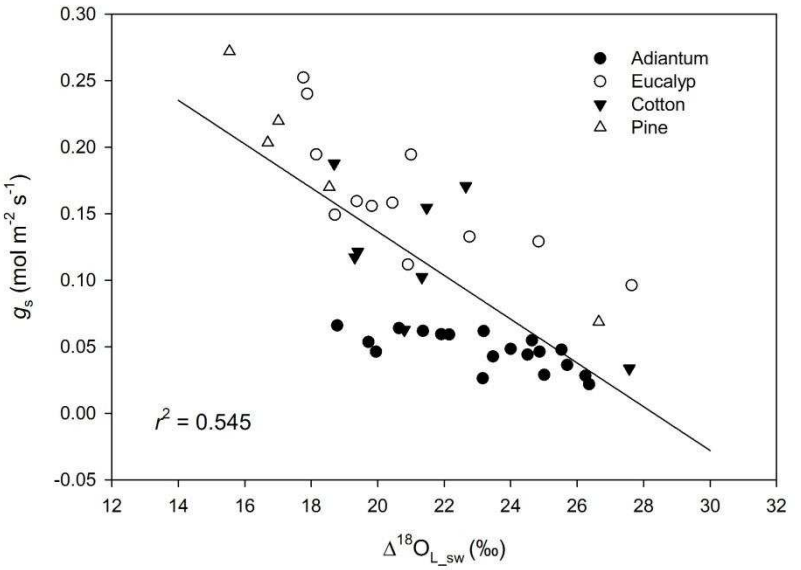

Figure 2.

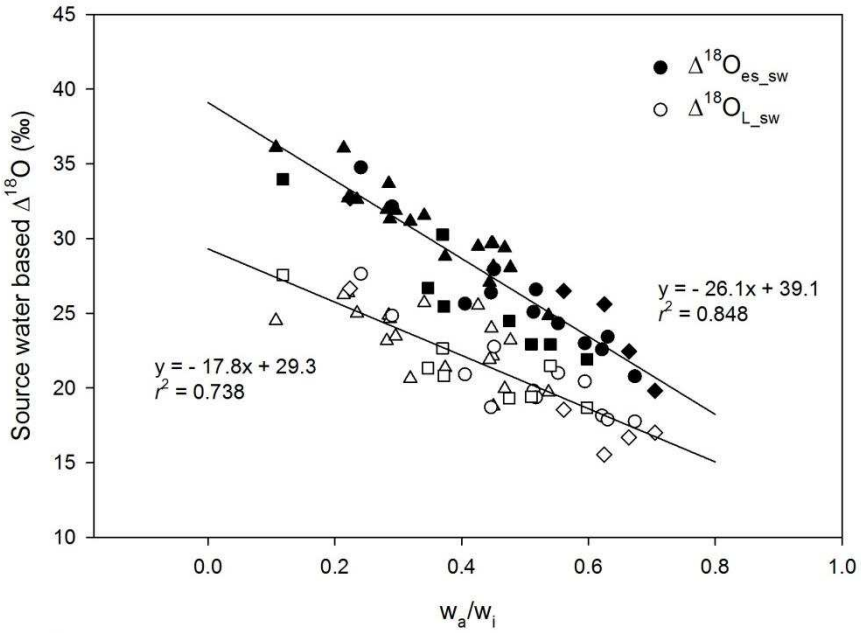

Figure 3.

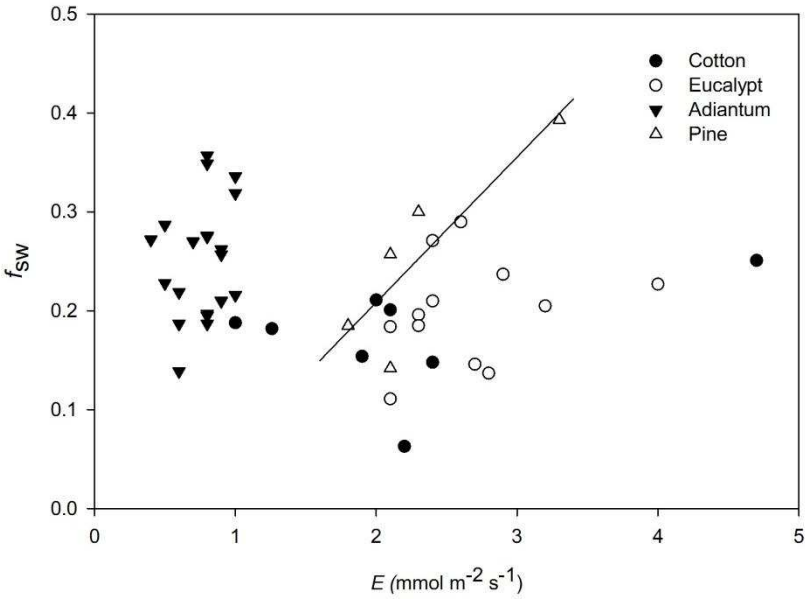

Figure 4.

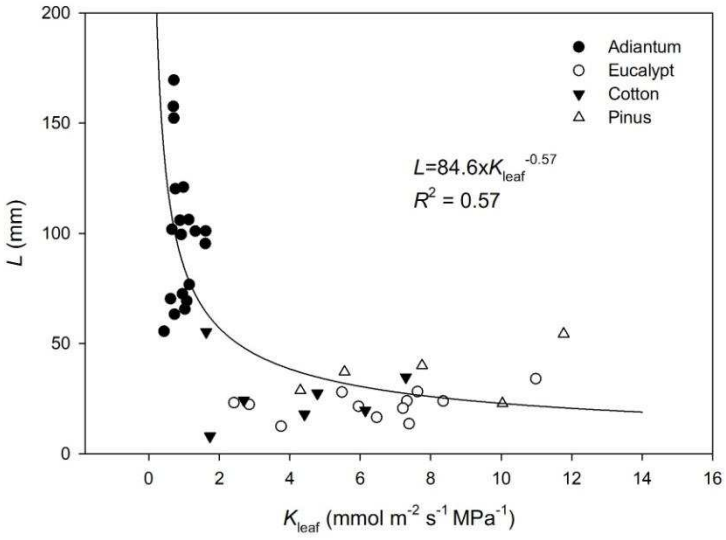
Adiantum
Eucalypt
Cotton
Pinus
L=84.6x$K_{leaf}^{-0.57}$
R^2 = 0.57
L (mm)
K_{leaf} (mmol m^{-2} s^{-1} MPa^{-1})
0
50
100
150
200
0
2
4
6
8
10
12
14
16

Figure 5.

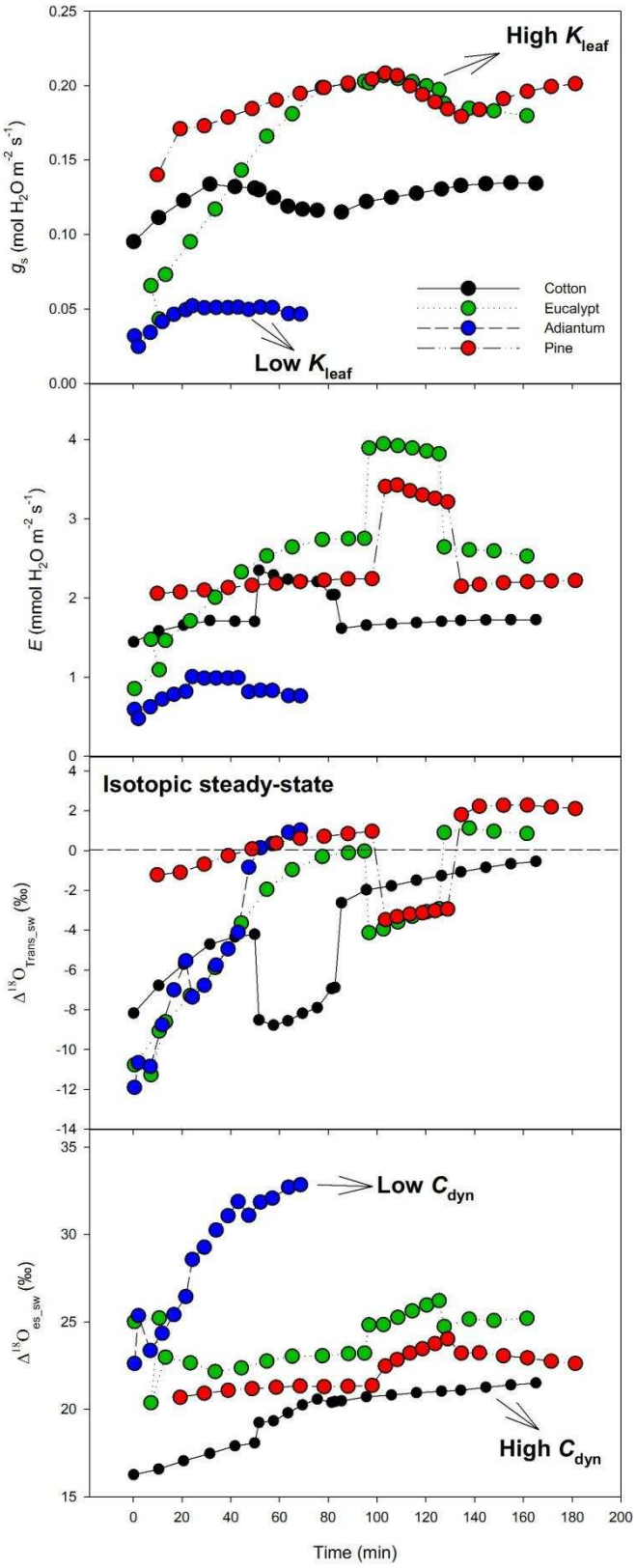
High K_{leaf}
Low K_{leaf}
Cotton
Eucalypt
Adiantum
Pine
g_s (mol H_2O m^{-2} s^{-1})
E (mmol H_2O m^{-2} s^{-1})
Isotopic steady-state
$\Delta^{18}O_{Trans\_sw}$ (‰)
Low C_{dyn}
High C_{dyn}
$\Delta^{18}O_{es\_sw}$ (‰)
Time (min)

Figure 6.

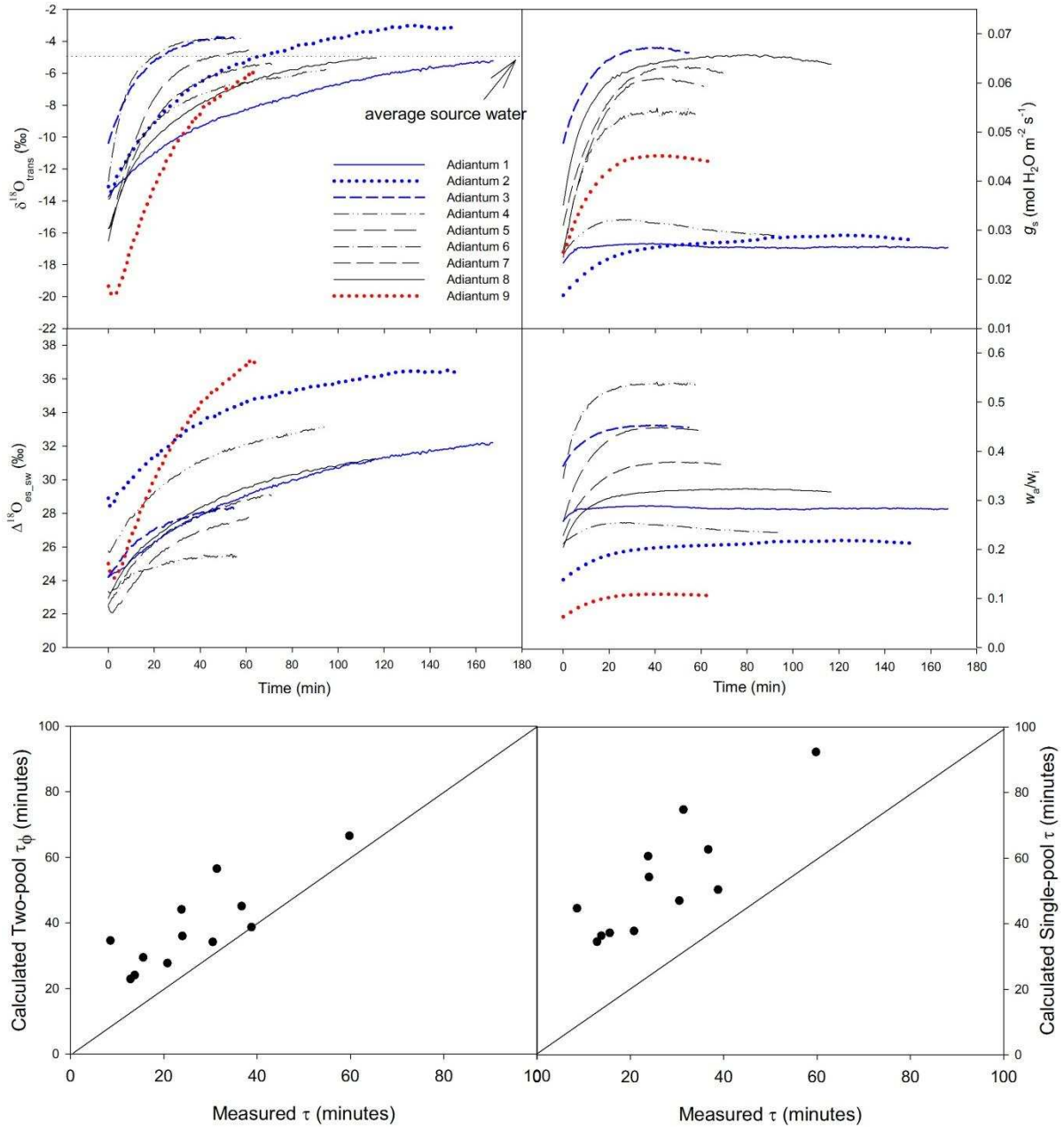
average source water
Adiantum 1
Adiantum 2
Adiantum 3
Adiantum 4
Adiantum 5
Adiantum 6
Adiantum 7
Adiantum 8
Adiantum 9
δ18Otrans (‰)
gs (mol H2O m-2 s-1)
Δ18Oes_sw (‰)
wa/wi
Time (min)
Time (min)
Calculated Two-pool τϕ (minutes)
Calculated Single-pool τ (minutes)
Measured τ (minutes)
Measured τ (minutes)

Figure 7.

CHAPTER 3

Leaf hydraulic vulnerability in two field-grown coffee cultivars under severe drought conditions

Samuel CV Martins, Leandro E Morais, Mateus Sanglard, Paulo Menezes-Silva, Rafael Mauri, Fábio M. DaMatta

Introduction

From all environmental resources, water is likely the most important resource determining plant distribution, growth, yield and survival (Engelbrecht et al., 2007; Zhao and Running, 2010). Plants are constantly threatened by the risk of desiccation through exposure to a drying soil or atmosphere and survival hinges on finding a strategy to optimise water loss and carbon gain (Brodribb et al., 2014). As water lost has to be replenished, xylem has a challenging task in supplying water to allow stomata aperture at the same time that physical tension increases its susceptibility to cavitation (Tyree et al., 1994). The risk of hydraulic failure depends on the extent that minimum xylem water potentials occurring under growth conditions (Ψ_{min}) are close to the water potential representing 50% loss of hydraulic conductivity (P_{50}) reflecting the hydraulic safety margin (HSM) for a given species (Meinzer et al., 2009).

Choat et al. (2012) recently reported that several plant species operate with narrow HSM, and therefore they are expected to be highly vulnerable to hydraulic dysfunctions that should be exacerbated due to the current and ongoing scenarios of increased frequency and severity of drought episodes (Allen et al., 2010). Although in their analysis Choat et al. (2012) have not considered other significant aspects associated with drought tolerance (see Klein et al., 2014), recent findings suggesting increased tree mortality linked to drought events (McDowell, 2008) point out for a hydraulic based view on how trees die when exposed to water deficit. Thus, the hydraulic vulnerability assessment coupled to future climate modelling can provide more robust predictions of changes in species' distribution or elaboration of climatic risk zoning for cultivated plants.

Coffee, a tropical woody crop, is one of the most important commodities in the international agricultural trade, representing a significant source of income to several Latin American, African and Asian countries. It is also one of most threatened species by global climate changes; depending on the climate change scenarios, extinction of native populations in Ethiopia (Davis et al., 2012) as well as remarkable reductions (up to 50%) of suitable areas for coffee cultivation have been predicted

(Bunn et al., 2014). In Brazil, the world's largest coffee producer, as well as in several other coffee growing countries, drought is considered to be the major environmental stress affecting coffee growth and production (DaMatta, 2004). Despite the growing body of information on the morphological and physiological mechanisms though which the coffee tree cope with drought stress (DaMatta, 2004; Pinheiro et al. 2005; Dias et al. 2007; Cavatte et al. 2012a), little is known on how hydraulic vulnerability, HSM and lethal water potentials are correlated in coffee. In earlier attempts, an exponential response of stem hydraulic conductance to leaf water potential (Ψ_l) was suggested (Tausend et al., 2000), implying cavitation to occur whenever $\Psi_l<0$; however, such an exponential behaviour could be due to the open vessel artefact (Cochard et al., 2013) which would overestimate the onset of cavitation. More recently, leaf vulnerability was assessed in four potted coffee cultivars by Nardini et al. (2014) who found P_{50} ranging from -0.6 to -1.0 MPa, which would imply that the coffee tree is highly vulnerable to drought. We herein suggest that such P_{50} values are highly unlikely to be observed under real field conditions given that coffee leaves reach Ψ_l as low as -1.1 MPa on a daily basis at field capacity (Dias et al., 2007; Cavatte et al., 2012). Alternatively, cavitation and repair could be routine in coffee plants acting as a trigger for stomata closure as suggested by Nardini et al. (2014). These conflicting results urge for a proper evaluation of hydraulic vulnerability in coffee plants grown under real field conditions not only to assess the ecological importance of cavitation but also to resolve the risk of death by hydraulic failure.

Another unknown aspect in coffee is whether xylem cavitation is involved in stomata closure as observed in several species (Cochard et al., 2002; Brodribb and Holbrook, 2003). Martins et al. (2014) demonstrated that a low capacity for water supply probably constrains stomata aperture under a high transpirational demand in coffee leaves. Indeed, stomata conductance (g_s) rapidly decreases in response to increasing vapour pressure deficit (VPD), irrespective of Ψ_l, suggesting a feed-forward regulation to minimise the risk of embolism (DaMatta and Ramalho, 2006). Interestingly, coffee seems to regulate g_s in such a way to optimise intrinsic water use efficiency (WUE_i) coupling water and carbon exchange in stomata control (Cornic, 2000; Martins et al., 2014). Such mechanism is expected to involve a sophisticated active control of stomata aperture, possibly linked to the phytohormone abscisic acid (ABA) (McAdam and Brodribb, 2011). Given that Batista et al. (2012) ruled out

feedback inhibition as limiting g_s throughout the day in coffee plants, it remains to be tested if cavitation can also have a role in governing stomata dynamics in this species.

Here we evaluated two field-grown coffee cultivars under severe (natural) drought and subsequent recovery with the following objectives: (1) to assess naturally occurring Ψ_{min} and determine reliable hydraulic safety margins; (2) to investigate diurnal hydraulic versus ABA-mediated stomata control and (3) to test whether loss of conductivity is significant in leaves expanded in the drought season. Assessment of these points will allow a better comprehension on how the coffee tree is affected by drought aiming at envisaging the importance of hydraulic failure for the plant survival and functioning.

Material and Methods

Plant material and experimental design

The experiment was carried out under field conditions on a Cambic Podzol, in Viçosa (20°45'S, 42°15'W, 650 m a.s.l.), southeastern Brazil. The site is characterised by a subtropical climate, with a mean annual temperature of 20°C, and receives an average rainfall of 1200 mm, mainly distributed from September to March (growing season). Two coffee cultivars, Catuaí (C. arabica L. 'Catuaí Vermelho IAC 44') and Hybrid 12 (a hybrid of C. arabica x C. racemosa Lour.), were investigated. Empirical observations from the field show that the Hybrid 12 endures drought stress much better than Catuaí; as a result, Hybrid 12, but not Catuaí, shows improved maintenance of leaf area and vigour under drought conditions and, therefore, has been empirically classified as drought-tolerant, whereas Catuaí has been classified, by comparison, as drought-sensitive. The trees have been cultivated at full sunlight conditions with no supplemental irrigation, as is usually performed in most coffee farms in southeastern Brazil. The coffee trees were grown at a spacing of 2.0 x 1.0 m in north-south oriented hedgerows. Six to seven trees, with approximately 2-m tall, were selected for uniformity and vigour and assigned in a completely randomised design. The experimental plot was one tree per hole. Annual precipitation in 2014 was 825 mm, the lowest one recorded over the last 25 years. Annual water deficit, calculated based on the estimation of climatic water balance, was 213 mm whereas the historical record for Viçosa is 60 mm (INMET, 2015). Annual water deficits higher than 150 mm are considered of high risk for coffee according to climatic zoning and not suitable for coffee cultivation (Zullo Jr. et al., 2011). Monthly precipitation and accumulated precipitation are shown in Fig. 1. From the expected

rainfall of 780 mm (historical average from January to October), only 460 mm had been recorded until October 2014. For the sake of simplicity, data herein shown were collected (on cloudless days) in three distinct periods: (i) drought period – measurements taken at the end of a natural long-term drought, i.e, in 17 October and 05 November 2014 (data were pooled); (ii) recovery phase –measurements recorded in 19 November 2014, i.e. 14 days after the onset of the rainy period (147 mm of accumulated rainfall); and the 'control' (reference) conditions –measurements made in 15 January 2015 (303 mm of accumulated rainfall). In January 2015, two sets of leaves were measured: leaves expanded in the rainy period (new leaves) and leaves expanded in the drought period (old leaves).

Leaf hydraulic vulnerability measurements

Leaf hydraulic measurements (K_{leaf}) were made in January 2015 in leaves developed in the wet season (expected to present maximum K_{leaf}) according to the standard protocol outlined by Brodribb and Cochard (2009). Detached shoots with at least three expanded leaf pairs from at least three plants were bench dried, and K_{leaf} was determined at intervals of 0.25-0.5 MPa (Ψ_l) by measuring the rehydration flux of water into leaves using a hydraulic flowmeter. The relationship between Ψ_l and K_{leaf} was used to determine the P_{50} (Ψ_l, at 50% loss of K_{leaf}) from a sigmoidal curve fitted to the pooled data from each genotype.

Leaf hydraulic measurements using the evaporative flux method

Leaves were measured between 0800 and 1600 h using the evaporative flux method (Sack et al. 2002; Brodribb & Holbrook 2006). Branches were collected in the field and brought to the laboratory where leaves were excised and then immediately re-cut under water. An entire mature leaf was then enclosed in an opaque lighted conifer chamber (Li6400-22L) connected to a portable open-flow gas exchange system (LI-6400XT, LI-COR, Lincoln, NE, USA). Measurements were performed under a photosynthetically active radiation (PAR) of 1,000 µmol photons m^{-2} s^{-1} at the leaf level and 400 µmol CO_2 mol^{-1} air. All measurements were performed at 25°C and vapour pressure deficit was maintained at c. 1.0 kPa. Leaves were allowed to reach a transpirational steady state (less than 10% variation over 180 s) and the resulting transpirational flux was recorded. Leaf water potential was measured with a Scholander-type pressure chamber (model 1000, PMS Instruments, Albany, NY, USA) and K_{leaf} was then calculated using the following equation:

$K_{leaf} = -E / \Psi_l$

where E is the transpirational flux and Ψ_l is the leaf water potential at steady state conditions. Leaf size was measured using a flatbed scanner in combination with the ImageJ software (National Institutes of Health, Bethesda, MD, USA).

Water relations, gas exchange and fluorescence measurements

Measurements of Ψ_l and instantaneous gas-exchange parameters were simultaneously performed using completely expanded leaves from the third or fourth pair from the apex of plagiotropic branches at 0800 h, 1200 h and 1600 h (Ψ_l was additionally assessed at predawn). Leaf Ψ_l was measured using the above mentioned pressure chamber. In October and January, fully expanded leaves were detached to produce pressure-volume curves, exactly as described in Pinheiro et al. (2005). From these curves, the osmotic potential at full turgor ($\Psi_{\pi(100)}$), the Ψ_l at the turgor loss point (Ψ_{TLP}), the relative water content at the turgor loss point (RWC_{TLP}), and the bulk modulus of elasticity (ε) were estimated. Hydraulic safety margins (HSM) were calculated as described in Choat et al. (2012) using the average of the four lowest Ψ_l measured under drought or control conditions as the value for Ψ_{min}. Then, a standard HSM based on P_{50} (HSM_{50}) or a more conservative HSM based on P_{88} (HSM_{88}), were calculated as:

$HSM_{50} = \Psi_{min} - P_{50}$ or $HSM_{88} = \Psi_{min} - P_{88}$

Leaf gas exchange parameters were determined simultaneously with measurements of chlorophyll (Chl) a fluorescence using the aforementioned gas-exchange system equipped with an integrated fluorescence chamber head (LI-6400-40, LI-COR Inc.). The net CO_2 assimilation rate (A), stomatal conductance to water vapour (g_s) and internal CO_2 concentration (C_i) were measured on attached leaves, under artificial PAR, i.e., 1,000 µmol photons m^{-2} s^{-1} at the leaf level and 400 µmol CO_2 mol^{-1} air. All measurements were performed under naturally fluctuating temperature and vapour pressure deficit conditions.

After registering the gas exchange parameters, the steady-state fluorescence yield (F_s) was measured after which a saturating white light pulse (8,000 µmol m^{-2} s^{-1}; 0.8 s) was applied to achieve the light-adapted maximum fluorescence (F_m'). The actinic light was then turned off and a far-red illumination was applied (2 µmol m^{-2} s^{-1}) to measure the light-adapted initial fluorescence (F_0'). The actual photosystem (PS) II photochemical efficiency (ϕ_{PSII}) was determined following the procedures of Genty

et al. (1989). The electron transport rate (ETR) was then calculated from ETR = ϕ_{PSII} β α PPFD, where α is leaf absorptance and β reflects the partitioning of absorbed quanta between PS II and I. The product β α determined for coffee was taken from Martins et al. (2014). Single point V_{cmax} was determined as described in Wilson et al. (2000) using the Rubisco kinetic properties determined for coffee taken from Martins et al. (2013) and values of A_n and ETR measured at 0800 h (when photosynthesis rates are at their maxima).

Statistical analysis

The data from the experiment were analyzed using a completely randomized design with six replicates. The data were subjected to an analysis of variance (two-way ANOVA with all main factors evaluated as fixed factors) that was performed using the general linear models (GLM) procedure of SAS (version 9.1.) adopting $\alpha = 0.05$. When any interaction was found significant, the Slice statement of GLM was used to interpret the dependency effect between factors.

Results

Leaf vulnerability curves followed a sigmoidal behaviour with K_{leaf} declining gradually as a function of Ψ_l. The Hybrid 12 displayed lower (more negative) P_{50} (26%) than Catuaí. In contrast, there were no cultivar differences in maximum fitted K_{leaf} which averaged on c. 2.6 mmol H_2O m^{-2} s^{-1} MPa^{-1} (Fig. 2). Predawn Ψ_l was c. -1.5 MPa in the dry season and was above -0.1 MPa when the rainy season started. Under drought, Catuaí and Hybrid 12 had their lowest Ψ_l values (c. -4 MPa) at midday and Ψ_l recovery was observed at the afternoon; such a recovery was more prominent in Catuaí. In the recovery and control conditions Ψ_l markedly increased in all time periods with the lowest values observed at midday (c. -1.6 MPa). In the recovery phase, there was no difference in Ψ_l from the morning to the afternoon for both cultivars. Catuaí exhibited the same previous behaviour under control conditions; the Hybrid 12, in turn, displayed a decreasing Ψ_l until midday, followed by a Ψ_l recovery in the afternoon (Fig. 2).

The variables of tissue water relations based on pressure-volume curves were similar for both cultivars under a same condition (drought or control) with the exception of ε, which was 50% higher in Catuaí in comparison with the Hybrid 12 under drought conditions (Table 1). Ψ_{TLP} was c. -2.3 and -1.9 MPa under drought and

control conditions, respectively; however, osmotic and elastic adjustments were significant only in Catuaí. K_{leaf} values measured by the evaporative flux method (averaged on 2.9 mmol H_2O m^{-2} s^{-1} MPa^{-1}) did not differ between cultivars or leaf age (Fig. 2). Hydraulic safety margins (HSM) based on P_{50} or P_{88} were negative, implying that loss of conductivity occurred, for both cultivars under drought. Positive HSM was found in the recovery and control conditions, but they were narrower in Catuaí (by approximately 0.5 MPa) than in the Hybrid 12 (Table 1).

Stomata conductance (g_s) was curvilinearly related to Ψ_l when all data were pooled (Fig. 3). The lower Ψ_l threshold for g_s under drought was associated with Ψ_l at P_{88} and most Ψ_l values observed at midday were more negative than those of Ψ_{TLP}. In contrast, under wet conditions, Ψ_{TLP} defined the lower Ψ_l for g_s values. Maximum g_s was greatly constrained throughout the day reaching c. 200, 100 and 60 mmol H_2O m^{-2} s^{-1} at 0800 h, 1200 h and 1600 h, respectively (Fig. 3). A_n and g_s values were significantly reduced by drought regardless of cultivar. In the recovery period, a 65% increase in g_s (relative to drought conditions) was observed for both cultivars at 0800 h. Regarding A_n, no changes occurred in the Hybrid 12 whereas Catuaí showed a 37% increase in comparison with drought conditions at 0800 h (Fig. 4). A_n and g_s values did not increase at 1200 h in the recovery period (relative to drought conditions), but values at 1600 h were comparable to control conditions. Under control conditions, A_n and g_s values were on average 50% higher than those obtained in the recovery period regardless of cultivar; in addition, no differences were observed between leaves expanded over the drought (old leaves) or wet (new leaves) period. A_n/g_s ratios ranged from 75 to 150 μmol CO_2 mol H_2O^{-1} with the highest values obtained at morning under drought conditions. Catuaí tended to have higher A_n/g_s ratios in the drought and recovery periods in comparison with control conditions; such a ratio varied inconsistently in the Hybrid 12 (Fig. 5). A_n and g_s were strongly correlated to each other regardless of cultivar, water regime or leaf age (R^2=0.90, P<0.001). No major differences in $V_{cmax\_single\ point}$ among water regimes were found, with an average value of 81 μmol CO_2 m^{-2} s^{-1} (Fig. 5). Finally, there was no clear pattern in ETR among water regimes; in any case the ETR values tended to be slightly lower in the afternoon as compared with their counterpart values measured at morning or midday, which did not differ from one another.

Discussion

The P_{50} values of coffee leaves is in the lower range reported for montane rainforest species (Blackman et al., 2010), which suggests that coffee should behave as a moderately tolerant species to hydraulic dysfunctions. Most importantly, our vulnerability curves revealed a sigmoidal behaviour, which is in sharp contrast with the linear behaviour proposed recently for coffee by Nardini et al. (2014). Hence, as opposed to the suggestion of Nardini et al. (2014), major cavitation events should not be routine in coffee under well-watered conditions. This statement is in line with what has empirically been observed in coffee plantations under field conditions (fast vigour recovery after long-term droughts) as well as with the proposed role for cavitation representing a threat to the mechanism of sap ascent that must be avoided (Delzon and Cochard, 2014). In any case, it must be emphasise that, under drought conditions, both cultivars operated with negative safety margins implying that hydraulic failure probably occurred in line with the findings of Choat et al. (2012) (Fig. 2 and Table 1). Indeed, Catuaí, the less drought tolerant cultivar, presented high rates of defoliation whereas the Hybrid 12 was able to retain much of its foliage (visual observation). In robusta coffee (C. canephora), for example, extensive leaf fall, that is characteristic of drought-sensitive genotypes, is believed to be a consequence rather than a defence strategy against drought stress since an improved water status in the remaining leaves is not observed (DaMatta, 2004).

Coffee seems to behave as an anisohydric species (Tardieu, 1993; Tausend et al, 2000), thus allowing midday Ψ_l to decline as soil Ψ declines with drought (Fig. 2) in order to maintain photosynthetic activity. Although such strategy maximises WUE_i, it may come at a cost of increased hydraulic dysfunction, reflecting the trade-off involving efficiency and safety (McDowell et al., 2008). Interestingly, the high variability in Ψ_l under drought (Fig. 3), which would be translated into 20 to 88% loss of conductivity, suggests this trade-off to happen at the plant level. Such variability may be a function of the high foliar plasticity in the coffee canopy (Matos et al., 2009) in addition to canopy control of g_s; Tausend et al. (2000b) showed that partial defoliation in coffee led to higher transpiration per unit leaf area associated with an increased stomata coupling with the surrounding atmosphere. Therefore, leaves that become suddenly exposed with the onset of defoliation and are not able to close stomata properly, may suffer major hydraulic dysfunction and probably fall whereas leaves which stayed in the safe Ψ_l region will survive. Accordingly, leaves that

"survived" the drought season (Fig. 4 and Table 1) presented similar K_{leaf} values to those of leaves that were developed in the rainy period, indicating that a hydraulic recovery occurred. Interestingly, the leaves expanded under drought were constrained at their maximum realizable g_s maybe due to cavitation fatigue from the recovery cycle (Hacke et al., 2001) (Fig. 4). Notably, loss of conductivity in leaves may happen in the within-xylem and outside xylem components (Scoffoni et al., 2014). As coffee has an important share of leaf resistances outside the xylem (Gascó et al., 2004) and the turgor loss point precedes P_{50} (Fig. 3), it is expected that loss of turgor cause a significant decline in K_{leaf} by affecting extra-xylary pathways (Brodribb and Holbrook, 2006). Such decline is simpler in nature to be reverted given that it does not depend on positive pressure to refill emboli (Holloway-Phillips and Brodribb, 2011). On the other hand, cavitation per se may have play a role in K_{leaf} loss at more negative Ψ_l; this may define the point of no return incurring leaf abscission (Blackman et al., 2009). We contend that Ψ_l at P_{88} possibly denotes a good proxy for leaf death and the upper Ψ threshold for plant death as tree mortality did not occur in this current study. Noteworthy, such results are in agreement with Urli et al. (2013) who found stem Ψ at P_{88} as the trigger for plant death in angiosperms. This statement well agrees with earlier attempts to measure stem hydraulic vulnerability in coffee which would predict coffee death to happen at -6 to -8 MPa stem Ψ (Tausend et al., 2000). In fact, this also corroborates experimental observation of predawn Ψ_l as low as -4 MPa in coffee plants without leading to plant death (DaMatta and Ramalho, 2006).

The incomplete recovery of A_n and g_s following rainfall (recovery phase; Fig. 4) likely indicates ABA accumulation as a way to regulate transpiration rates, thus promoting gradual hydraulic repair by limiting the rate of stomatal reopening (Lovisolo et al. 2008). Moreover, even with constrained g_s, Ψ_l at the morning and afternoon reached similar or more negative values in comparison with those found in the fully-recovered leaves ('control' conditions) when g_s values were twice as high, evidencing post-drought hydraulic loss (Fig. 3 and 4). Such persistent loss of conductivity possibly reflects cavitation in stem xylem, which is likely to require zero or positive root pressure for repair (Ewers et al., 1997), thus demanding an extended period of rainfall and longer time period. Indeed, maximum gas exchange rates were observed two months after the beginning of the rainy period.

Regarding stomata control, coffee leaves show a tight coordination between A_n and g_s, thus ultimately resulting in extremely high WUE_i values (Medrano et al., 2009) under drought with little, if at all, variations throughout the day (Fig. 5). However, such efficiency comes at the cost of reaching Ψ_l closer to values leading to c. 20% loss of conductivity and loss of turgor. At this point, it is likely that short-term diurnal g_s adjustments rely on fast/active mechanisms involving ABA synthesis and catabolism in leaves to close stomata and allow plant rehydration as clearly seen at the afternoon (Fig. 3). Such stomata control of xylem embolism has been reported in several species (Salleo et al., 2000; Nardini et al.; 2001; Cochard et al., 2002; Brodribb et al., 2003), which suggests a role for cavitation as a hydraulic signal promoting stomata closure. However, the mechanisms by which stomata could sense cavitation and adjust g_s remain controversial (Zufferey et al., 2011). In a recent study Scoffoni et al. (2014) propose that leaf shrinkage may play a role in K_{leaf} loss, but this is unlikely to be the case of coffee taking into account its very rigid cell walls (high ε, Table 1). In any case, high extra-vascular resistances in coffee (Gascó et al., 2004) may increase internal water deficits near to the sites of evaporation, therefore augmenting guard cell sensitivity to ABA (Tardieu and Davis, 2003; McAdam et al., 2011). We suggest ABA as playing a major role at this g_s control as feedback inhibition by carbohydrate accumulation seems not occur in coffee plants under normal growth conditions (DaMatta et al., 2008; Batista et al., 2012). Nevertheless, we cannot discard an intrinsic guard-cell response to Ψ_l or leaf turgor as both passive and active mechanisms likely interact controlling stomata apertures (Brodribb and McAdam, 2013; McAdam and Brodribb, 2014). We believe that reductions in leaf turgor in turn causes reductions in guard cell turgor and thus probably diminishing g_s at the morning under drought; but, as the leaf dries out, a passive mechanism alone cannot guarantee full stomata closure because of mechanical advantage of epidermal cells (Franks, 2013). Thus, active mechanisms probably ABA-mediated come into action to ensure proper closure at the afternoon to avoid damaging Ψ_l to occur. In any case, differential leaf sensitivity to ABA is likely to occur given the high range of Ψ_l found mainly under drought (Fig. 3). This suggests that some leaves cannot reach sufficient stomata closure and further ABA-sensitivity studies are necessary to better elucidate the contribution of passive and active mechanisms controlling coffee stomata.

Another important outcome of our study was the confirmation that, even under severe drought, carbon gain in coffee is strongly limited by diffusive limitations as evidenced by nearly constant values of ETR and V_{cmax} (Fig. 4 and 5) (Galle et al., 2009). We have previously demonstrated in potted coffee seedlings that gas exchanges are constrained by a limited hydraulic architecture (Martins et al., 2014) linked to a low K_{leaf} that limits water supply and ultimately restricts water demand. Such hydraulic limitation is expected to be exacerbated under real plantation conditions, where high temperatures and energy load maximise the evaporative demand. Thus, the narrow and negative safety margins found in this study would concern the worst case scenario for coffee. Interestingly, coffee leaves present a lower P_{50} than would be expected considering its evolution under a wet, shady environment (Sylvain, 1955; Blackman et al., 2012). As this improved tolerance to hydraulic dysfunction can be a result from breeding programs conducted under full sun conditions, it is imperative to assess the natural hydraulic plasticity in coffee from a conservation perspective. A complicating factor to model coffee mortality will likely be the interaction between death by hydraulic failure and/or by carbon starvation (McDowell et al., 2011). We contend that hydraulic failure will be the major concern for coffee grown in open areas whereas carbon starvation may be the case for shaded coffee. Results from Cavatte et al. (2012a) support this assertion as droughted shade plants presented lower starch concentrations but higher midday Ψ_l than did the sun plants. In any case, from a survival perspective, coffee seems to be well-adapted to tolerate drought, with stems apparently very tolerant to hydraulic dysfunction, capacity to perform elastic and osmotic adjustments (Table 1), and a high capacity to make over new leaves in addition to the ability to resprout (personal observations). On the other hand, the operation under narrow safety margins risking the loss of metabolic costly leaves and dispendious nitrogen (Cavatte et al., 2012b, Martins et al., 2014b) is not interesting from an economical perspective. Foliage loss will contribute negatively to final yield at the short-term and foliage recovery will deplete plant internal reserves at the long term, reducing the lifespan of coffee plantations (DaMatta et al., 2010). Both factors contribute to diminishing revenue streams from the coffee crop in a scenario of increased drought frequency.

Conclusion

As other angiosperms, the coffee tree operates under narrow safety margins even under well-watered growth conditions and it is subjected to hydraulic failure

upon severe drought events. Recovery of gas exchange to maximum rates took place two months after the beginning of the rainy period, suggesting the need for positive root pressures to refill xylem emboli. Difference in the level of foliage retention after drought between cultivars appears to be related to lower leaf vulnerability to hydraulic dysfunction, despite minor alteration in gas exchange parameters. In any case, leaves that did not cross a given threshold for leaf abscission, likely to be the Ψ_l at P_{88}, recovered from hydraulic loss presenting K_{leaf} similar to the new leaves that were developed over the rainy season, but constrained at their maximum realizable g_s. Under wet conditions, stomata aperture is likely regulated to prevent loss of conductivity of reaching levels higher than c. 30%. The advantage of such risky strategy is the maximisation of WUE_i, which may come at the cost of foliage loss. Further studies to determine hydraulic vulnerability in stems and roots as well in other varieties, are of utmost importance for a proper assessment of the impact climate changes will have for the coffee crop.

References

Allen CD, Macalady AK, Chenchouni H, et al. 2010. A global overview of drought and heat-induced tree mortality reveals emerging climate change risks for forests. Forest Ecology and Management **259**, 660–684.

Batista KD, Araújo WL, Antunes WC, Cavatte PC, Moraes GABK, Martins SCV, DaMatta FM. 2012. Photosynthetic limitations in coffee plants are chiefly governed by diffusive factors. Trees **26**, 459–468.

Blackman CJ, Brodribb TJ, Jordan GJ. 2009. Leaf hydraulics and drought stress: response, recovery and survivorship in four woody temperate plant species. Plant, Cell & Environment **32**, 1584–1595.

Blackman CJ, Brodribb TJ, Jordan GJ. 2010. Leaf hydraulic vulnerability is related to conduit dimensions and drought resistance across a diverse range of woody angiosperms. New Phytologist **188**, 1113–1123.

Blackman CJ, Brodribb TJ, Jordan GJ. 2012. Leaf hydraulic vulnerability influences species' bioclimatic limits in a diverse group of woody angiosperms. Oecologia **168**, 1–10.

Brodribb TJ, Cochard H. 2009. Hydraulic failure defines the recovery and point of death in water-stressed conifers. Plant Physiology **149**, 575–584.

Brodribb TJ, Holbrook MN. 2003. Stomatal closure during leaf dehydration, correlation with other leaf physiological traits. Plant Physiology **132**, 2166–2217.

Brodribb TJ, Holbrook NM. 2006. Declining hydraulic efficiency as transpiring leaves desiccate: two types of response. Plant, Cell & Environment **29**, 2205–2215.

Brodribb TJ, Holbrook NM, Edwards EJ, Gutierrez MV. 2003. Relations between stomatal closure, leaf turgor and xylem vulnerability in eight tropical dry forest trees. Plant, Cell and Environment **26**, 443–450.

Brodribb TJ, McAdam SAM. 2013. Abscisic acid mediates a divergence in the drought response of two conifers. Plant Physiology **162**, 1370–1377.

Brodribb TJ, McAdam SAM, Jordan GJ, Martins SCV. 2014. Conifer species adapt to low-rainfall climates by following one of two divergent pathways. Proceedings of the National Academy of Sciences of the United States of America **111**, 14489-14493.

Bunn C, Läderach P, Ovalle Rivera O, Kirschke D. 2014. A bitter cup: climate change profile of global production of Arabica and Robusta coffee. Climatic Change. doi 10.1007/s10584-014-1306-x

Cavatte PC, Oliveira AAG, Morais LE, Martins SCV, Sanglard LMVP, DaMatta FM. 2012a. Could shading reduce the negative impacts of drought on coffee? A morphophysiological analysis. Physiologia Plantarum **144**, 111–122.

Cavatte PC, Rodríguez-López NF, Martins SCV, Mattos MS, Sanglard LMVP, Damatta FM. 2012b. Functional analysis of the relative growth rate, chemical composition, construction and maintenance costs, and the payback time of Coffea arabica L. leaves in response to light and water availability. Journal of Experimental Botany **63**, 3071–3082.

Choat B, Jansen S, Brodribb TJ, et al. 2012. Global convergence in the vulnerability of forests to drought. Nature **491**, 752–756.

Cochard H, Badel E, Herbette S, Delzon S, Choat B, Jansen S. 2013. Methods for measuring plant vulnerability to cavitation: a critical review. Journal of Experimental Botany **64**, 4779–4791.

Cochard H, Coll L, Roux X Le, Améglio T. 2002. Unraveling the effects of plant hydraulics on stomatal closure during water stress in walnut. Plant Physiology **128**, 282–290.

Cornic G. 2000. Drought stress inhibits photosynthesis by decreasing stomatal aperture - Not by affecting ATP synthesis. Trends in Plant Science **5**, 187–188.

DaMatta FM. 2004. Exploring drought tolerance in coffee : a physiological approach with some insights for plant breeding. Brazilian Journal of Plant Physiology **16**, 1–6.

DaMatta FM, Cunha RL, Antunes WC, Martins SCV, Araújo WL, Fernie A, Moraes, GABK. 2008. In field-grown coffee trees source-sink manipulation alters photosynthetic rates, independently of carbon metabolism, via alterations in stomatal function. New Phytologist **178**, 348–357

DaMatta, FM, Ramalho, JDC. 2006. Impact of drought and temperature stress on coffee physiology and production: a review. Brazilian Journal of Plant Physiology **18**, 55–81.

DaMatta FM, Ronchi CP, Maestri M, Barros RS. 2010. Coffee: environment and crop physiology. In: DaMatta, FM (Ed.), Ecophysiology of Tropical Tree Crops. Nova Science Publishers, New York, USA, pp. 181–216.

Davis AP, Gole TW, Baena S, Moat J. 2012. The impact of climate change on indigenous arabica coffee (Coffea arabica): predicting future trends and identifying priorities. PLoS ONE **7**, e47981.

Delzon S, Cochard H. 2014. Recent advances in tree hydraulics highlight the ecological significance of the hydraulic safety margin. New Phytologist **203**, 355–358.

Dias PC, Araujo WL, Moraes GABK, Barros RS, DaMatta FM. 2007. Morphological and physiological responses of two coffee progenies to soil water availability. Journal of Plant Physiology **164**, 1639–1647.

Engelbrecht BMJ, Comita LS, Condit R, Kursar TA, Tyree MT, Turner BL, Hubbell SP. 2007. Drought sensitivity shapes species distribution patterns in tropical forests. Nature **447,** 80–82.

Ewers FW, Cochard H, Tyree MT. 1997. A survey of root pressures in vines of a tropical lowland forest. Oecologia **110,** 191–196.

Franks PJ. 2013. Passive and active stomatal control: either or both? New Phytologist **198**, 325–327.

Galle A, Florez-Sarasa I, Tomas M, Pou A, Medrano H, Ribas-Carbo M, Flexas J. 2009. The role of mesophyll conductance during water stress and recovery in tobacco (Nicotiana sylvestris): acclimation or limitation? Journal of Experimental Botany **60**, 2379–2390.

Gascó A, Nardini A, Salleo S. 2004. Resistance to water flow through leaves of Coffea arabica is dominated by extra-vascular tissues. Functional Plant Biology **31**, 1161-1168.

Hacke UG, Stiller V, Sperry JS, Pittermann J, McCulloh KA. 2001. Cavitation fatigue. embolism and refilling cycles can weaken the cavitation resistance of xylem. Plant physiology **125**, 779–786.

Holloway-Phillips M-M, Brodribb TJ. 2011. Minimum hydraulic safety leads to maximum water-use efficiency in a forage grass. Plant, Cell & Environment **34**, 302–313.

Klein T, Yakir D, Buchmann N, Grünzweig JM. 2014. Towards an advanced assessment of the hydrological vulnerability of forests to climate change-induced drought. New Phytologist **201**, 712–716.

Lovisolo C, Perrone I, Hartung W, Schubert A. 2008. An abscisic acid-related reduced transpiration promotes gradual embolism repair when grapevines are rehydrated after drought. New Phytologist **180,** 642–651

Martins SC V, Araújo WL, Tohge T, Fernie AR, DaMatta FM. 2014. In high-light-acclimated coffee plants the metabolic machinery is adjusted to avoid oxidative stress rather than to benefit from extra light enhancement in photosynthetic yield. PloS ONE **9**, e94862.

Martins SCV, Galmés JG, Cavatte PC, Pereira LF, Ventrella MC, Damatta FM. 2014. Understanding the low photosynthetic rates of sun and shade coffee leaves: bridging the gap on the relative roles of hydraulic, diffusive and biochemical constraints to photosynthesis. PloS ONE **9**, e95571.

Martins SCV, Galmés JG, Molins A, DaMatta FM. 2013. Improving the estimation of mesophyll conductance: on the role of electron transport rate correction and respiration. Jornal of Experimental Botany **64**, 3285-3298.

Matos FS, Wolfgramm R, Gonçalves F V, Cavatte PC, Ventrella MC, DaMatta FM. 2009. Phenotypic plasticity in response to light in the coffee tree. Environmental and Experimental Botany **67**, 421–427.

Medrano H, Flexas J, Galmés J. 2009. Variability in water use efficiency at the leaf level among Mediterranean plants with different growth forms. Plant Soil **317**, 17-29.

McAdam SAM, Brodribb TJ. 2012. Stomatal innovation and the rise of seed plants. Ecology Letters **15**, 1–8.

McAdam SAM, Brodribb TJ. 2014. Separating active and passive influences on stomatal control of transpiration. Plant Physiology **164**, 1578–1586.

McAdam SAM, Brodribb TJ, Ross JJ, Jordan GJ. 2011. Augmentation of abscisic acid (ABA) levels by drought does not induce short-term stomatal sensitivity to CO_2 in two divergent conifer species. Journal of Experimental Botany **62**, 195–203.

McDowell NG. 2011. Mechanisms linking drought, hydraulics, carbon metabolism, and vegetation mortality. Plant Physiology **155**, 1051–1059.

McDowell N, Pockman WT, Allen CD, Breshears DD, Cobb N, Kolb T, Plaut J, Sperry J, West A, Williams DG, et al. 2008. Mechanisms of plant survival and mortality during drought: why do some plants survive while others succumb to drought? New Phytologist **178**, 719–739.

Meinzer FC, Johnson DM, Lachenbruch B, McCulloh KA, Woodruff DR. 2009. Xylem hydraulic safety margins in woody plants: coordination of stomatal control of xylem tension with hydraulic capacitance. Functional Ecology **23**, 922–930.

Nardini A, Tyree MT, Salleo S. 2001. Xylem cavitation in the leaf of Prunus laurocerasus L. and its impact on leaf hydraulics. Plant Physiology **125,** 1700–1709.

Nardini A, Ounapuu-Pikas E, Savi T. 2014. When smaller is better: leaf hydraulic conductance and drought vulnerability correlate to leaf size and venation density across four Coffea arabica genotypes. Functional Plant Biology **41**, 972-983.

Pinheiro HA, DaMatta FM, Chaves AR, Loureiro ME, Ducatti C. 2005. Drought tolerance is associated with rooting depth and stomatal control of water use in clones of Coffea canephora. Annals of Botany **96**, 101–108.

Sack L. 2002. The hydraulic conductance of the angiosperm leaf lamina: a comparison of three measurement methods. Journal of Experimental Botany **53**, 2177–2184.

Salleo S, Lo Gullo MA, Raimondo F, Nardini A. 2001. Vulnerability to cavitation of leaf minor veins: any impact on leaf gas exchange? Plant, Cell & Environment **24,** 851–859.

Scoffoni C, Vuong C, Diep S, Cochard H, Sack L. 2014. Leaf shrinkage with dehydration: coordination with hydraulic vulnerability and drought tolerance. Plant Physiology **164**, 1772–1788.

Sylvain P. 1955. Some observations on Coffea arabica L. in Ethiopia. Turrialba **5**, 37-53.

Tardieu F. 1993. Will increases in our understanding of soil-root relations and root signaling substantially alter water flux models? The Philosophical Transactions of the Royal Society of London Serie B **341**, 57–66.

Tardieu F, Davies WJ. 1993. Integration of hydraulic and chemical signalling in the control of stomatal conductance and water status of droughted plants. Plant Cell & Environment **16,** 341–349.

Tausend PC, Goldstein G, Meinzer FC. 2000a. Water utilization, plant hydraulic properties and xylem vulnerability in three contrasting coffee (Coffea arabica) cultivars. Tree Physiology **20**, 159–168.

Tausend PC, Meinzer FC, Goldstein G. 2000b. Control of transpiration in three coffee cultivars: the role of hydraulic and crown architecture. Trees **14,** 181-190.

Tyree, MT, Davis SD, Cochard H. 1994. Biophysical perspectives of xylem evolution: is there a trade-off to hydraulic efficiency for vulnerability to dysfunction? International Association Wood Anatomists Journal **15,** 335-360.

Urli M, Porté AJ, Cochard H, Guengant Y, Burlett R, Delzon S. 2013. Xylem embolism threshold for catastrophic hydraulic failure in angiosperm trees. Tree Physiology **33**, 672–683.

Wilson KB, Baldocchi DD, Hanson PJ. 2000. Quantifying stomatal and non-stomatal limitations to carbon assimilation resulting from leaf aging and drought in mature deciduous tree species. Tree Physiology **20**, 787–797.

Zhao M, Running SW. 2010. Drought-induced reduction in global terrestrial net primary production from 2000 through 2009. Science **329**, 940-943.

Zufferey V, Cochard H, Ameglio T, Spring JL, Viret O. 2011. Diurnal cycles of embolism formation and repair in petioles of grapevine (Vitis vinifera cv. Chasselas). Journal of Experimental Botany **62**, 3885–3894.

Table 1. Water potential at the turgor loss point (Ψ_{TLP}, MPa), osmotic potential at full turgor ($\Psi_{\pi(100)}$, MPa), relative water content at the turgor loss point (RWC_{TLP}, %), bulk modulus of elasticity (ε, MPa), leaf hydraulic conductance measured with the evaporative flux method (K_{leaf} EFM, mmol H_2O m^{-2} s^{-1} MPa^{-1}), and hydraulic safety margins ($\Psi_{min} - P_x$, MPa) based on P_{50} or P_{88} of coffee plants. When underlined, means for drought-stressed plants differ from those for control plants; * denotes differences between cultivars ($P \leq 0{\cdot}05$). For the K_{leaf} measurements, drought refers to a leaf expanded under drought, but measured at the same time as the leaves that developed upon the wet season.

	Catuaí		Hybrid 12	
	Drought	Control	Drought	Control
Ψ_{TLP}	-2.29	<u>-1.87</u>	-2.21	-1.96
$\Psi_{\pi(100)}$	-1.89	<u>-1.44</u>	-1.79	-1.63
RWC_{TLP}	91.8	89.2	93.0	89.7
ε	24.1*	<u>15.5</u>	16.1	15.2
K_{leaf} EFM	3.10	3.24	3.31	2.31
$\Psi_{min\_drought} - P_{50}$	-1.83		-1.38	
$\Psi_{min\_drought} - P_{88}$	-0.54		-0.13	
$\Psi_{min\_wet} - P_{50}$	0.52		1.06	
$\Psi_{min\_wet} - P_{88}$	1.81		2.31	

Figure legends

Figure 1. Monthly and accumulated precipitation in Viçosa, southeastern Brazil. Historical averages concern the period from 1961-2014. Annual precipitation in 2014 was 825 mm, the lowest recorded in the last 25 years.

Figure 2. Responses of leaf hydraulic conductance (K_{leaf}) to declining leaf water potential (Ψ_l) during dehydration and the diurnal Ψ_l time-course in two coffee cultivars. Curves fitted are sigmoidal functions. Horizontal dotted lines indicate P_{50} in the Ψ_l time-course graphs. Only significant differences among means for water regimes within time are shown, as denoted by different letters; * denotes difference between cultivars within a given water regime ($P<0.05$). Each bar represents the mean ($n = 6$) ± SE.

Figure 3. Pooled data showing the diurnal general relationships between stomatal conductance (g_s) and percentage loss of conductance (PLC) as affected by increasingly negative leaf water potential (Ψ_l). Dashed and dotted vertical lines indicate the Ψ_l at 50% or 88% PLC. Heavy dashed lines indicate the water potential at turgor loss (Ψ_{TLP}). Note the high amplitude in Ψ_l measured at the drought season at 0800 h and 1200 h.

Figure 4. Time-course of net CO_2 assimilation rate (A_n), stomatal conductance (g_s), and electron transport rate (ETR) as measured in two field-grown coffee cultivars grown under full sun conditions and different water conditions. Only significant differences among means for water conditions within a given time are shown, as denoted by different letters; * denotes difference between cultivars within a given water regime ($P<0.05$). Each bar represents the mean ($n = 6$) ± SE.

Figure 5. Time-course of intrinsic water efficiency (A_n/g_s), maximum carboxylation capacity based at a single point ($V_{cmax\_single\ point}$) and the pooled relationship between A_n and g_s as measured in two field-grown coffee cultivars planted under full sun conditions and different water regimes. Only significant differences between means for water regimes within a same time are shown ($P<0.05$), as denoted by different letters. Each bar represents the mean ($n = 6$) ± SE.

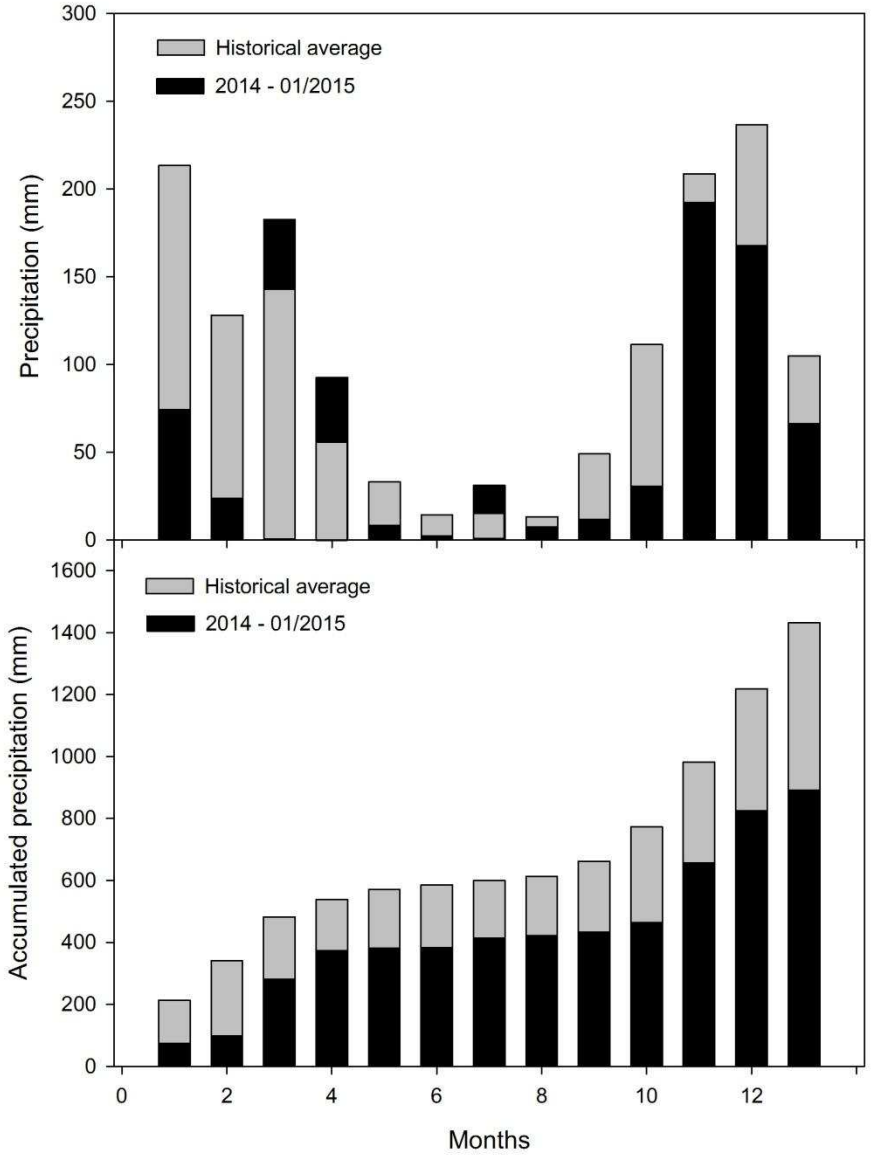
Historical average
2014 - 01/2015
Precipitation (mm)
300
250
200
150
100
50
0
Historical average
2014 - 01/2015
Accumulated precipitation (mm)
1600
1400
1200
1000
800
600
400
200
0
0
2
4
6
8
10
12
Months

Figure 1.

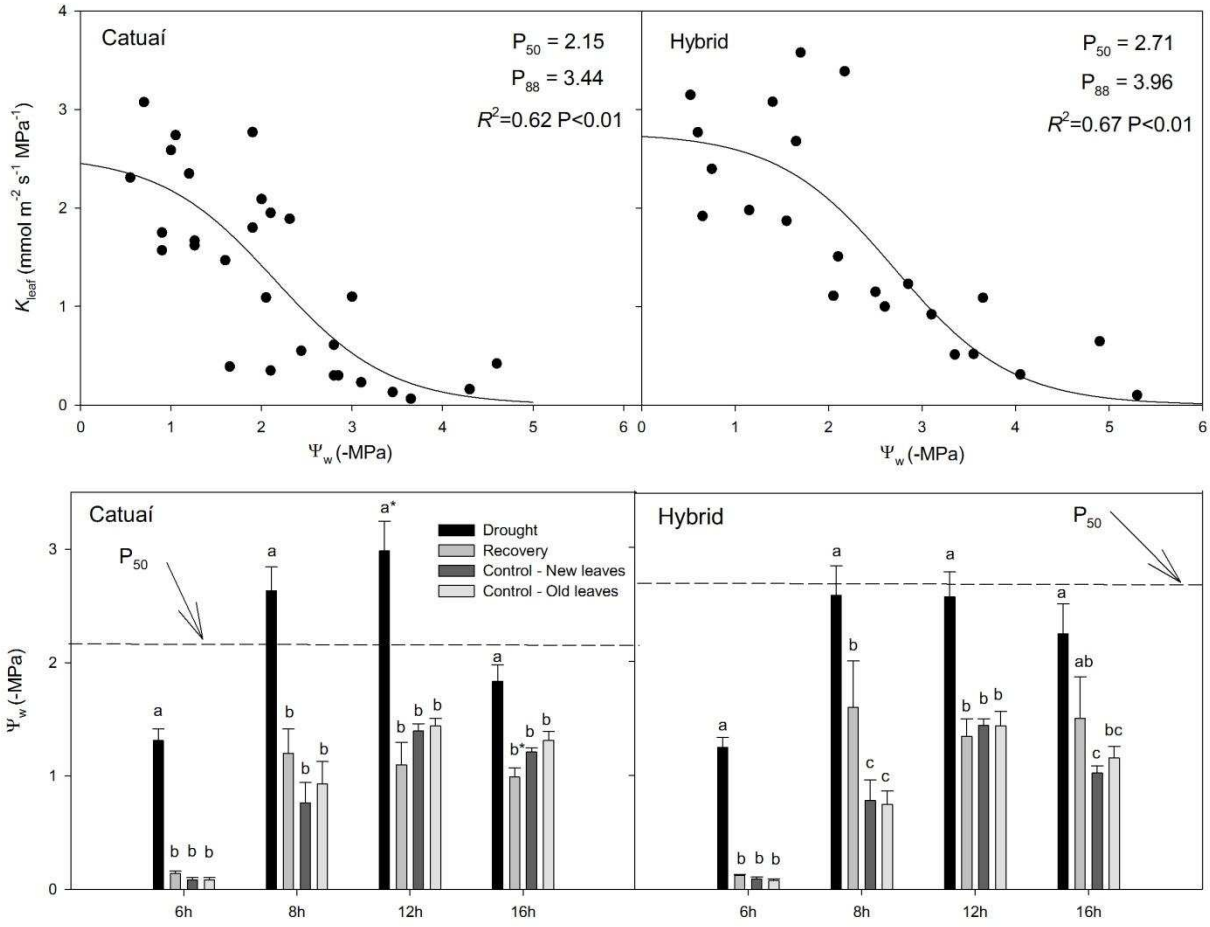
Catuaí
P50 = 2.15
P88 = 3.44
R2=0.62 P<0.01
Hybrid
P50 = 2.71
P88 = 3.96
R2=0.67 P<0.01
Kleaf (mmol m-2 s-1 MPa-1)
Ψw (-MPa)
Drought
Recovery
Control - New leaves
Control - Old leaves
P50
6h
8h
12h
16h

Figure 2.

Figure 3

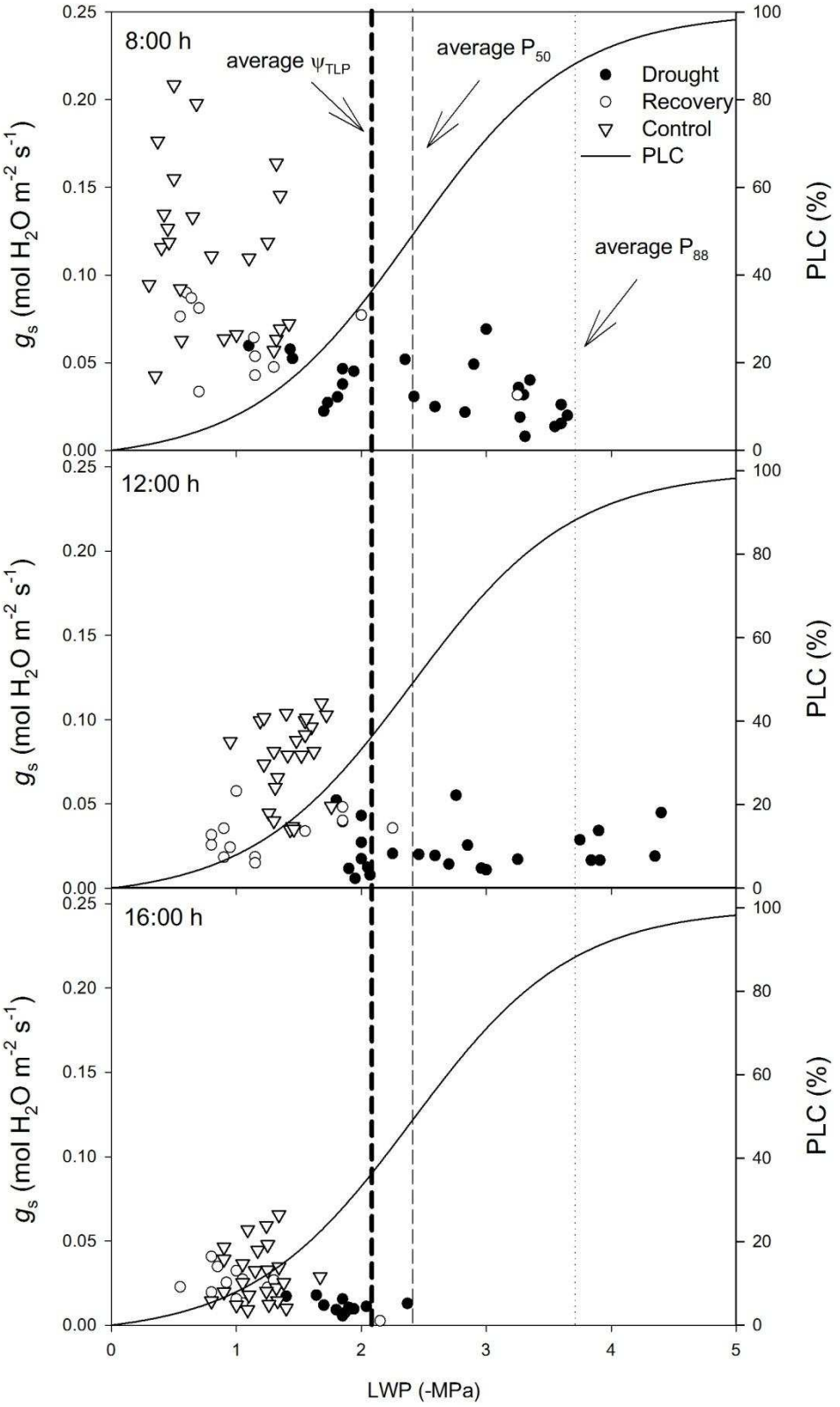
8:00 h
12:00 h
16:00 h
average ψ_{TLP}
average P_{50}
average P_{88}
Drought
Recovery
Control
PLC
g_s (mol H_2O m^{-2} s^{-1})
PLC (%)
LWP (-MPa)

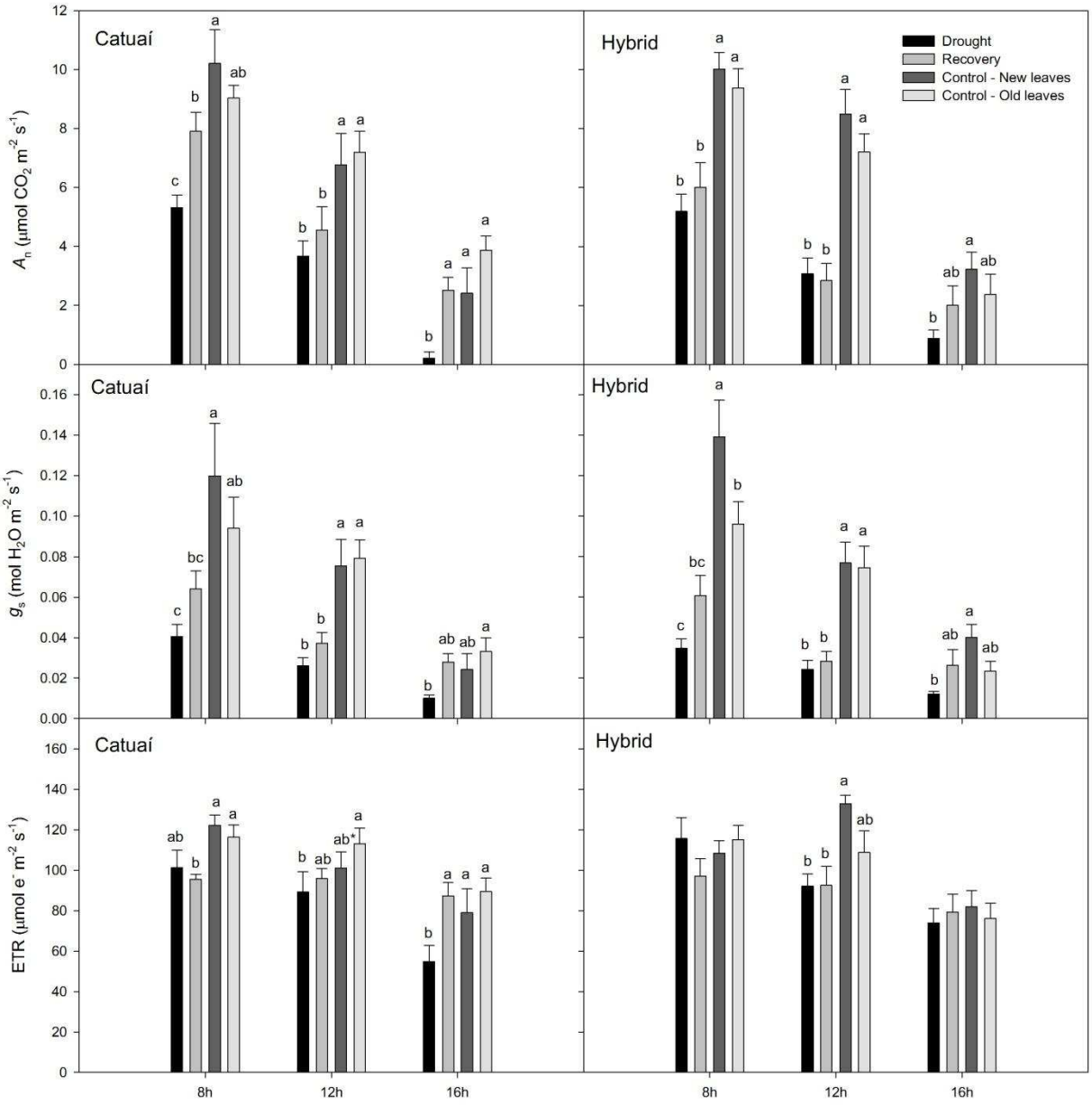
Catuaí
Hybrid
Drought
Recovery
Control - New leaves
Control - Old leaves
A_n (µmol CO_2 m^{-2} s^{-1})
g_s (mol H_2O m^{-2} s^{-1})
ETR (µmol e^- m^{-2} s^{-1})
8h
12h
16h

Figure 4.

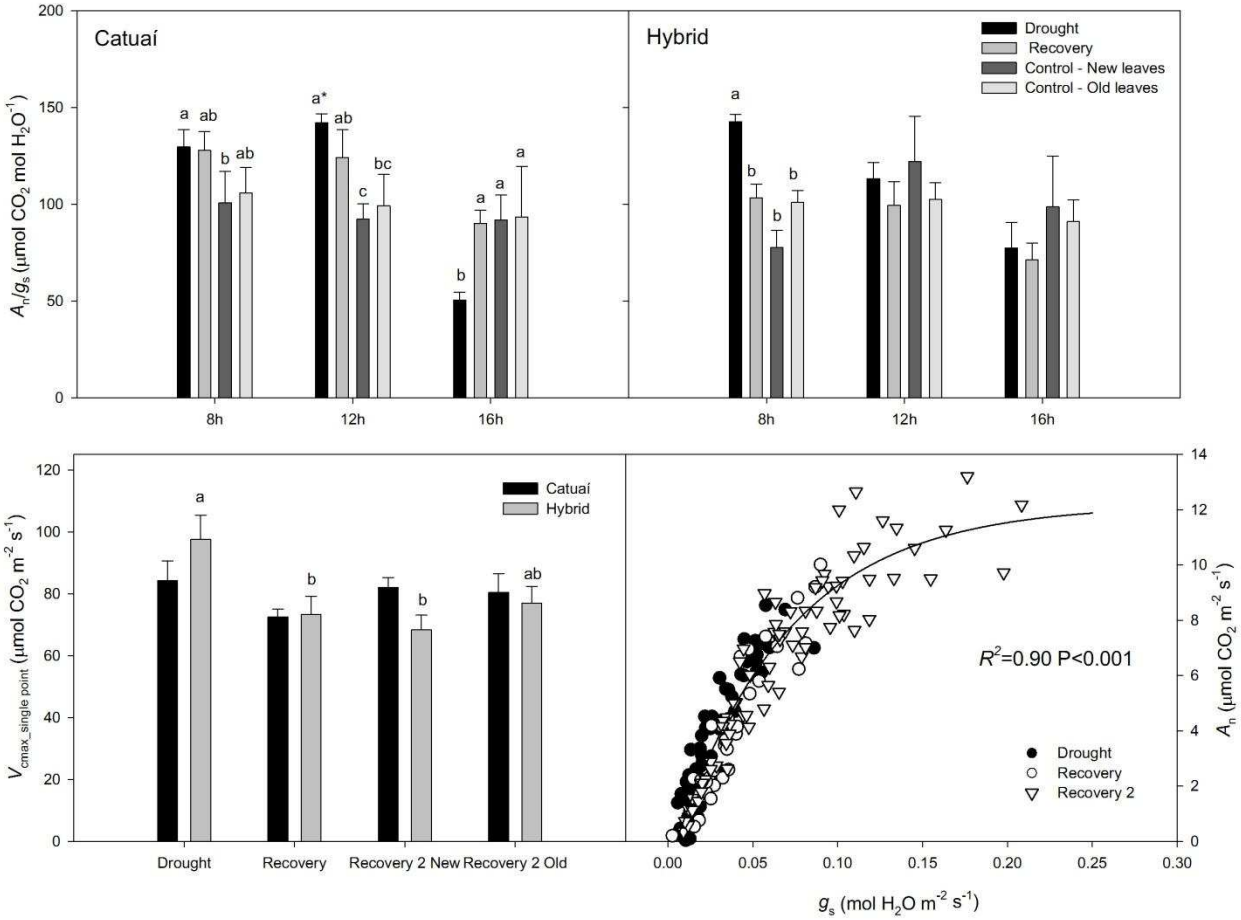
Catuaí
Hybrid
Drought
Recovery
Control - New leaves
Control - Old leaves
A_n/g_s (µmol CO_2 mol H_2O^{-1})
8h
12h
16h
$V_{cmax\_single\ point}$ (µmol CO_2 m^{-2} s^{-1})
Catuaí
Hybrid
Drought
Recovery
Recovery 2 New
Recovery 2 Old
R^2=0.90 P<0.001
Drought
Recovery
Recovery 2
A_n (µmol CO_2 m^{-2} s^{-1})
g_s (mol H_2O m^{-2} s^{-1})

Figure 5.

GENERAL CONCLUSIONS

We have demonstrated the importance of hydraulic parameters in determining g_s dynamics in response to VPD. Our data evidenced that leaf anatomy, through changes in dynamic capacitance and/or water content, had a significant effect on the speed of stomata movements in ferns and conifers, thus leading to closure rates as fast as those seen in angiosperms.

Our water enrichment experiment provided additional evidence in support for the two pool model in three out of four species with contrasting leaf structure and drew attention for a possible interplay between vein density and the associated ground tissues as determinants of the fraction of unenriched water. We proposed that an increased radial resistance for water transport in ferns can have a role in constraining the mixing of enriched and unenriched water; also, it highlights the usefulness of species with low water content in the study of water stable isotopes given the reduced time required to reach the isotopic steady state.

Leaf hydraulic vulnerability assessment showed that the coffee tree operates under narrow safety margins even under normal growth conditions and it is subjected to hydraulic failure upon severe drought events. There seems to be hydraulic variability in coffee, as the cultivar with the leaves less vulnerable to drought stress displayed higher foliage retention after a long-term drought event. We also found that stomata control in coffee under wet conditions appears to be regulated to avoid major loss of conductivity and it is limited to the water potential at the turgor loss point. Further studies to determine hydraulic vulnerability in stems and roots as well in other varieties will be of extreme importance to a proper assessment of the impact climate change will have for the coffee crop.